

# Modelling the technical influence of randomly distributed solar PV uptake on electrical distribution networks

by

Anrich Frederik Willem Steyn



*Thesis presented in partial fulfilment of the requirements for  
the degree of Master of Engineering (Electrical) in the  
Faculty of Engineering at Stellenbosch University*

Supervisor: Dr. A.J. Rix

April 2019

# Declaration

I have read and understand the Stellenbosch University Policy on Plagiarism and the definitions of plagiarism and self-plagiarism contained in the Policy [Plagiarism: The use of the ideas or material of others without acknowledgement, or the re-use of one's own previously evaluated or published material without acknowledgement or indication thereof (self-plagiarism or textrecycling)].

I also understand that direct translations are plagiarism, unless accompanied by an appropriate acknowledgement of the source. I also know that verbatim copy that has not been explicitly indicated as such, is plagiarism.

I know that plagiarism is a punishable offence and may be referred to the University's Central Disciplinary Committee (CDC) who has the authority to expel me for such an offence.

I know that plagiarism is harmful for the academic environment and that it has a negative impact on any profession.

Accordingly all quotations and contributions from any source whatsoever (including the internet) have been cited fully (acknowledged); further, all verbatim copies have been expressly indicated as such (e.g. through quotation marks) and the sources are cited fully.

I declare that, except where a source has been cited, the work contained in this assignment is my own work and that I have not previously (in its entirety or in part) submitted it for grading in this module/assignment or another module/assignment.

Date: ..... April 2019 .....

# Abstract

## Modelling the technical influence of randomly distributed solar PV uptake on electrical distribution networks

A.F.W. Steyn

*Department of Electrical and Electronic Engineering,  
University of Stellenbosch,  
Private Bag X1, Matieland 7602, South Africa.*

Thesis: MEng (Electrical)

April 2019

The solar photovoltaic (PV) industry has seen an exponential growth over the last decade, prompted mainly by government incentives and -regulations. Although the global PV industry is dominated by large, utility-scale PV plants, there has been an increase in the uptake of distributed generation (DG) in the form of residential-, commercial- and industrial rooftop PV systems. Globally, utilities are confronted with the issue of integrating DG into electrical distribution networks. The introduction of DG via renewable energy technologies will cause a metamorphosis of conventional passive power systems into active power systems. DG will influence the technical characteristics of conventional power systems, posing technical challenges with regards to operation and control of the power system.

This project investigates network integration of distributed rooftop PV systems on three distribution networks (one residential, one commercial and one industrial) in Cape Town, South Africa. The residential and commercial networks are owned and operated by the City of Cape Town Municipality, whereas the industrial network is owned and operated by Eskom, the South African national electricity utility. Amidst the lack of a South African national standard with regard to distributed PV installations, the aim is to start to fill a void in the understanding of PV network integration, in order to provide Eskom and CCT, as well as other local municipalities, with a better understanding of the technical effects of PV on distribution networks, as well as the PV hosting capacity of these distribution networks.

This project develops a methodology that can be used to model the technical influence of randomly distributed solar PV uptake on electrical distribution networks. This study focuses solely on the technical effects of voltage rise and equipment overload as network constraints for allowable PV uptake. The methodology first develops techniques with which to model network topology, -loads and PV generators. Subsequently, a simulation methodology is developed and applied to the distribution networks by means of algorithms developed in Digsilent Programming Language.

For the residential- and industrial area, the amount of PV-eligible roof space provides potential PV generation capacity that far exceeds the load requirements of the area. It is shown that allowable PV installations on the residential LV networks vary between 187 kW - 373

kW, and allowable PV penetration levels vary between 82% - 150%. Conductor overload and overvoltage constrain allowable PV uptake on the residential LV networks, whereas the residential MV/LV transformers provide adequate capacity to handle much higher PV penetration levels. The industrial network has the lowest allowable PV penetration level (31 %) due to transformers being overloaded by large PV systems. The commercial area experiences no limit to the uptake of PV, since there is not enough PV-eligible roofspace, and subsequent potential PV generation capacity, to cause network problems.

This project concludes guidelines as to the PV hosting capacity of a sample residential-, commercial- and industrial network. The results of this project provide a better understanding to utilities in terms of the technical limits that dictate PV uptake for different types of networks, as well as the corresponding PV penetration levels. The presented methodology can be used as a starting point for future studies, and can be adapted and extended to consider other technical effects of DG on distribution networks.

# Uittreksel

## Modellering van die tegniese invloed van lukrake-verspreide PV-stelsels op elektriese distribusie-netwerke

*(“Modelling the technical influence of randomly distributed solar PV uptake on electrical distribution networks”)*

A.F.W. Steyn

*Departement Elektriese en Elektroniese Ingenieurswese,  
Universiteit van Stellenbosch,  
Privaatsak X1, Matieland 7602, Suid Afrika.*

Tesis: MIng (Elektries)

April 2019

Die sonfotovoltaïese (PV) industrie het oor die afgelope dekade wêreldwyd eksponensiële groei getoon. Hierdie groei kan hoofsaaklik toegeskryf word aan regerings se regulasies en aansporings. Alhoewel die industrie deur grootskaalse sonplase oorheers word, is daar ook 'n merkbare toename in verspreide generasie (VG) deur middel van residensiële-, kommersiële- en industriële PV-stelsels wat op dakke aangebring word. Kragvoorsieners ervaar wêreldwyd 'n uitdaging om VG in elektriese distribusie-netwerke te integreer. Toename in VG, deur middel van hernubare tegnologieë, sal die tradisionele passiewe kragstelsels 'n gedaantewisseling laat ondergaan. Die tegniese eienskappe van tradisionele kragstelsels sal beïnvloed word deur VG, wat uitdagings in terme van netwerk-operasie en -beheer kan veroorsaak.

Hierdie projek stel dit ten doel om netwerk-integrasie van dakgemonteerde PV-stelsels te ondersoek. Drie verskillende distribusie-netwerke, waaronder 'n residensiële-, kommersiële- en industriële netwerk, word in hierdie opsig ondersoek. Al drie netwerke is in Kaapstad, Suid-Afrika. Die residensiële- en kommersiële netwerke word deur die Kaapstad munisipaliteit besit en bestuur, terwyl die industriële netwerk deur Eskom, Suid-Afrika se nasionale kragvoorsiener, besit en bestuur word. Te midde van die afwesigheid van 'n amptelike Suid-Afrikaanse nasionale standaard wat verspreide PV-stelsels reguleer, poog hierdie projek om 'n leemte in die verstaan van PV netwerk-integrasie te vul. Die doel is om Eskom, Kaapstad munisipaliteit, asook ander plaaslike munisipaliteite te help om 'n beter begrip te ontwikkel in terme van die tegniese invloede wat verspreide PV-stelsels op distribusie-netwerke kan hê. Daar moet ook meer te wete gekom word oor die kapasiteit van PV-stelsels wat deur distribusie-netwerke gehuisves kan word.

Hierdie projek ontwikkel 'n metodologie wat gebruik kan word om die tegniese invloed van lukrake-verspreide PV-stelsels op distribusie-netwerke te modelleer. Slegs twee tegniese invloede word in hierdie opsig oorweeg - spanningstyging en oorlading van netwerktoerusting. Die metodologie ontwikkel eerstens tegnieke waarmee die netwerktopologie, -laste en PV-stelsels gemodelleer kan word. Daarna word 'n simulasiemetodologie ontwikkel en toegepas op die distribusie-netwerke deur middel van algoritmes wat in Digsilent Programmingstaal

ontwikkel is.

In die residensiële- en industriële area, is daar só baie dakspasie beskikbaar vir PV-stelsels, dat 'n situasie kan ontstaan waar die potensiele generasie-opbrengs van die area die lasver-eistes van die area ver kan oorskry. Dit word aangetoon dat die toegelate PV-installasies op die laagspanning residensiële netwerke vanaf 187 kW - 373 kW kan beloop, en die toe-gelate PV-penetrasie vlakke tussen 82% - 150%. Oorlading van geleiers en spanningstyging is die twee tegniese invloede wat die hoeveelheid toegelate PV-stelsels op die residensiële laagspanningsnetwerke beperk, terwyl die residensiële transformators genoegsame kapasiteit het om baie hoër PV-penetrasievlakke te akkommodeer. Die industriële netwerk het die laagste toegelate PV-penetrasievlakke (31%) as gevolg van die feit dat transformators deur groot PV-stelsels oorlaai word. In die kommersiële area is geen beperking in terme van PV-opname teëgekome nie, aangesien daar nie genoegsame dakspasie is om 'n genoegsame generasie-opbrengs te vestig wat netwerk probleme kan veroorsaak nie.

Die projek ontwikkel riglyne in terme van die PV kapasiteit van die drie bestudeerde voorbeeld-netwerke. Die resultate van hierdie projek verskaf 'n beter begrip aan kragvoorsieners in terme van die tegniese beperkings wat PV-opname vir verskillende netwerk-tipes beperk, tesame met die ooreenkomstige PV-penetrasievlakke. Die voorgestelde metodologie kan ge-bruik word as 'n beginpunt vir toekomstige studies, en ook aangepas en uitgebrei word om ander tipes tegniese invloede wat PV-stelsels op distribusie-netwerke kan hê, te ondersoek.

# Acknowledgements

I would like to extend my gratitude towards the following parties:

- Eskom Power Plant Engineering Institute (EPPEI) for funding this research.
- Dr A.J. Rix from the Department of Electrical and Electronic Engineering at the University of Stellenbosch, who acted as academic supervisor for this work and provided assistance that contributed towards the success of this project.
- Zoe Lincoln from Eskom Distribution, for acting as industrial mentor as part of the EPPEI programme, and for providing data and assistance that contributed towards the success of this project.
- Mziwamadoda Tsholoba from City of Cape Town Municipality, for providing data and assistance that contributed towards the success of this project.
- The Centre for Renewable and Sustainable Energy Studies (CRSES) at Stellenbosch University, the City of Cape Town Municipality, and Eskom Distribution for providing data and resources.
- My family and friends for their continued support throughout this project and the entire course.

# List of Publications

A.F.W. Steyn, J.C. Bekker, "Study of the harmonics generated by old and new streetlight technologies", in Proc. 25th Southern African Universities Power Engineering Conference, Stellenbosch, South Africa, 30 January - 1 February 2017.

A.F.W. Steyn, A.J. Rix, "Investigating the effects of distributed PV generation on electrical distribution grids: A Cape Town residential network case study", in Proc. 5th Southern African Solar Energy Conference, Durban, South Africa, 25-27 June 2018.



# Dedications

*Dedicated to my mom and dad.*

# Contents

<b>Declaration</b>	<b>i</b>
<b>Abstract</b>	<b>ii</b>
<b>Uittreksel</b>	<b>iv</b>
<b>Acknowledgements</b>	<b>vi</b>
<b>List of Publications</b>	<b>vii</b>
<b>Dedications</b>	<b>viii</b>
<b>Contents</b>	<b>ix</b>
<b>List of Figures</b>	<b>xii</b>
<b>List of Tables</b>	<b>xv</b>
<b>Nomenclature</b>	<b>xvi</b>
<b>1 Introduction</b>	<b>1</b>
1.1 Project Background . . . . .	1
1.2 Project Objectives . . . . .	1
1.3 Project Applicability . . . . .	2
1.4 Thesis Structure . . . . .	2
<b>2 PV Systems</b>	<b>4</b>
2.1 Introduction . . . . .	4
2.2 Global PV Industry . . . . .	4
2.3 South African PV Industry . . . . .	6
2.4 Distributed PV Generation in Cape Town . . . . .	7
2.4.1 Overview . . . . .	7
2.4.2 Supply Utilities . . . . .	7
2.4.3 SSEG . . . . .	8
2.4.4 Requirements and Restrictions for SSEG in Cape Town . . . . .	9
2.4.5 Metering and Tariffs for SSEG in Cape Town . . . . .	9
2.5 PV System Topologies . . . . .	10
2.5.1 Overview . . . . .	10
2.5.2 Off-grid PV Systems . . . . .	10
2.5.2.1 Off-grid PV System With Battery Storage . . . . .	10
2.5.2.2 Off-grid PV System Without Battery Storage . . . . .	11
2.5.3 Grid-connected PV Systems . . . . .	11

2.5.3.1	Grid-connected PV System With Reverse Power Flow Capability . . . . .	11
2.5.3.2	Grid-connected PV System With Reverse Power Blocking . . . . .	12
2.6	Grid Connection of PV Systems . . . . .	12
<b>3</b>	<b>Electrical Power Systems</b>	<b>14</b>
3.1	Introduction . . . . .	14
3.2	History of Power Systems . . . . .	14
3.3	Power System Components . . . . .	15
3.4	Electrical Distribution Systems . . . . .	16
3.4.1	Overview . . . . .	16
3.4.2	Distribution Line Parameters . . . . .	16
3.4.3	MV Distribution . . . . .	19
3.4.3.1	MV Radial System . . . . .	19
3.4.3.2	MV Loop System . . . . .	19
3.4.3.3	MV Network System . . . . .	20
3.4.4	LV Distribution . . . . .	21
3.4.4.1	Individual MV/LV Transformer Per Customer System . . . . .	21
3.4.4.2	Common LV Main System . . . . .	22
3.4.4.3	LV Network System . . . . .	22
3.4.4.4	Spot Network System . . . . .	23
3.4.5	Distribution System Equipment . . . . .	24
3.4.5.1	Voltage Transformation . . . . .	24
3.4.5.2	Voltage Regulation . . . . .	25
3.4.5.3	Protection . . . . .	26
3.5	Technical Effects of DG on Electrical Distribution Networks . . . . .	27
3.5.1	Overview . . . . .	27
3.5.2	Reverse Power Flow . . . . .	28
3.5.3	Equipment Overload . . . . .	29
3.5.4	System Losses . . . . .	29
3.5.5	Voltage Variations . . . . .	30
3.5.6	Protection Systems . . . . .	34
3.5.7	Reactive Power . . . . .	34
3.5.8	Harmonics . . . . .	35
3.5.9	System Frequency . . . . .	36
3.5.10	Interconnected Networks . . . . .	37
3.5.11	Summary . . . . .	37
<b>4</b>	<b>Modelling and Simulation Methodology</b>	<b>40</b>
4.1	Introduction . . . . .	40
4.2	Networks Overview . . . . .	40
4.3	Modelling Methodology . . . . .	42
4.3.1	Network Topology Modelling . . . . .	42
4.3.2	Network Load Modelling . . . . .	49
4.3.3	Network Generation Modelling . . . . .	52
4.3.3.1	Solar Panel Hosting Capacity . . . . .	52
4.3.3.2	Solar Radiation Data and Terrain Horizon . . . . .	54
4.3.3.3	Generation Profile Simulation . . . . .	56
4.4	Simulation Methodology . . . . .	57
4.4.1	Simulation Data . . . . .	57

4.4.1.1	Minimum Load . . . . .	59
4.4.1.2	Maximum Generation . . . . .	61
4.4.1.3	Summary . . . . .	62
4.4.2	Software Development . . . . .	64
4.4.3	PV Penetration Definition . . . . .	64
4.4.3.1	Network MD Simulations . . . . .	65
4.4.3.2	PV Placement Simulations . . . . .	67
<b>5</b>	<b>Results</b>	<b>70</b>
5.1	Introduction . . . . .	70
5.2	Network MD Results . . . . .	70
5.3	PV Penetration Results . . . . .	70
5.3.1	Results Analysis Method . . . . .	70
5.3.2	Case Study 1: Residential Network . . . . .	72
5.3.2.1	Sunrise Isolated LV Network . . . . .	72
5.3.2.2	Fish Isolated LV Network . . . . .	73
5.3.2.3	Lion Isolated LV Network . . . . .	74
5.3.2.4	Oak Isolated LV Network . . . . .	75
5.3.2.5	Market Isolated LV Network . . . . .	76
5.3.2.6	Beach Isolated LV Network . . . . .	77
5.3.2.7	Grave Isolated LV Network . . . . .	78
5.3.2.8	Residential Interconnected MV/LV Network . . . . .	79
5.3.3	Case Study 2: Commercial Network . . . . .	80
5.3.4	Case Study 3: Industrial Network . . . . .	81
5.3.5	Results Summary and Discussion . . . . .	82
<b>6</b>	<b>Conclusions and Recommendations</b>	<b>88</b>
6.1	Introduction . . . . .	88
6.2	Project Purpose . . . . .	88
6.3	Evaluation of Project Objectives . . . . .	88
6.4	Project Findings and -Contributions . . . . .	89
6.5	Closing Remarks . . . . .	91
	<b>Appendices</b>	<b>92</b>
<b>A</b>	<b>Residential Network Information</b>	<b>93</b>
A.1	Residential Network Topology . . . . .	93
A.2	Residential Network Cables . . . . .	103
A.3	Residential Network Transformers . . . . .	103
<b>B</b>	<b>Commercial Network Information</b>	<b>104</b>
B.1	Commercial Network Topology . . . . .	104
B.2	Commercial Network Cables . . . . .	105
B.3	Commercial Network Transformers . . . . .	105
<b>C</b>	<b>Industrial Network Information</b>	<b>107</b>
C.1	Industrial Network Topology . . . . .	107
C.2	Industrial Network Cables . . . . .	108
C.3	Industrial Network Transformers . . . . .	109
	<b>List of References</b>	<b>110</b>

# List of Figures

2.1	Global PV Capacity Growth 2007-2017 . . . . .	5
2.2	Global PV Capacity Growth 2007-2017 by Country . . . . .	5
2.3	Global PV Power Potential . . . . .	6
2.4	South Africa PV Power Potential . . . . .	6
2.5	Electricity Distribution Licensee Area Boundaries Map . . . . .	8
2.6	Off-grid PV System With Battery Storage . . . . .	11
2.7	Grid-connected PV System with Reverse Power Flow Capability . . . . .	12
2.8	Grid-connected PV System With Reverse Power Blocking . . . . .	12
2.9	Grid-connected PV System Components . . . . .	13
3.1	Distribution Line . . . . .	16
3.2	MV Radial System . . . . .	19
3.3	MV Loop System . . . . .	20
3.4	MV Network System . . . . .	21
3.5	Individual MV/LV Transformer Per Customer System . . . . .	21
3.6	Common LV Main System . . . . .	22
3.7	LV Network System . . . . .	23
3.8	Spot Network System . . . . .	23
3.9	HV/MV Transformer . . . . .	24
3.10	MV/LV Transformer . . . . .	25
3.11	Distribution Substation Voltage Regulators . . . . .	26
3.12	Shunt Capacitor Bank . . . . .	26
3.13	Pole-mount Recloser . . . . .	27
3.14	One-bus Power System with DG . . . . .	28
3.15	Generic Daily Load Profiles for Residential-, Commercial- and Industrial Networks	28
3.16	Distribution Line with Distributed Generation . . . . .	31
3.17	Summary of NRS 097-2-3 PV Penetration Specifications . . . . .	38
4.1	Residential Network Area . . . . .	41
4.2	Commercial Network Area . . . . .	41
4.3	Industrial Network Area . . . . .	42
4.4	Residential MV Network SLD . . . . .	43
4.5	Residential LV Networks . . . . .	44
4.6	Example of Residential Network LV Kiosks . . . . .	45
4.7	Commercial MV Network SLD . . . . .	46
4.8	Industrial MV Network SLD . . . . .	48
4.9	Example of Residential Area Building Footprint Sizes . . . . .	51
4.10	Example of Polygons Indicating Roof Space with PV Potential in Residential Area	52
4.11	Example of Polygons Indicating Roof Space with PV Potential in Commercial Area	53
4.12	Example of Polygons Indicating Roof Space with PV Potential in Industrial Area	53
4.13	Residential Area Horizon- and Sunpath Diagram . . . . .	55

4.14	Commercial Area Horizon- and Sunpath Diagram . . . . .	55
4.15	Industrial Area Horizon- and Sunpath Diagram . . . . .	55
4.16	Cape Town Global Irradiation . . . . .	58
4.17	Residential Area Total Daily Load Profile . . . . .	60
4.18	Commercial Area Total Daily Load Profile . . . . .	60
4.19	Industrial Area Total Daily Load Profile . . . . .	60
4.20	Residential Area Total Daily PV Generation Profile Utilising Maximum PV-eligible Roofsace . . . . .	61
4.21	Commercial Area Total Daily PV Generation Profile Utilising Maximum PV-eligible Roofsace . . . . .	61
4.22	Industrial Area Total Daily PV Generation Profile Utilising Maximum PV-eligible Roofsace . . . . .	62
4.23	Residential Area Total Daily Net Load Profiles with Varying PV Generation . .	62
4.24	Commercial Area Total Daily Net Load Profiles with Varying PV Generation . .	63
4.25	Industrial Area Total Daily Net Load Profiles with Varying PV Generation . . .	63
4.26	Feeder MD Algorithm Flowchart . . . . .	66
4.27	PV Placement Algorithm Flowchart . . . . .	69
5.1	Sunrise Isolated LV Network Maximum Voltage Results . . . . .	72
5.2	Sunrise Isolated LV Network Maximum Line Loading Results . . . . .	73
5.3	Sunrise Isolated LV Network Maximum Transformer Loading Results . . . . .	73
5.4	Fish Isolated LV Network Maximum Voltage Results . . . . .	73
5.5	Fish Isolated LV Network Maximum Line Loading Results . . . . .	74
5.6	Fish Isolated LV Network Maximum Transformer Loading Results . . . . .	74
5.7	Lion Isolated LV Network Maximum Voltage Results . . . . .	74
5.8	Lion Isolated LV Network Maximum Line Loading Results . . . . .	75
5.9	Lion Isolated LV Network Maximum Transformer Loading Results . . . . .	75
5.10	Oak Isolated LV Network Maximum Voltage Results . . . . .	75
5.11	Oak Isolated LV Network Maximum Line Loading Results . . . . .	76
5.12	Oak Isolated LV Network Maximum Transformer Loading Results . . . . .	76
5.13	Market Isolated LV Network Maximum Voltage Results . . . . .	76
5.14	Market Isolated LV Network Maximum Line Loading Results . . . . .	77
5.15	Market Isolated LV Network Maximum Transformer Loading Results . . . . .	77
5.16	Beach Isolated LV Network Maximum Voltage Results . . . . .	77
5.17	Beach Isolated LV Network Maximum Line Loading Results . . . . .	78
5.18	Beach Isolated LV Network Maximum Transformer Loading Results . . . . .	78
5.19	Grave Isolated LV Network Maximum Voltage Results . . . . .	78
5.20	Grave Isolated LV Network Maximum Line Loading Results . . . . .	79
5.21	Grave Isolated LV Network Maximum Transformer Loading Results . . . . .	79
5.22	Residential Interconnected MV/LV Network: MV Network Maximum Voltage Results . . . . .	79
5.23	Residential Interconnected MV/LV Network: LV Network Maximum Voltage Results . . . . .	80
5.24	Residential Interconnected MV/LV Network Maximum Line Loading Results . .	80
5.25	Residential Interconnected MV/LV Network Maximum Transformer Loading Results . . . . .	80
5.26	Commercial Network: MV Network Maximum Voltage Results . . . . .	81
5.27	Commercial Network Maximum Line Loading Results . . . . .	81
5.28	Commercial Network Maximum Transformer Loading Results . . . . .	81
5.29	Industrial Network: MV Network Maximum Voltage Results . . . . .	82

5.30	Industrial Network Maximum Line Loading Results . . . . .	82
5.31	Industrial Network Maximum Transformer Loading Results . . . . .	82
A.1	LV Networks SLD Legend . . . . .	93
A.2	Sunrise LV Network SLD . . . . .	93
A.3	Fish LV Network SLD . . . . .	94
A.4	Lion LV Network SLD . . . . .	94
A.5	Oak LV Network SLD . . . . .	95
A.6	Market LV Network SLD . . . . .	95
A.7	Beach LV Network SLD . . . . .	96
A.8	Grave LV Network SLD . . . . .	97

# List of Tables

3.1	Major Power Systems Milestones . . . . .	15
3.2	Voltage Level Classification . . . . .	15
3.3	Typical Eskom Operating Voltages . . . . .	16
3.4	NRS 048-2 Voltage Specifications . . . . .	33
3.5	NRS 048-2 Harmonics Specifications . . . . .	36
3.6	NRS 048-2 Frequency Specifications . . . . .	36
3.7	Individual Generation Limits for Shared LV Feeders . . . . .	38
4.1	Residential LV Networks Overview . . . . .	44
4.2	Summary of Network Characteristics . . . . .	49
4.3	Available Roof Space for PV Installations . . . . .	54
4.4	Reference PV System . . . . .	56
4.5	Network Violation Thresholds: Network MD Simulations (Passive Network) . . . . .	65
5.1	Network MD Results . . . . .	70
5.2	Network Violation Thresholds: PV Penetration Simulations (Active Network) . . . . .	71
5.3	PV Penetration Results for Scenarios Utilising Maximum PV-eligible Roofspace . . . . .	83
5.4	Maximum Allowable PV According to Each Network Violation . . . . .	83
5.5	Summary of PV Penetration Results . . . . .	84
A.1	Residential Network LV Kiosks Phase Allocation . . . . .	97
A.1	Residential Network LV Kiosks Phase Allocation - continued from previous page . . . . .	98
A.1	Residential Network LV Kiosks Phase Allocation - continued from previous page . . . . .	99
A.2	Residential Network MV Cable Composition . . . . .	100
A.3	Residential Network LV Cable Composition . . . . .	100
A.3	Residential Network LV Cable Composition - continued from previous page . . . . .	101
A.3	Residential Network LV Cable Composition - continued from previous page . . . . .	102
A.4	Residential Network Cable Characteristics . . . . .	103
A.5	Residential Network MV/LV Transformers . . . . .	103
B.1	Commercial Network MV Cable Composition . . . . .	104
B.1	Commercial Network MV Cable Composition - continued from previous page . . . . .	105
B.2	Commercial Network Cable Characteristics . . . . .	105
B.3	Commercial Network MV/LV Transformers . . . . .	105
B.3	Commercial Network MV/LV Transformers - continued from previous page . . . . .	106
C.1	Industrial Network MV Cable Composition . . . . .	107
C.1	Industrial Network MV Cable Composition - continued from previous page . . . . .	108
C.2	Industrial Network Cable Characteristics . . . . .	108
C.3	Industrial Network MV/LV Transformers . . . . .	109



# Nomenclature

## Acronyms

<i>AC</i>	Alternating Current
<i>CCT</i>	City of Cape Town Municipality
<i>CG</i>	Central Generation
<i>CRSES</i>	Centre for Renewable and Sustainable Energy Studies
<i>DC</i>	Direct Current
<i>DG</i>	Distributed Generation
<i>DK</i>	Distribution Kiosk
<i>DPL</i>	Digsilent Programming Language
<i>EVR</i>	Electronic Voltage Regulator
<i>HV</i>	High Voltage
<i>HVDC</i>	High Voltage Direct Current
<i>LV</i>	Low Voltage
<i>MD</i>	Maximum Demand
<i>MK</i>	Metering Kiosk
<i>MPPT</i>	Maximum Power Point Tracker
<i>MV</i>	Medium Voltage
<i>NERSA</i>	National Energy Regulator of South Africa
<i>NMD</i>	Notified Maximum Demand
<i>OLTC</i>	On Load Tap Changer
<i>PCC</i>	Point of Common Coupling
<i>PV</i>	Photovoltaic
<i>QoS</i>	Quality of Supply
<i>REIPPPP</i>	Renewable Energy Independent Power Producer Procurement Programme
<i>RMS</i>	Root Mean Square
<i>RoCoF</i>	Rate of Change of Frequency
<i>RPP</i>	Renewable Power Plant
<i>SLD</i>	Single-line Diagram
<i>SSEG</i>	Small-Scale Embedded Generation
<i>THD</i>	Total Harmonic Distortion
<i>VAR</i>	Volt-ampere Reactive

# Chapter 1

## Introduction

### 1.1 Project Background

The solar photovoltaic (PV) industry has seen an exponential growth over the last decade. Although the global PV industry is dominated by large, utility-scale PV plants, there has been an increase in the uptake of distributed generation (DG) in the form of residential-, commercial- and industrial rooftop PV systems. [1, 2]

Traditionally, global power systems have been reliant on central generation (CG) via coal power plants [3]. These power systems are designed for unidirectional power flow, from source to load [4]. The growth of the global PV industry, prompted mainly by government incentives and regulations [1, 5], will see significant changes in the conventional way that electricity has been supplied and utilised. The introduction of DG via renewable energy technologies will cause a metamorphosis of conventional passive power systems into active power systems. DG will influence the technical characteristics of conventional power systems, posing technical challenges with regard to operation and control of the power system [6].

The topic of network integration of DG is receiving widespread attention. Questions are posed regarding the technical effects of DG, the DG hosting capacity of conventional power systems due to technical constraints, as well as the network adjustments needed to address the technical issues associated with DG network integration. Globally, utilities are confronted with the issue of integrating DG into electrical distribution networks [7]. This project investigates this issue, with focus placed on South African distribution networks, in order to help local stakeholders better understand the impacts of DG.

### 1.2 Project Objectives

This project investigates network integration of distributed rooftop PV systems, with the focus restricted to residential-, commercial- and industrial distribution networks. Three distribution networks (one residential, one commercial and one industrial) in Cape Town, South Africa, are selected as case studies. The residential and commercial networks are owned and operated by the City of Cape Town Municipality (CCT), whereas the industrial network is owned and operated by Eskom, the South African national electricity utility. The aim is to start to fill a void in the understanding of PV network integration, in order to provide Eskom and CCT, as well as other local municipalities, with a better understanding of the technical effects of PV on distribution networks, as well as the PV hosting capacity of these distribution networks.

The project first investigates literature surrounding the topics of PV systems and electrical power systems. The aim is to provide a firm understanding of PV systems, conventional power systems, and ultimately the status quo when PV- and conventional power systems are integrated. Thereafter, this project proposes a methodology with which to achieve the following objectives for the three networks:

- Model the network topologies.
- Model the electrical loads.
- Determine the PV uptake potential, in terms of the amount of available roofspace for PV installations.
- Model the power supply from rooftop PV systems.
- Develop software with which to perform network studies.
- Investigate the occurrence of voltage rise and equipment overload when PV is integrated into the networks.
- Determine the PV hosting capacity (allowable PV penetration level), as well as the restraining technical issue that is the bottleneck to further PV uptake.

### 1.3 Project Applicability

In the lack of proper national legislation with regards to grid-connected PV installations in South Africa, CCT has aligned with the NRS 097-2-3 specification in determining the amount of allowable PV penetration on a distribution network. The justification of this remains in question, and the application thereof may therefore be overly restrictive, and possibly pose an unnecessary bottleneck to the uptake of PV.

The findings of this project provides a new reference point to Eskom, CCT and other local municipalities with regards to the technical effects of PV on distribution networks, as well as the PV hosting capacity of distribution networks. More important, however, is that this project develops a reproducible methodology that can be uniformly applied to any electrical distribution network, so that comparable results are yielded when any distribution network, in the presence of distributed PV generation, is studied.

### 1.4 Thesis Structure

This thesis is structured as follows:

Chapter 2: This chapter provides an overview of PV systems. An overview of the global status of the PV industry is provided, as well as the PV industry in South Africa. Thereafter, the current status of distributed PV generation in Cape Town is discussed, with an overview of the current regulations in place in this regard within CCT. This is followed by a basic introduction to PV systems, with a discussion on the different PV system topologies and grid-connection of PV systems.

- Chapter 3: This chapter provides an overview of electrical power systems. A brief history of power systems is presented, followed by a discussion of the different components that constitute a conventional power system. Thereafter, conventional distribution systems are considered in more detail, with a review of distribution network parameters, -topologies and -equipment. Subsequently, active power systems, with integrated DG, are considered, with an overview of the technical effects of DG on electrical distribution networks. An overview of the NRS specifications applicable to distribution system operation in South Africa is provided alongside the discussion on the technical effects of DG on electrical distribution networks.
- Chapter 4: Chapter 4 presents the modelling and simulation methodology that is followed in this project. An overview of the case study networks are provided, followed by a discussion detailing the modelling procedure followed to represent the topologies, loads and PV generators of the case study networks. The chapter concludes with a discussion of the simulation procedure followed, and associated software employed in the network studies.
- Chapter 5: This chapter provides all the results obtained via the network studies, followed by a summary and discussion of the results.
- Chapter 6: This chapter draws conclusions on the results and information brought to light by the project, and provides recommendations for future work.

# Chapter 2

## PV Systems

### 2.1 Introduction

This chapter elaborates on the global- and South African PV industry, and discusses the current status of distributed PV regulations in Cape Town. Thereafter, a basic introduction to PV system topologies is provided, followed by a closer look at grid-connection of PV systems.

### 2.2 Global PV Industry

The global PV industry has seen an exponential growth over the last decade. The increased adoption of PV can be attributed to several factors [1, 2, 5, 8]:

- Government and municipal incentives, -policies and -regulations,
- Environmental awareness,
- Decreasing cost of PV panels,
- Economic competitiveness of PV electricity,
- Rising demand for access to electricity,
- Rising utility electricity prices,
- The need to diversify the energy mix.

In 2017, PV added more generation capacity to the global power generation pool than any other generation technology, with a 98 GW<sub>DC</sub> capacity contribution. This rapid increase was prompted mainly by China, which showcased a growth in installations of more than 50%. In terms of cumulative installed capacity, the current world dominators are China, USA, Japan, Germany and Italy, whilst Germany, Japan, Belgium, Italy and Australia are global leaders in terms of per capita PV capacity. The main contributors of newly installed capacity in 2017 were China, USA, India, Japan and Turkey. Figure 2.1 shows the global annual additions and -cumulative capacity of PV for 2007-2017, and figure 2.2 shows the global cumulative PV capacity for 2007-2017 by country. It can be seen that the global cumulative installed PV capacity amounted to 402 GW<sub>DC</sub> at the end of 2017. [1]

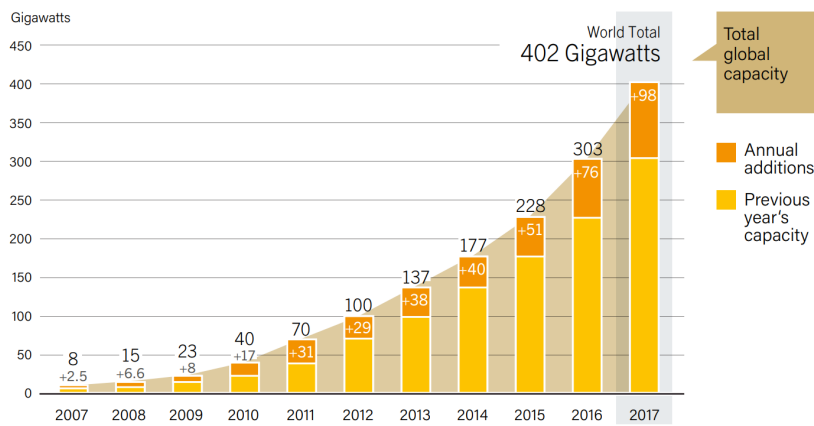


Figure 2.1: Global PV Capacity Growth 2007-2017 [1]

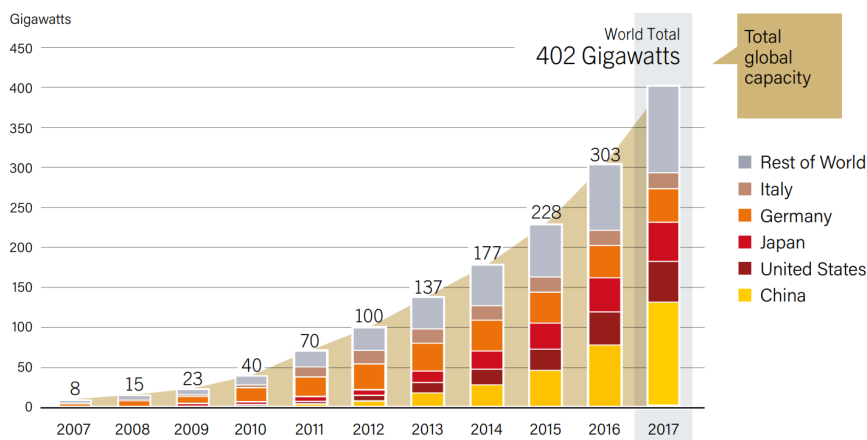


Figure 2.2: Global PV Capacity Growth 2007-2017 by Country [1]

Of the 53.1  $\text{GW}_{\text{DC}}$  capacity added by China in 2017, 19.4  $\text{GW}_{\text{DC}}$  was distributed PV. Although it is still a small market-segment compared to utility scale PV projects, rooftop PV is the fastest growing PV sector in India. 1.1  $\text{GW}_{\text{DC}}$  of residential PV systems were added in Japan in 2017, and a doubling in community-based PV projects were observed for the same time period. In Thailand, there has been a proliferation in companies that install rooftop PV. Spain's 145 % increase in PV capacity in 2017 was dominated by rooftop PV. The rising of electricity prices and improving competitiveness of PV economics prompted a 1.3  $\text{GW}_{\text{DC}}$  increase in Australia's PV market in 2017, bringing the total capacity to 7.2  $\text{GW}_{\text{DC}}$ . Australia's 2017 growth was dominated by distributed residential PV installations. At the end of 2017, a cumulative capacity of almost 1.8 million distributed rooftop PV systems were operating in Australia. In Brazil and Mexico, increase in distributed PV generation is currently prompted by high electricity prices, as well as the incentive of net-metering. [1]

Although the global PV market is currently being dominated by utility-scale PV plants, the growth in distributed PV applications is clearly visible. This discussion clearly illustrates the relevance of this study - a growing global PV market, and associated increased distributed PV installations, spurs the need for studying the network integration of distributed PV systems. The proliferation of renewable energy technologies, specifically PV, will change the face of existing power systems, and it is imperative to understand how this will influence the technical operation of the power system.

## 2.3 South African PV Industry

Figure 2.3 shows the global PV power generation potential. Inspection of figure 2.3 shows that South Africa has amongst the best solar resource in the world. When looking at the South African regional PV power potential, shown in figure 2.4, it can be seen that the Northern Cape has the highest PV power potential in South Africa. It is for this reason that the Northern Cape is home to several utility-scale PV plants, which were installed as part of South Africa's Renewable Energy Independent Power Producer Procurement Programme (REIPPPP). South Africa added 13 MW<sub>DC</sub> of PV in 2017, for a total of 1.8 GW<sub>DC</sub> PV installed [1].

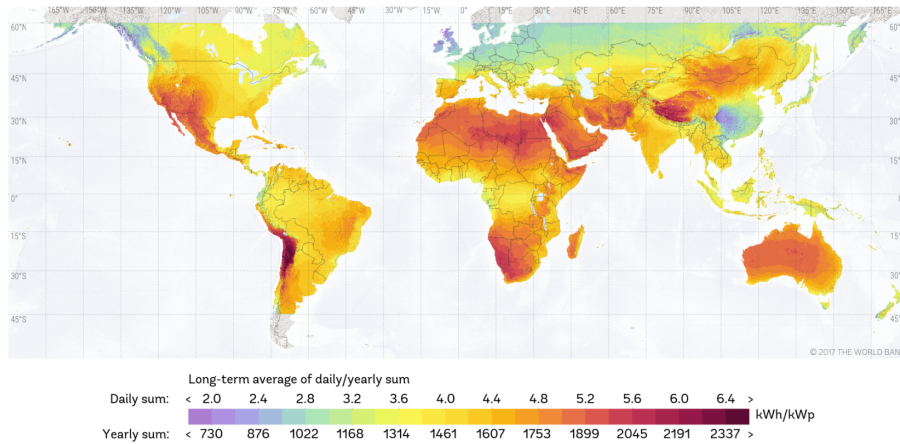


Figure 2.3: Global PV Power Potential [9]

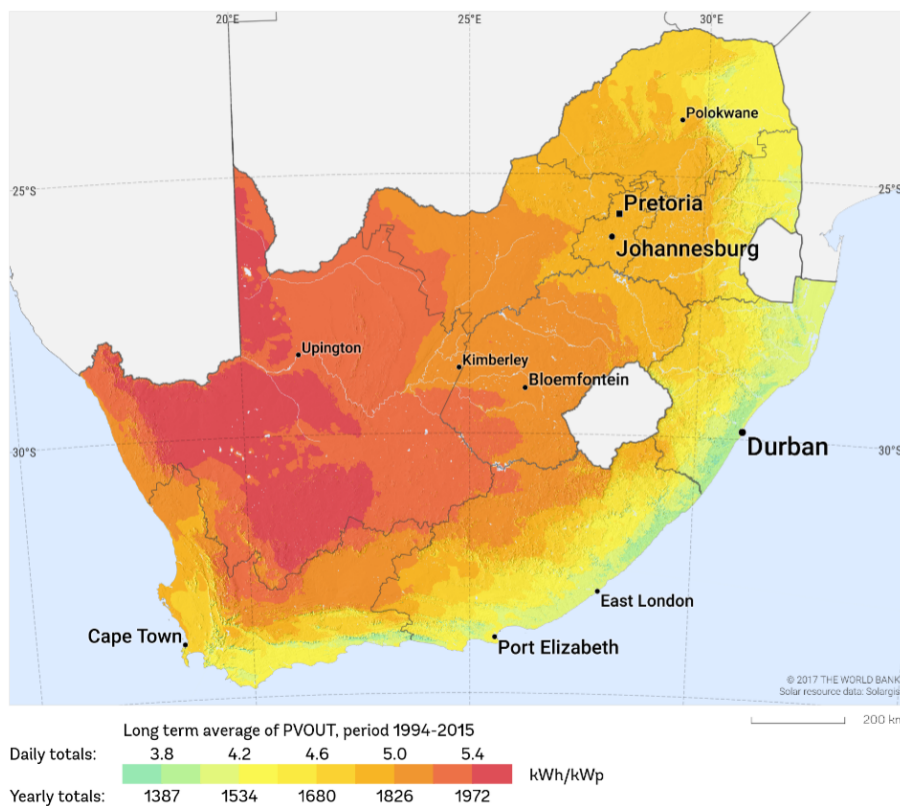


Figure 2.4: South Africa PV Power Potential [9]

In 2017, CCT claimed on its website that it aims to source 10% of its electricity by means of renewable energy sources by 2020, indicating that rooftop PV systems penetration is expected to increase within this municipality [10]. In a report released in July 2015 by the Centre for Renewable and Sustainable Energy Studies (CRSES) at Stellenbosch University [11], it is indicated that there was, at the time, 10,2 MW of registered distributed PV installations connected in the Western Cape Province (this excludes off-grid installations and utility-scale plants as part of the REIPPPP). Currently, CCT claims to have more than 24 MVA of registered solar PV systems [12], which clearly indicates the rapid growth in PV systems uptake over the last few years.

## 2.4 Distributed PV Generation in Cape Town

### 2.4.1 Overview

This section provides an overview of the current status of distributed PV generation in Cape Town, with focus on the current regulations in place in this regard in Cape Town.

### 2.4.2 Supply Utilities

Within the boundaries of CCT, 75% of electricity consumers are served by CCT, while Eskom supplies the remaining 25% [13]. A map of the boundaries for the electrical distribution licensees is shown in figure 2.5. Standalone PV systems (not grid-connected) are allowed within CCT and Eskom supply areas. Grid-tied PV systems are allowed in CCT supply areas (subject to approval), whereas, according to documentation dating to March 2016, grid-connected systems are prohibited in Eskom supply areas [14]. In a 2018 update of the same document, CCT state that an Eskom-supplied property owner in Cape Town must enquire with Eskom to determine if a proposed grid-connected PV system will be allowed [13]. Scholtz et. al [2] report in a 2017 World Wildlife Fund report that Eskom, in the lack of a national regulatory framework, currently considers grid-connection requests on a case-to-case basis, and only allow MV-connected customers the option to export excess PV generation to the network.



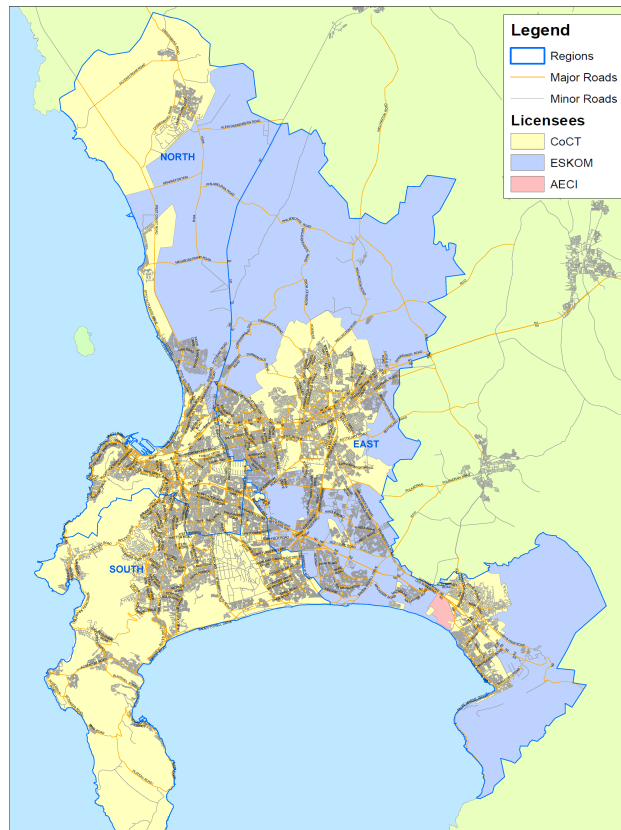


**Figure 2.5:** Electricity Distribution Licensee Area Boundaries Map[15]

### 2.4.3 SSEG

Although electrical installations are subject to wiring standards in South Africa, there is no national standard dedicated to PV installations [13]. In the lack thereof, CCT has aligned with the NRS 097-2-3 specification, along with other standards and regulations, in establishing a framework which provides a legal process whereby a PV system may be grid-connected. In this regard, CCT has published a document titled *Requirements for small-scale embedded generation: Application process to become a small-scale embedded generator in the City of Cape Town* [16], which provides a comprehensive guideline regarding the grid-connection of DG in Cape Town.

Small-scale embedded generation (SSEG) refers to an embedded generator with a capacity of under 1 MVA. In the context of PV, this capacity refers to the maximum output of the system's inverter. Embedded generation refers to a generation system that is connected on the customer side of the electricity meter, hence it is embedded in the electrical network. The generated electricity is primarily for the customer's own use, but during periods of excess generation, the customer's system can feed power into the utility electrical network. Furthermore, SSEG is classified by CCT according to two different customer types, one being residential, and the other being commercial/industrial. Written consent must be obtained from the Director of the Electricity Services Department before connection to a CCT network will be allowed. The aforementioned document, which details the application process to be followed to grid-connect SSEG, does not apply to DG systems larger than 1 MVA. Grid-connection of a DG system larger than 1 MVA, requires a personal meeting with CCT in order to establish the process to be followed and the requirements to be satisfied. Furthermore, a National Energy Regulator of South Africa (NERSA) generating licence will

need to be obtained. [16]

#### 2.4.4 Requirements and Restrictions for SSEG in Cape Town

As part of the application process for grid-connection of SSEG, a PV system must comply with all of the following standards and regulations [16]:

- Electricity Regulation Act, Act 4 of 2006,
- Electricity Regulation Amendment Act, Act 28 of 2007,
- CCT Electricity Supply By-Law,
- SANS 10142- Parts 1 to 4: The Wiring of Premises,
- SANS 474/ NRS 057 Code of Practice for Electricity Metering,
- NRS 048: Electricity Supply - Quality of Supply,
- NRS 097-1: Code of Practice for the interconnection of embedded generation to electricity distribution networks: Part 1 MV and HV,
- NRS 097-2: Grid interconnection of embedded generation: Part 2 Small-scale embedded generation,
- South African Distribution Code, -Grid code, -Renewable Power Plants Grid Code,
- Occupational Health and Safety Act, No. 85 of 1993.

If a grid-connected PV system does not comply with the above standards and regulations, it cannot be commissioned and grid-connected to a CCT network. It must be noted that SSEG that is connected to the network through a reverse power flow blocking relay, is still considered to be grid-connected and must comply with the same standards and regulations as SSEG with reverse power flow capability. Furthermore, two additional conditions apply before approval may be granted. The first condition is that the SSEG owner must be a net consumer, which means that the SSEG owner must purchase more electricity over a continuous 12-month period from CCT than they feed back into the network. The SSEG owner can therefore not be a net generator. The second condition is that the electricity that the SSEG system generates, must be for own use, and cannot be sold to a third party. The SSEG installation may also only be on the property where the electricity is used. If an SSEG system is decommissioned, CCT must be formally notified. [16]

#### 2.4.5 Metering and Tariffs for SSEG in Cape Town

Metering changes need to be made when an SSEG system is grid-connected to a CCT network. If an SSEG system with reverse power flow capability is installed, the customer's electricity meter needs to be changed accordingly. The customer's meter has to be changed to a bi-directional credit meter, capable of measuring energy flow in both directions, regardless of whether the customer previously had a conventional credit- or prepayment meter installed. If an SSEG with reverse power blocking is installed, the customer is required to make use of a prepayment meter, provided that they draw a current of less than 100 A. If the customer's system has reverse power blocking, but they draw a current of more than 100 A, a bi-directional credit meter has to be installed. Conventional prepayment- and credit meters are not allowed to run backwards. [16]

In CCT, different customers are placed on different electricity consumption tariffs, based on the criteria that the customer satisfies. Customers are classified according to criteria such as the type of customer (residential or commercial/industrial), the amount of power and energy they use, the time of power usage, as well as the voltage level at which they are supplied. A daily service charge, for network operation costs, may also apply to non-residential customers. [17]

The tariff structure changes when a customer connects SSEG with reverse power flow capability to the network. All SSEG customers, including residential, are subject to a daily service charge. Under certain scenarios, the electricity consumption tariff may also change for some customers, and all customers are placed on a feed-in tariff, whereby they are compensated for electricity that they export to the network. [17]

## 2.5 PV System Topologies

### 2.5.1 Overview

Distributed PV systems can be categorised as either being an off-grid system, or a grid-connected system. As the name suggests, an off-grid system functions independent of the network, while a grid-connected system is connected to the utility electrical network. Furthermore, an off-grid system can either operate in conjunction with a battery storage system, or can be a standalone system with no storage capability. A grid-connected system can be classified according to whether or not the system allows for reverse power flow. This section discusses the different PV system topologies. [13, 18]

### 2.5.2 Off-grid PV Systems

#### 2.5.2.1 Off-grid PV System With Battery Storage

An off-grid PV system with battery storage is shown in figure 2.6. The solar panels (1) convert sunlight into direct current (DC) electricity. The generated DC electricity charges a battery bank (4). A charge controller (2) controls the battery charging process. An inverter (5) is used to convert the DC electricity of the battery bank into alternating current (AC) electricity so that the electricity may be utilised. The PV system has its own distribution board (3), as well as its own electrical circuitry (6) that is independent of the conventional electrical network. The conventional utility electrical network (7) can still be connected to the existing conventional electricity meter (8) and the conventional distribution board (9) will operate as usual. [13]

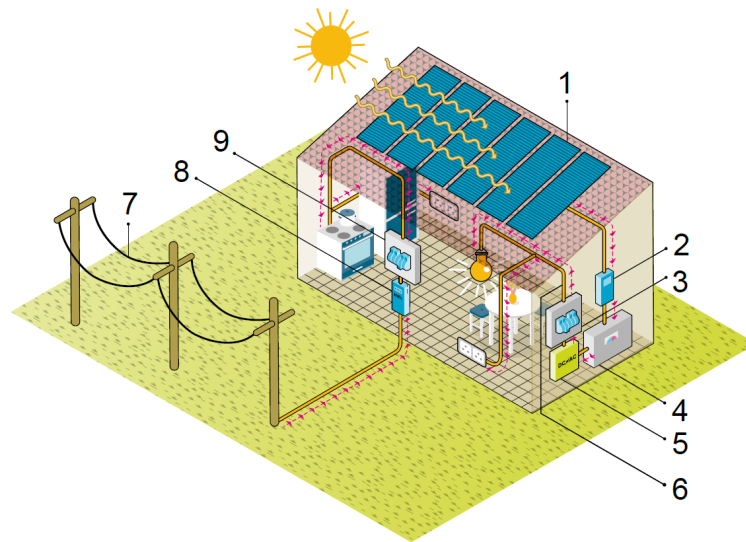


**Figure 2.6:** Off-grid PV System with Battery Storage (adapted from [13])

### 2.5.2.2 Off-grid PV System Without Battery Storage

An off-grid PV system without battery storage operates in the same way as an off-grid solar PV system with battery storage, with the difference being the absence of a battery bank and a charge controller. If no storage is available, electricity must be utilised as it is generated and electrical energy cannot be stored for later use.

## 2.5.3 Grid-connected PV Systems

### 2.5.3.1 Grid-connected PV System With Reverse Power Flow Capability

A grid-connected PV system with reverse power flow capability is shown in figure 2.7. The solar panels (1) convert sunlight into DC electricity. An inverter (3) converts the generated DC electricity into AC electricity, which feeds the existing distribution board (2). A bi-directional electricity meter (4) should be installed between the distribution board and utility electrical network. This type of system can export electricity (5) to the utility electrical grid when the PV system generates more electricity than what is being consumed by the building load. The utility may then credit the customer for the generated electricity. When the building uses more electricity than what is being generated by the PV system, such as during peak consumption, or at night, the customer can import electricity (6) from the utility electrical network (7). A hybrid grid-connected system can also be installed, which includes battery storage. [13]

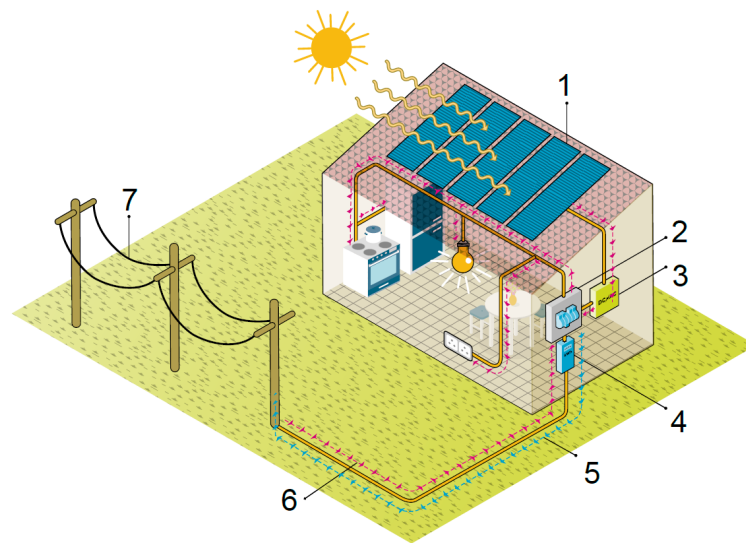


**Figure 2.7:** Grid-connected PV System With Reverse Power Flow Capability (adapted from [13])

### 2.5.3.2 Grid-connected PV System With Reverse Power Blocking

A grid-connected PV system with reverse power blocking is shown in figure 2.8. The solar panels (1) convert sunlight into DC electricity. An inverter (3) converts the generated DC electricity into AC electricity, which feeds the existing distribution board (2). No excess power can be exported from the distribution board to the utility network. A bi-directional- or prepayment electricity meter (4) should be installed between the distribution board and utility electrical network. When the building uses more electricity than what is being generated by the solar PV system, such as during peak consumption, or at night, the customer can import electricity (5) from the utility electrical network (6). [13]

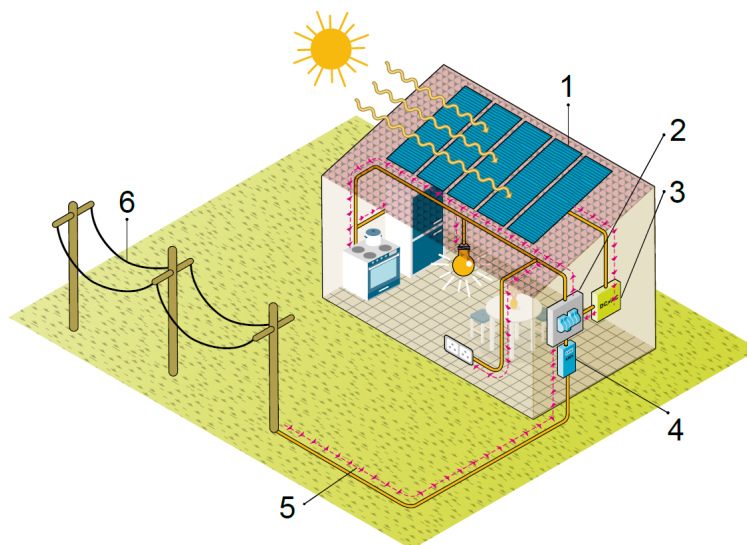


**Figure 2.8:** Grid-connected PV System with Reverse Power Blocking (adapted from [13])

## 2.6 Grid Connection of PV Systems

A more detailed version of a grid-connected PV system with reverse power flow capability is shown in figure 2.9, where all the typical physical components of a single-inverter grid-

connected residential PV system is shown. PV panels can be connected in series or parallel, and use a combination of the two configurations. The configuration varies across different applications. In the figure shown, series strings of solar PV panels carry DC electricity through DC cabling to a DC combiner box, where all the strings are electrically connected. The DC combiner box typically includes blocking diodes, a fuse for each string, and a lightning surge arrester. The combined DC electricity is then carried to an array disconnect switch, which can electrically isolate the PV panels from the system. From the array disconnect switch, DC electricity is carried to the power conditioning unit, which typically includes a maximum power point tracker (MPPT) and an inverter. [18]

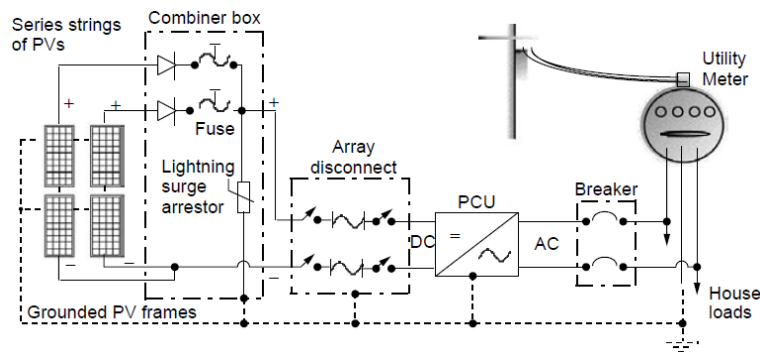


**Figure 2.9:** Grid-connected PV System Components [18]

The MPPT is a control unit designed to keep the PV panels operating at the optimum point on their I-V curves, so that maximum power output from each panel is maintained during operation. The main function of the inverter is to convert DC electricity to AC electricity. Furthermore, a grid-tie inverter has to perform additional functions. The inverter must monitor the network voltage, phase and frequency so as to ensure that the PV system is electrically synchronised with the utility electrical network. The inverter must also instantly disconnect from the utility electrical network when there is an outage on the utility electrical network. When the PV system malfunctions, the inverter should also instantly disconnect from the utility electrical network. The AC output of the inverter is connected to the distribution board through AC circuit breakers. A bi-directional electricity meter is connected between the distribution board and the utility electrical network. [18]

Many different configurations for PV systems exist. In addition to the arrangement of the panels in series and parallel, different inverter configurations also exist. In the above example, the system is using a single, centralised inverter. Instead of using a centralised inverter for the entire system, each string or panel can be fitted with its own string- or micro-inverter. The onus lies with the system designer to decide on an appropriate system layout.

# Chapter 3

## Electrical Power Systems

### 3.1 Introduction

A discussion of power systems design and -operation is appropriate, in order to comprehend and analyse the effects that rooftop PV systems will have on conventional electrical distribution networks. This chapter first provides an overview of conventional electrical power systems. A brief history of power systems is presented, followed by a discussion of the different components that constitute a conventional power system. Thereafter, conventional distribution systems are considered in more detail, with a review of distribution network parameters, -topologies and -equipment. Finally, active power systems, with integrated DG, are considered, with an overview of the technical effects of DG on electrical distribution networks. An overview of the NRS specifications applicable to distribution system operation in South Africa is provided alongside the discussion on the technical effects of DG on electrical distribution networks.

### 3.2 History of Power Systems

Electrical power systems have been present for over a century and have developed over the years by means of several discoveries and inventions. Current power systems are primarily three-phase AC systems, although high voltage direct current (HVDC) systems are also used for transmission in some applications. In the early days of electrical power systems, a battle existed between AC and DC systems. AC has proven to be the more attractive option for bulk generation, -transmission and distribution of electricity. However, both AC and DC play a crucial role in modern power systems, and conversion between AC and DC constitutes a significant field of power systems engineering. Table 3.1 provides some major historical milestones that contributed to the development of electrical power systems.

**Table 3.1:** Major Power Systems Milestones [18, 19, 20]

Year	Milestone
1820	Relationship between electricity and magnetism confirmed by H.C. Oersted
1821	First electric motor by M. Faraday
1831	Principles of electromagnetic induction by M. Faraday
1882	First electric streetlights in Africa installed in Kimberley
1882	Pearl Street Station opened by Edison
1883	Transformer invented by L. Gaulard and J. Gibbs
1888	Induction motor and polyphase AC systems by N. Tesla
1890	First single-phase AC transmission system in USA
1891	First three-phase AC transmission system in Germany
1893	First three-phase AC transmission system in USA

### 3.3 Power System Components

Generation, transmission and distribution are the three major components of a power system. Conventional power plants convert fossil fuels into electric energy. Step-up transformers at power plant substations are used to increase the voltage, so that power may be transmitted at high voltages in order to reduce transmission line losses. From power plant substations, the transmission system transports bulk power at high voltage (HV), until it reaches transmission substations. At transmission substations, the voltages are reduced but still kept at HV. Power is then transmitted to load centres via the subtransmission system. At distribution substations, which are supplied by the subtransmission system, the voltage is reduced to medium voltage (MV). The MV distribution system supplies MV/LV transformers, which step down the voltage to its final customer utilisation low voltage (LV) level. Light industrial customers may be directly supplied by the MV distribution system, while heavy industrial loads may be supplied directly via the subtransmission system.

In South Africa, Eskom is the electricity utility that is responsible for national bulk generation and -transmission of electricity [21]. In areas where distribution is not done by local municipalities, Eskom also acts as distributor. In this project, voltage levels are defined in a South African context and shown in Table 3.2. Table 3.3 shows typical Eskom operating voltages of the different power system components.

**Table 3.2:** Voltage Level Classification [16, 21]

Voltage Classification	Voltage Level
LV	$V \leq 1 \text{ kV}$
MV	$1 \text{ kV} < V \leq 33 \text{ kV}$
HV	$V > 33 \text{ kV}$



**Table 3.3:** Typical Eskom Operating Voltages [21, 22]

Power System Component	Voltage Level
Generation	22 kV
Transmission	275 kV, 400 kV, 765 kV
Subtransmission	132 kV
MV Distribution	11 kV, 22 kV, 33 kV
LV Distribution	400/230 V

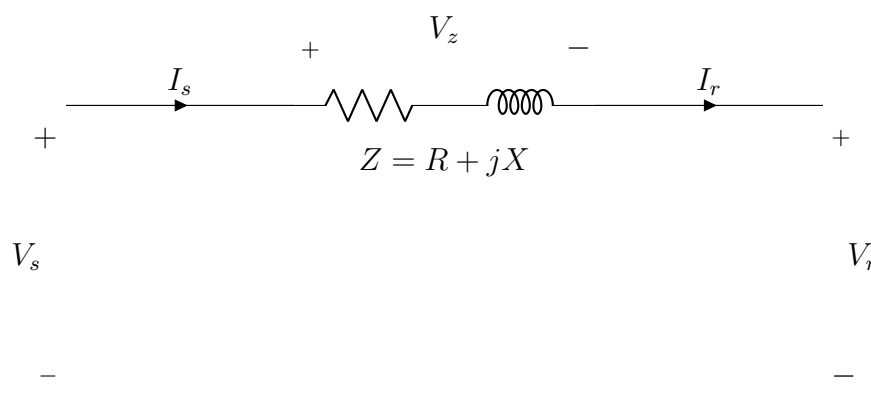
## 3.4 Electrical Distribution Systems

### 3.4.1 Overview

Distribution is the third and final major component of a power system. Distribution networks are supplied by the subtransmission network, and run from distribution substations to electrical loads of customers. Distribution networks can furthermore be divided into MV distribution- and LV distribution systems. This section discusses distribution line parameters, MV- and LV distribution, as well as important distribution system equipment. It is important to keep in mind that the discussion in section 3.4 on electrical distribution systems, relates to conventional electrical distributions systems, without integrated DG. In section 3.5, the discussion will shift focus towards active power systems, with integrated DG. It is also important to keep in mind that although the fundamentals of power systems are universally applicable, the operation, control and topologies of power systems may differ across countries or utilities. As an example, parameters such as voltage operating levels and transformer sizing may differ across sources. Where applicable, reference will be made to typical parameters as used by CCT and Eskom.

### 3.4.2 Distribution Line Parameters

Distribution lines can either be overhead lines, as is typical in rural areas, or underground cables, as is typical in urban areas. Transmission lines that are shorter than 80 km are known as short transmission lines. A distribution line can therefore be modelled with the same parameters as a short transmission line, where shunt admittance is neglected [19]. Only the series impedance of the line is included. A distribution line, with series impedance, and no integrated DG, is shown in figure 3.1, where  $V_s$  represents the sending-end voltage and  $V_r$  represents the receiving-end voltage.

**Figure 3.1:** Distribution Line

The impedance of the line,  $Z$ , is represented by equation (3.1):

$$Z = R + jX \quad (3.1)$$

where

$Z$  = Series impedance ( $\Omega$ )

$R$  = Series resistance ( $\Omega$ )

$X$  = Series reactance ( $\Omega$ )

The flow of electric current in the distribution line will cause a series voltage drop,  $V_z$ , where the voltage drop is represented by equation (3.2):

$$\begin{aligned} V_z &= V_s - V_r \\ &= I_s \cdot Z \end{aligned} \quad (3.2)$$

Substituting equation 3.1 into equation 3.2, yields equation (3.3):

$$V_z = I_s \cdot (R + jX) \quad (3.3)$$

The complex power supplied by the sending end,  $S_s$ , is given by equation (3.4)

$$S_s = V_s \cdot I_s^* \quad (3.4)$$

Rearrangement of equation (3.4) yields the line current,  $I_s (= I_r)$ , as given by equation (3.5):

$$\begin{aligned} I_s^* &= \frac{S_s}{V_s} \\ &= \frac{P + jQ}{V_s} \\ I_s &= \left( \frac{P + jQ}{V_s} \right)^* \\ &= \frac{P - jQ}{V_s} \end{aligned} \quad (3.5)$$

Substituting equation (3.5) into equation (3.3), yields equation (3.6):

$$\begin{aligned} V_z &= \left( \frac{P - jQ}{V_s} \right) \cdot (R + jX) \\ &= \frac{PR + QX}{V_s} + \frac{j(PX - QR)}{V_s} \end{aligned} \quad (3.6)$$

Due to a small difference between the sending- and receiving end voltage angle [23], equation 3.6 can then be simplified to equation (3.7):

$$V_z = \frac{PR + QX}{V_s} \quad (3.7)$$

The receiving-end voltage can then be represented by equation (3.8):

$$\begin{aligned} V_r &= V_s - V_z \\ &= V_s - \frac{PR + QX}{V_s} \end{aligned} \quad (3.8)$$

Distribution networks typically have high  $R/X$  ratios [24], i.e. they are resistive networks. Furthermore, typically  $P \gg Q$  [24], hence  $PR \gg QX$ . The derived equations clearly show that the receiving end voltage will be lower than the sending end voltage.

The series impedance for power lines can also be expressed per unit length. The total line impedance is then obtained by multiplying the impedance per unit length with the line length. Total line impedance increases as a function of length, and therefore the series voltage drop along a distribution line will also increase as a function of line length. The voltage profile along a distribution line will vary according to the load profile. Under the condition of no-load, no current will flow in the line, resulting in no series voltage drop and a receiving-end voltage that will match the sending-end voltage. As the load increases, the line current will increase, and the series voltage drop will increase. During low-load conditions, the receiving-end voltage of a distribution line will be close to the sending-end voltage, but during high-load conditions, the voltage drop along the line can cause the receiving-end voltage to be considerably lower than the sending-end voltage. The voltage along a distribution line must always be kept within regulatory limits. The distribution system must be designed in such a way that the maximum and minimum allowed voltages are respected under any load condition.

The distribution system consists of distribution substations, as well as MV- and LV distribution systems. The distribution substations are supplied by HV subtransmission systems. Inside the distribution substation, transformers known as HV/MV transformers are used to lower the HV subtransmission voltages to MV distribution voltages. The MV distribution system is then used for local distribution, which can either be by means of overhead lines or underground cables. The MV distribution system supplies transformers, known as MV/LV transformers, which then step down the voltage further to LV distribution voltages. These MV/LV transformers can either be installed on poles, as for overhead lines, or on ground level plinths or in vaults for underground cables. The LV distribution system then supplies customers with either single-phase or three-phase power. [19]

South African urban distribution networks generally consist of 11 kV MV distribution systems supplying 400 V LV distribution systems via MV/LV distribution transformers [25]. In South Africa, three-phase, three-wire delta systems are the standard for MV distribution systems, while three-phase, four-wire Y-connected systems are the standard for LV distribution systems [21]. The MV distribution system includes three systems [19]:

1. MV radial systems,
2. MV loop systems,
3. MV network systems.

The LV distribution system includes four systems [19]:

1. Individual MV/LV transformer per customer system,
2. Common LV main system,
3. LV network system,
4. Spot network system.

The different MV- and LV distribution systems are discussed in subsequent sections.

### 3.4.3 MV Distribution

#### 3.4.3.1 MV Radial System

An MV radial system is shown in figure 3.2. MV radial systems are economical and have found widespread use. They are often used in areas with low load-density. Separate three-phase feeders branch from a distribution substation bus in a radial fashion, each supplying a different geographical area. Each three-phase feeder can be protected at the distribution substation or elsewhere on the feeder with a recloser (in the case of an overhead line), or a circuit breaker (for underground cables). Lateral lines branch out from the three-phase feeders. The laterals are connected through fuses, so that a fault on an individual lateral line may be cleared without interrupting the entire feeder. Each distribution feeder can also be divided into different sections by means of sectionalising fuses. When a part of the feeder is faulted, the fault on that part can be cleared without interrupting service to unfaulted sections upstream. Shunt capacitor banks may be installed along the feeder to improve power factor, reduce line losses and also reduce voltage drop. During emergency conditions, feeders can be connected to an adjacent feeder from a different distribution substation (only if the system has been designed as such for feeder redundancy) through a tie switch that is normally open. Unfaulted sections of the problematic feeder can then be temporarily supplied from an adjacent feeder. [19]

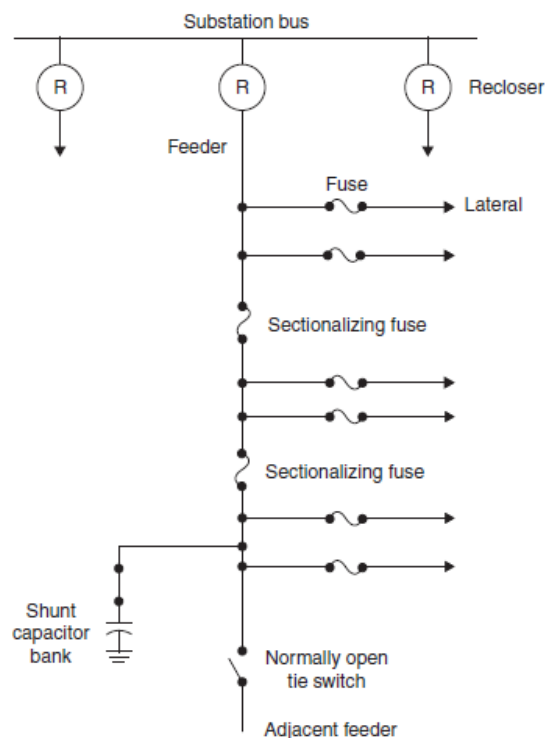
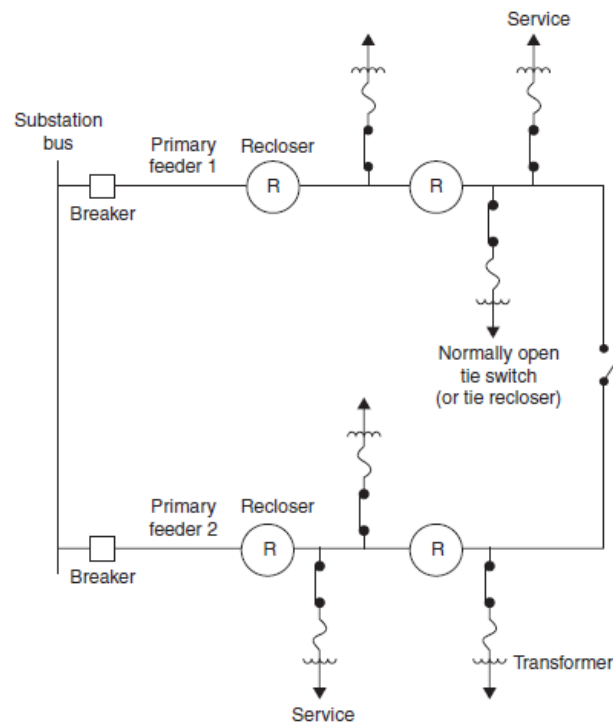


Figure 3.2: MV Radial System [19]

#### 3.4.3.2 MV Loop System

An overhead MV loop system is shown in figure 3.3. An underground MV loop system has a similar topology, with the absence of reclosers. The primary loop system is used in areas where high reliability is a priority. Different feeders, which originate from the same substation bus, loop around a load area. There is a tie switch between the different feeders, which may be open under normal operating conditions if the network is operated radially,

but permanently closed in systems that permanently operate as a loop, in order to provide high service reliability. Each feeder supplies its own loads (if operated radially), but if need be, the tie switch can be closed so that the loads of a faulted feeder may be fed from the other feeder. In looped operation, the tie-point will be permanently closed. This system therefore provides a two-way feed from the substation. The individual feeder conductors are sized to carry the load of the entire loop. Conductors that branch off from the primary feeders are isolated by circuit breakers or fuses. This two-feeder loop with two-way feed, can be extended to a multi-feeder loop with multi-way feed. [19]



**Figure 3.3:** MV Loop System [19]

### 3.4.3.3 MV Network System

An MV network system is shown in figure 3.4. The MV network system provides higher reliability than the radial and loop systems, and will typically be found where high load densities are present, such as in city centres. Various substations feed several feeders which are interconnected in a mesh. These substations are compact unit substations that are smaller than conventional distribution substations. Circuit breakers at the substations, and fuses on the MV network, are used to clear network faults. [19]

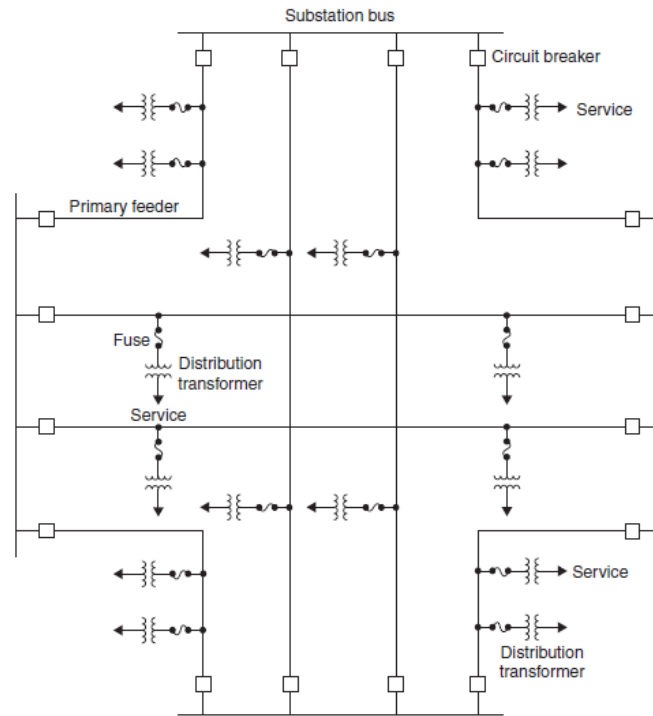


Figure 3.4: MV Network System [19]

### 3.4.4 LV Distribution

#### 3.4.4.1 Individual MV/LV Transformer Per Customer System

An individual MV/LV transformer per customer system is shown in figure 3.5. In this system, an MV feeder supplies an MV/LV transformer through protective equipment such as a fuse or circuit breaker. The MV/LV transformer supplies an individual customer on the LV distribution system. This type of system is applicable in rural areas, where customers are separated by long distances and long LV conductors would be impractical (due to losses and voltage drop). An individual MV/LV transformer per customer is also useful to supply a large individual load, such as a commercial building. [19]

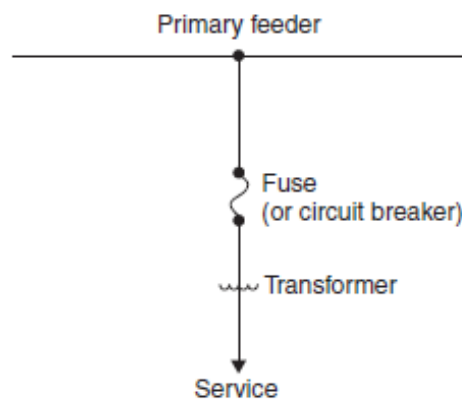


Figure 3.5: Individual MV/LV Transformer Per Customer System [19]

### 3.4.4.2 Common LV Main System

A common LV main system is shown in figure 3.6. In this system, an MV feeder supplies one or more MV/LV transformers through protective equipment such as fuses or circuit breakers. A shared common LV main is supplied by the MV/LV transformer(s). An individual MV/LV transformer therefore supplies several customers along the common LV main, as opposed to each customer having an individual MV/LV transformer. The common LV main may also be divided into different sections by means of an insulator or sectionalising fuse, or could be completely electrically isolated from adjacent LV mains - each LV section is then supplied by a different MV/LV transformer. [19]

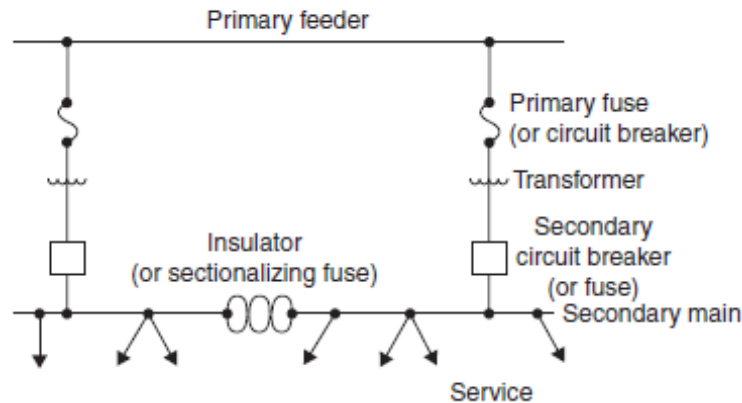


Figure 3.6: Common LV Main System [19]

### 3.4.4.3 LV Network System

An LV network system is shown in figure 3.7. In this system, two or more MV feeders supply an underground LV network through network transformers. Each network transformer is protected by a network protector circuit breaker. This system provides high service reliability and is used in areas where high load densities are present, such as in city centres. The outage of an MV feeder or a fault on the LV mains does not result in customer outages, since there are several MV feeders in parallel that supply the LV network, and the LV mains also operate in parallel to supply customer loads. When a line section is faulted, the customer will be supplied via a different parallel path. The system is designed in such a way that the load is distributed equally among all the network transformers. [19]

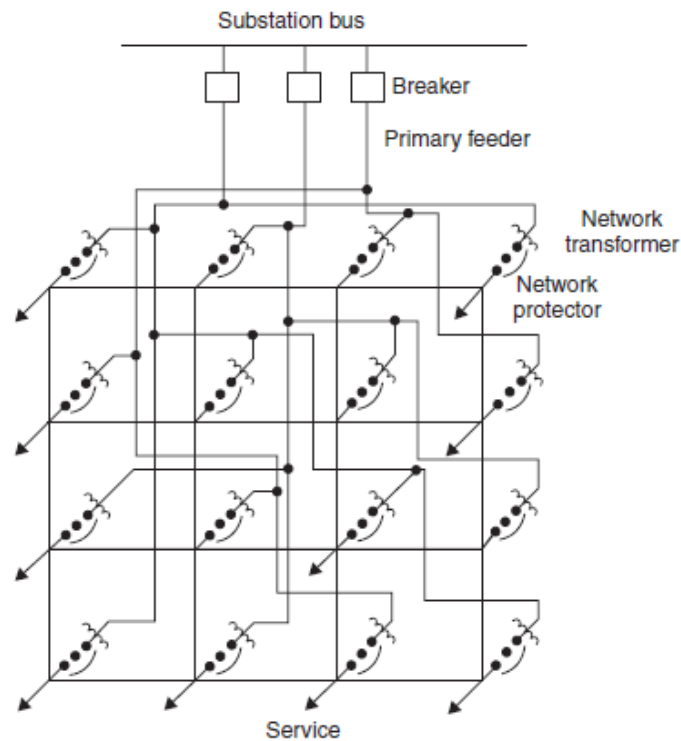


Figure 3.7: LV Network System [19]

#### 3.4.4.4 Spot Network System

A spot network system is shown in figure 3.8. In this system, an LV spot network bus is supplied via two or more MV feeders through network transformers. Each network transformer is also protected by a network protector circuit breaker. The spot network bus supplies an individual, concentrated load such as a commercial building. This system provides high service reliability, as the LV bus is continuously supplied via a number of different MV feeders. Outage of a primary feeder will therefore not result in customer interruption. The spot network bus is protected by cable limiters or fuses. [19]

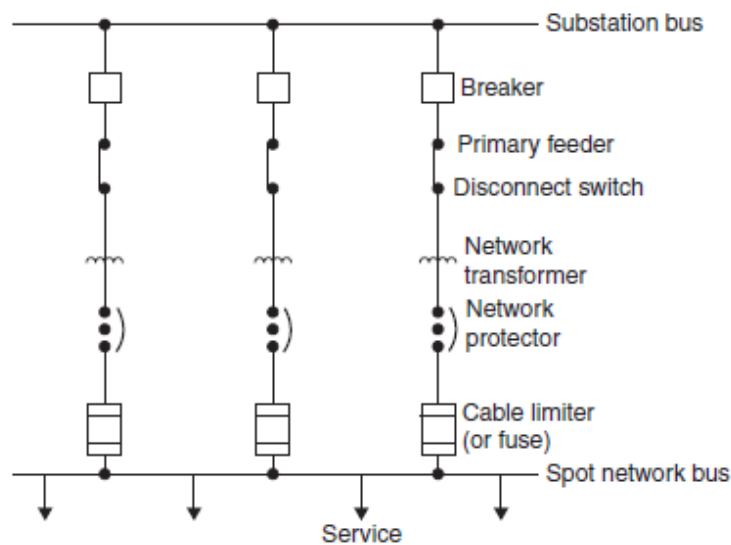


Figure 3.8: Spot Network System [19]



### 3.4.5 Distribution System Equipment

#### 3.4.5.1 Voltage Transformation

At distribution substations, HV subtransmission voltages are lowered to MV distribution voltages. This is done by means of HV/MV transformers. An example of an HV/MV transformer is shown in figure 3.9. HV/MV transformers have typical ratings in the 2.5-75 MVA range. CCT utilises 40 MVA- and 50 MVA HV/MV transformers in the two CCT networks in the case studies, as will be seen later. HV/MV transformers typically use mineral oil as insulator and coolant. Copper and core losses heat up the transformer, therefore additional cooling mechanisms such as oil circulating pumps and external radiators may also be used. The same transformer may have multiple ratings, such as a rating when the transformer is being operated with only passive cooling, or a different rating when active cooling methods such as oil circulating pumps or radiators with fans are applied. The transformer can be operated under a higher loading when active cooling methods are used, as opposed to only passive cooling. HV/MV transformers may sometimes be operated above their nameplate capacity. The allowable duration and extent of the overload depends on the transformer characteristics and the transformer loading under normal conditions. [19]



**Figure 3.9:** HV/MV Transformer [26]

MV/LV transformers are used to lower MV distribution voltages to LV distribution voltages. An example of an MV/LV transformer is shown in figure 3.10. MV/LV transformers can be single- or three-phase, with typical ratings in the 5-500 kVA (single-phase) range and 30-5000 kVA (three-phase) range. MV/LV transformers can either be installed on poles, on ground level plinths or in vaults. Large MV/LV transformers (300-2500 kVA range) known as network transformers (mentioned in subsection 3.4.4.3 and subsection 3.4.4.4) are used to supply LV network- and spot network systems. The CCT utilises 100-, 160-, 315-, 500-, 800-, 1000- and 1600 kVA MV/LV transformers in the two CCT networks in the case studies, and Eskom utilises 100-, 200-, 315-, 500- and 1000 kVA MV/LV transformers in the Eskom case study network, as will be seen later. MV/LV transformers can be liquid-filled or dry-type, with the latter being less durable than the former and not normally being loaded above nameplate capacity. [19]



Figure 3.10: MV/LV Transformer [27]

### 3.4.5.2 Voltage Regulation

As shown in subsection 3.4.2, there will be a series voltage drop along a distribution line when a line current flows. Loads are distributed along the distribution line, and will have a supply voltage that is dependent on its location relative to the distribution substation. The load at the end of the line will have the lowest supply voltage, due to the voltage drop across the entire length of the line (assuming no voltage compensation, DG, or Ferranti effect). It is important to keep voltages across the entire length of the line within specified maximum and minimum regulatory limits, under any load condition. Various voltage regulation devices are used to keep the voltage profile along a distribution line near constant under various load conditions. The most commonly used are transformer on load tap changers (OLTCs), voltage regulators, as well as shunt capacitors.

HV/MV transformers typically have OLTCs that automatically adjust voltage levels as needed. The primary or secondary windings have several taps, or tap positions, to which the primary- or secondary conductors can be electrically connected in order to adjust the turns ratio, and hence the voltage levels, of the transformer. Voltage regulators, which are basically automatically adjustable autotransformers, can also be used for voltage adjustment. Voltage regulators can be single- or three-phase and can be installed at distribution substations (typically where transformers with no OLTCs are present) or on distribution lines, as is typical with Eskom [28]. Distribution substation voltage regulators are shown in figure 3.11.



**Figure 3.11:** Distribution Substation Voltage Regulators [29]

Shunt capacitor banks are another way of improving voltage regulation on a distribution line. Shunt capacitors are primarily used on the MV distribution system. Shunt capacitors can help to improve the system power factor and reduce the total current flowing in the distribution line. A lower distribution line current reduces line losses and results in lower voltage drops along the line, which helps to improve voltage regulation. Shunt capacitor banks can either be fixed installations, which are permanently connected, or switched banks, which may be switched on during high-load conditions. A shunt capacitor bank is shown in figure 3.12.



**Figure 3.12:** Shunt Capacitor Bank [30]

### 3.4.5.3 Protection

Distribution systems are protected by reclosers, circuit breakers, sectionalisers and fuses. Reclosers and circuit breakers operate in conjunction with instrument transformers and overcurrent relays, which are used to trigger breakers under fault conditions. A recloser has the same function as that of a circuit breaker, with the additional functionality of being able to reclose itself after opening during a fault condition. Many faults on overhead distribution lines are temporary of nature. Reclosers close the circuit after a set time delay, and will remain closed if the temporary fault has been cleared. If the fault persists, the recloser will

open again. The recloser will repeat this open-close procedure for a set number of cycles before it will lockout, and permanently interrupt the faulted circuit. Devices known as sectionalisers are used in conjunction with reclosers. Sectionalisers operate in synchronism with reclosers, and use recloser open-close cycles to determine the location of a fault, so that the sectionaliser can isolate the faulted part of the distribution line. The upstream, unfaulted regions can be re-energised so that service interruptions are kept to a minimum. A pole-mount recloser is shown in figure 3.13. Fuses, devices that destruct when a specified fault current flows through it, can also be used to protect against overcurrent.

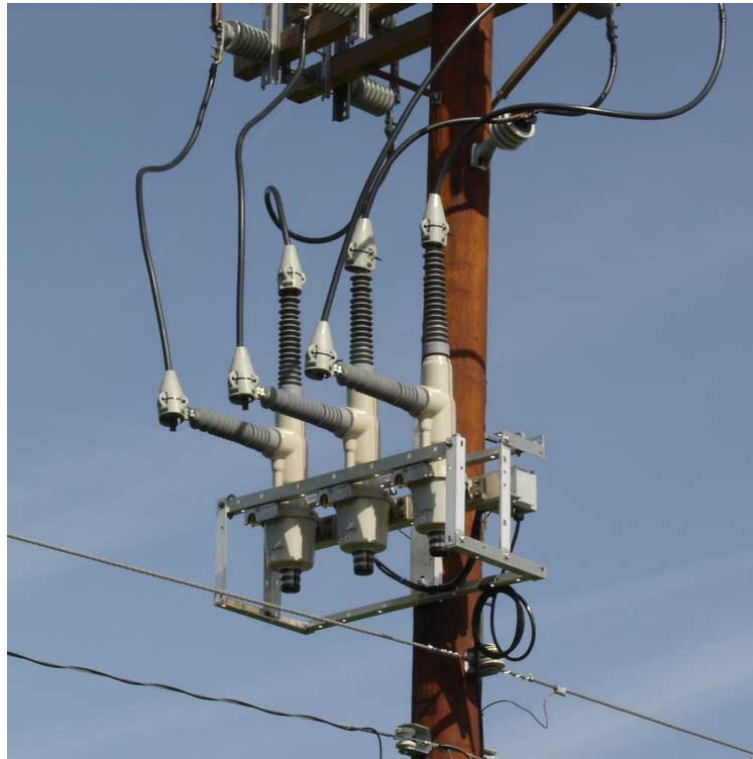


Figure 3.13: Pole-mount Recloser [31]

## 3.5 Technical Effects of DG on Electrical Distribution Networks

### 3.5.1 Overview

The technical performance of power systems is influenced by the introduction of DG, which may have beneficial or adverse technical effects on power systems, depending on a number of factors. This section focuses on the technical effects, both beneficial and adverse, brought about by the introduction of DG into power systems. As will be shown, many of the technical effects are linked, and occur as a consequence of another. Reverse power flow, equipment overload, system losses, voltage variations, as well as impacts on protection systems, -reactive power, -harmonics, -system frequency and -interconnected networks are discussed. Finally, a summary of the variables influencing the extent of the technical effects of DG, is provided.

### 3.5.2 Reverse Power Flow

Consider a single-line diagram (SLD) of a one-bus power system in figure 3.14. For simplicity, line parameters are omitted and the system is operating at unity power factor.

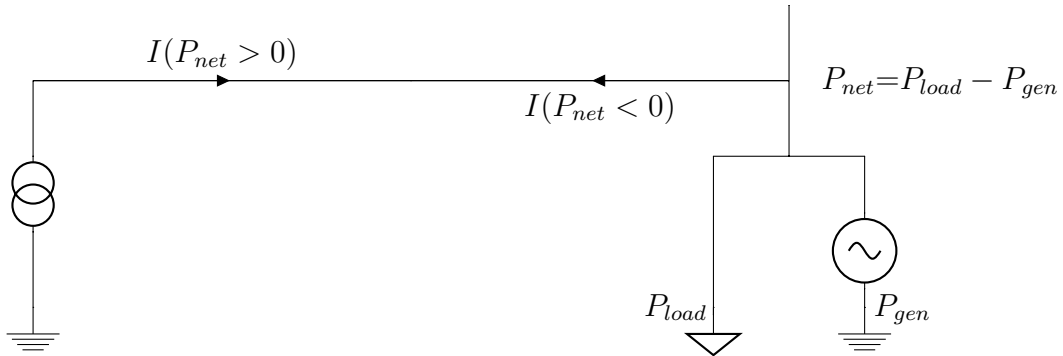


**Figure 3.14:** One-bus Power System with DG

Figure 3.14 can be used to explain the occurrence of power flow reversal in a power system with DG. The net load of the system,  $P_{net}$ , is given by equation (3.9):

$$P_{net} = P_{load} - P_{gen} \quad (3.9)$$

where  $P_{load}$  is the active power consumed by the load, and  $P_{gen}$  is the active power supplied by the DG. In a conventional power system,  $P_{gen} = 0$ , and hence  $P_{net} = P_L$ , a positive quantity, corresponding with unidirectional power flow from source to load. When the value of  $P_{gen}$  exceeds that of  $P_{load}$ , the resultant net load becomes negative, corresponding with reverse power flow. The load node effectively becomes the generator node in the power system, and power flows in the opposite direction of conventional design. In order to understand how reverse power flow will practically occur in a system, it is necessary to study the issue of generator-load mismatch. Consider figure 3.15, which shows generic daily load profiles of a residential, commercial and industrial network, along with a PV generation profile.

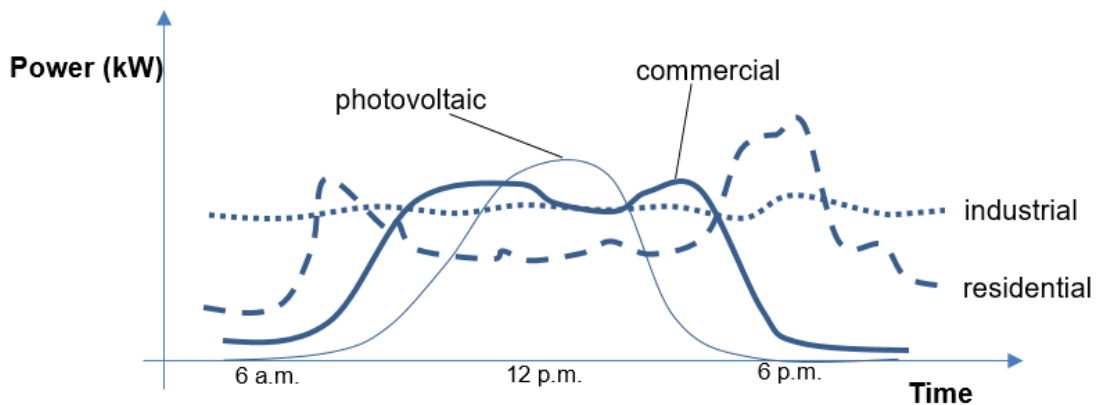


**Figure 3.15:** Generic Daily Load Profiles for Residential-, Commercial- and Industrial Networks [32]

The morning and evening peaks of the residential load profile can clearly be distinguished, as well as the occurrence of maximum PV generation with low residential load (compared to

evening- and morning peaks) around midday. The commercial load profile ramps up during daytime, corresponding to daytime commerce during work hours. The industrial load profile remains fairly constant throughout the day, as is typical in an industrial area with continuous manufacturing/processing. The mismatch between load and generation is seen to be most severe for residential networks, in terms of a sag in load coinciding with peak generation. This mismatch is typically most severe for sunny summer days around noon, when PV generators are at peak generation output. There tends to be much better correlation between load and DG in the case of commercial- and industrial networks.

During an investigation of the effects of PV installations on a residential network in Austin, Toliyat et al. [33] discovered issues of unbalance due to single-phase connected PV generators on a three-phase network. Although their work is focused on voltage unbalance (discussed in subsection 3.5.5), it provides a basis on which to understand the occurrence of unbalanced reverse power flow in three-phase systems with single-phase loads. This will typically be on LV residential distribution networks, where customers may be connected to individual phases. Mismatch between load and generation on one phase, will cause reverse power flow on that particular phase. Situations might arise when DG may cause reverse power flow in one phase, whilst a DG system in another phase might not, bringing about the occurrence of unbalanced reverse power flow. Several technical issues can be introduced by reverse power flow, and will be discussed in subsequent sections.

### 3.5.3 Equipment Overload

The issue of equipment overload is a direct consequence of reverse power flow, discussed in subsection 3.5.2. Excessive reverse power flow may lead to thermal overload of conductors and transformers. Carefully sized PV systems and constrained penetration levels can alleviate loading on substation equipment, transformers and conductors, prolonging the lifespan of the equipment. However, excessive reverse power flow will have the opposite effect.

Uçar et al. [34] investigated the effects of PV penetration on distribution transformer aging. In the study, it is shown that if PV is matched to not exceed local load, it can extend the lifetime of distribution transformers. The reason for this, is that if local PV production supplies load nodes, the transformer will see a decrease in downstream demand, i.e. the transformer will not have to supply all the load, prolonging the lifespan of the transformer. The converse, however, is also true. PV production that exceeds local load, will cause reverse power flow, and if significant enough, can overload the transformer and cause a reduction in lifespan. Watson et al. [35] studied the impacts of PV penetration on an LV network in New Zealand. It is shown that low levels of PV penetration can reduce thermal loading of conductors, but only up to a certain threshold, whereafter the number of overloaded conductors increase as reverse power flow begins to dominate with increased PV penetration.

### 3.5.4 System Losses

The issue of system losses is a direct consequence of reverse power flow, discussed in subsection 3.5.2. Consider equation (3.10), which gives the active power loss,  $P_{loss}$ , in a conductor:

$$P_{loss} = I^2 \cdot R \quad (3.10)$$

Equation (3.10) can be extended to equation (3.11), which gives the summated losses for all the conductors in a network:

$$P_{loss}(total) = \sum_{n=1}^k I_n^2 \cdot R_n \quad (3.11)$$

where

$n$  = branch  $n$  in the network

$k$  = total number of branches in the network

$I_n$  = current in branch  $n$

$R_n$  = resistance of branch  $n$

The power supplied by a distribution substation,  $P_{substation}$  has two components - the line losses, as well as the network loads, and is given by equation (3.12):

$$\begin{aligned} P_{substation} &= P_{loss}(total) + P_{loads}(total) \\ &= \sum_{n=1}^k I_n^2 \cdot R_n + \sum_{i=1}^j P_i \end{aligned} \quad (3.12)$$

where

$i$  = load  $i$  in the network

$j$  = total number of loads in the network

$P_i$  = active power of load  $i$

Analysis of equation (3.12) shows that the introduction of PV can reduce  $P_{loads}(total)$ , which results in a lower line current needed to supply loads, and consequently reduces line- and substation losses. Once again, the converse is also true. A scenario of net-generation by DG will result in reverse power flow, and if severe enough, can increase line- and substation losses beyond that which is normally seen under passive, load-only conditions. Méndez Quezada et al. [36] assessed the annual energy losses for different levels of DG penetration in a distribution network. Their study found that the introduction of low levels of DG initially decreases energy losses, up until a point is reached where losses are at a minimum. If DG penetration levels are further increased, losses increase again. In extreme cases, the losses in the network were five times higher than that observed with no DG installed.

### 3.5.5 Voltage Variations

In figure 3.1 in subsection 3.4.2, a diagram was presented for a distribution line operating under passive conditions, with no DG. In order to understand how voltage rise may occur in the presence of DG, it is necessary to adjust the diagram for active conditions. Figure 3.16 shows the adjusted diagram for a distribution line with DG. The nomenclature has been adjusted to cater for the introduction of DG. Where the passive model had a *sending end* and *receiving end* of the line, the active model has a *sending end* and *generation end*. The receiving side of the passive model, now has generation added to its terminals, and the voltage at the generator connection point is denoted as  $V_g$ . Note that the polarity of  $V_g$  is reversed, along with the direction of  $I_g$ . This corresponds to a power flow reversal.

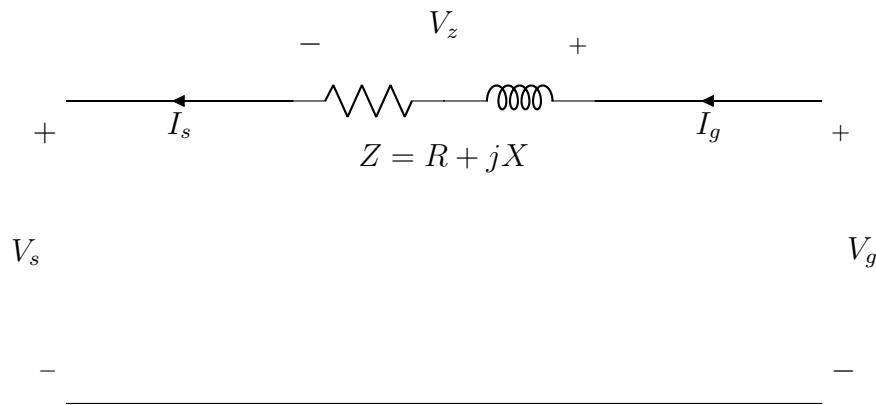


**Figure 3.16:** Distribution Line with Distributed Generation

The impedance of the line,  $Z$ , is represented by equation (3.13):

$$Z = R + jX \quad (3.13)$$

where

$Z$  = series impedance ( $\Omega$ )

$R$  = series resistance ( $\Omega$ )

$X$  = series reactance ( $\Omega$ )

The flow of electric current in the distribution line will cause a series voltage drop,  $V_z$ , where the voltage drop is represented by equation (3.14):

$$\begin{aligned} V_z &= V_g - V_s \\ &= I_g \cdot Z \end{aligned} \quad (3.14)$$

Substituting equation (3.13) into equation (3.14), yields equation (3.15):

$$V_z = I_g \cdot (R + jX) \quad (3.15)$$

The complex power supplied by the generation end,  $S_g$ , is given by equation (3.16)

$$S_g = V_g \cdot I_g^* \quad (3.16)$$

Rearrangement of equation (3.16) yields the line current,  $I_g (= I_s)$ , as given by equation (3.17):

$$\begin{aligned} I_g^* &= \frac{S_g}{V_g} \\ &= \frac{P \pm jQ}{V_g} \\ I_s &= \left( \frac{P \pm jQ}{V_g} \right)^* = \frac{P \mp jQ}{V_g} \end{aligned} \quad (3.17)$$

Substituting equation (3.17) into equation (3.15), yields equation 3.18:



$$\begin{aligned}
V_z &= \left( \frac{P \mp jQ}{V_g} \right) \cdot (R + jX) \\
&= \frac{PR \pm QX}{V_g} + \frac{j(PX \pm QR)}{V_g}
\end{aligned} \tag{3.18}$$

Due to a small difference between the sending- and receiving end voltage angle [23], equation 3.18 can then be simplified to equation 3.19:

$$V_z = \frac{PR \pm QX}{V_g} \tag{3.19}$$

The generation-end voltage can then be represented by equation (3.20):

$$\begin{aligned}
V_g &= V_s + V_z \\
&= V_s + \frac{PR \pm QX}{V_g}
\end{aligned} \tag{3.20}$$

$Q$  can be either positive or negative, depending on whether the generator is supplying or absorbing reactive power. Analysis of equation (3.20) shows how voltage rise may occur in the presence of DG. Since distribution networks typically have high  $R/X$  ratios [24], i.e. they are resistive networks, along with the fact that typically  $P \gg Q$  [24], it is apparent that  $PR \gg QX$ , therefore the second term in equation (3.20) will be positive. This clearly shows the voltage rise at the generating end of the distribution line. Inter-node potential differences may be established between nodes in the network, result to directional changes of current flows. Currents may flow both downstream and upstream in the same network, depending on DG location and size. In this regard, Aziz & Ketjoy [37] state that the voltage rise associated with PV installations on LV networks is highly influenced by the location and concentration of PV installations along a feeder. DG may improve the voltage along a feeder, acting as a voltage regulator, but only under conditions of adequate sizing and location.

Masters [24] suggest the following methods to combat voltage rise associated with DG penetration on MV networks:

- Lower the substation voltage,
- Allow DG to contribute to volt-ampere reactive (VAR) control,
- Employ line voltage regulators,
- Increase conductor sizes,
- Curtail DG under low-load conditions.

Nye [38] investigated methods to increase DG penetration when uptake is constrained by voltage regulation. OLTC setpoint reduction, VAR control and implementation of EVRs (electronic voltage regulators) were some of the proposed methods that could successfully be implemented to achieve this objective.

Voltage regulation for passive feeders was discussed in subsection 3.4.5.2. The idea of employing voltage regulators in an active network, as suggested by Masters[24] and Nye [38], brings another potential adverse effect of DG to light. Voltage regulation devices such as capacitor banks, line voltage regulators, and OLTCs, which boost voltage in passive power

systems, can raise overvoltages that occur due to DG penetration, even higher. Voltage regulation equipment, designed for unidirectional power flow, operate in such a way as to keep downstream voltages within regulatory limits, up to the end of the feeder. The placement of DG downstream of a voltage regulator, could interfere with the conventional operation of voltage regulation equipment and confuse the regulators, resulting in difficulty of voltage control [39]. DG can also cause increased operation of voltage regulation equipment such as OLTCs, resulting in equipment wearing. The coordination and control of conventional voltage regulation equipment therefore needs to be revised in the presence of DG.

Another voltage issue associated with DG penetration, is voltage unbalance. This is typical on an LV network with single-phase customers. Yang et al. [40] state that it is not an uncommon scenario to observe overvoltage in only one of the three phases in an LV system, since single-phase PV systems and existing unbalanced loads contribute to voltage imbalance on the network. Habijan et al. [41] investigated unbalance in LV networks with DG, and found scenarios where reverse power flow occurred in some phases, but not the others, i.e. the one phase is a net generator, whilst the others are net consumers. This results in a scenario where the phase with the dominant net production has the highest voltage, while the lowest voltage occurs on the phase with the dominant net load. In order to facilitate increased PV penetration levels in three-phase LV networks, it becomes a requirement to apply load- and DG balancing techniques to the network.

Cloud transients can also introduce voltage variation issues in a network with integrated PV. This results in a rapid decrease in output power from PV systems, which could result in voltage fluctuations, voltage flicker and voltage instability [39, 42, 43]. A condition could arise where PV systems are operating at full power, when a cloud transient abruptly changes PV output power. As a consequence, the utility instantaneously has to supply the network loads via the substation when PV generation falls away. Fluctuation in PV output power causes fluctuating demands from the utility side. This can cause problems with voltage control on MV networks, due to the inability of the transmission system to instantaneously react to this rapid demand increase [37].

The NRS voltage specifications applicable to distribution system operation in South Africa, is shown in table 3.4.

**Table 3.4:** NRS 048-2 Voltage Specifications [44]

<b>Voltage Level</b>	<b>Compatibility Level</b>	<b>Maximum Deviation Limit</b>
< 500	± 10%	± 15%
≥ 500	± 5%	± 10%

The compatibility level assessment for voltage is done with the lowest and highest 10-minute root mean square (RMS) value, which is not exceeded for 95% of the time (95th percentile), and the maximum deviation limit assessment is done with the lowest and highest 10-minute RMS value, for an assessment period that shall last at least one week. The voltage unbalance compatibility level for three-phase LV, MV and HV networks is 2%, whereas 3% applies in the case of single-phase networks. [44]

### 3.5.6 Protection Systems

The introduction of DG can influence the normal operation of network protection systems. DG can interfere with conventional operation of protection schemes, and adversely affects conventional protection systems coordination. Devices such as circuit breakers, reclosers and fuses are used for overcurrent protection in distribution networks. The protection system will typically be configured to have main protection (which operates first to isolate the fault), and backup protection, which operates in the case of main protection failure [45]. Under fault conditions, protective relays must clear the faults so as to isolate only the faulted section of the network. A downstream fault must be isolated by the main protection for that faulted feeder section, and not result in tripping of an upstream network section by an upstream protective relay (this should only happen in the event of primary protection failure) [46].

Under increased DG penetration, fault current magnitude could increase, since DG will contribute to the fault current. An increased fault current can lead to equipment damage, and necessitate upgrades to higher-rated protection equipment. The direction of fault currents could also reverse. Furthermore, DG may lead to nuisance tripping of protection equipment. [48]

Protection relays are coordinated with particular methods in order to correctly distinguish the appropriate relay that must open a breaker for a particular fault. As an example, relays can be configured by time settings in order to first open the breaker closest to the fault, or they can be configured by knowing in advance what the fault current at particular sections of the network will be [47]. Without considering the intricate details of protection systems schemes, it can be seen how DG may disturb and desensitise conventional protection relay operation, possibly leading to undetected faults or delayed breaker tripping. Furthermore, if DG units do not disconnect fast enough during network faults, they can interfere with the auto-reclosing sequence of reclosers. Another issue is the possible occurrence of unintentional islanding, a condition whereby DG energises a network section that is supposed to be de-energised due to the occurrence of a fault, posing risk to utility workers. [46]

### 3.5.7 Reactive Power

In a conventional, passive power system, the utility fulfills the active and reactive power needs of the network and its associated loads. Consider the scenario of a high penetration of PV installations on a network, operating at unity power factor. This presents a typical scenario, where a PV installer is required by regulations to operate the PV system at unity power factor. As a local example, in South Africa NERSA stipulates through version 2.9 (July 2016) of the Grid Connection Code for Renewable Power Plants (RPPs) [49] that LV-connected DG with capacities  $\leq 100$  kVA, should operate at unity power factor. Another reason for choosing to operate a system at unity power factor, apart from being required to do so, is that a PV installer often does not have any incentive to provide reactive power support to the network as an ancillary service [50].

The connection of DG to a network does not alter the requirements of loads on the network - loads will still operate according to conventional active and reactive power requirements. The PV systems will supply active power to the loads, but the reactive power requirements of loads will still need to be fulfilled by the utility. From a network perspective, a reduction in active power requirements, accompanied by unchanged reactive power requirements, results in a poorer network operating power factor. A common way to perform power-factor correction is by means of shunt capacitors. However, PV inverters can be configured to pro-

vide reactive power support to the network, and hence improve the network operating power factor [51]. Peng et al. [50] investigated load power factor correction by means of inverter VAR control, using different control techniques. Their work shows that local VAR control on inverters can successfully be used to restore network operating power factor. While investigating the power factor in a distribution network with integrated PV, Ciric & Markovic [52] also noticed the trend of decreasing power factor under increasing PV penetration.

### 3.5.8 Harmonics

PV systems are connected to the network via grid-tie inverters. Inverter power electronics have the potential to add harmonics to the grid, adversely affecting the Quality of Supply (QoS). Harmonics injected into the network via inverters may significantly increase harmonic distortion levels, especially if a large number of inverters are installed on the network [53]. When inverters from the same manufacturer are connected to the same network, the like-order harmonics add [54].

The presence of harmonics may, in turn, introduce a variety network issues such as [55]:

- Voltage- and current sinusoid distortion,
- Skin effect heating of transformer windings and conductors,
- Overheating of equipment,
- High neutral currents heating neutral conductors,
- Power factor reduction,
- Malfunctioning protection relays,
- Communication circuit interference.

Chidurala et al. [56] investigated the harmonic impact of PV-inverters on unbalanced distribution networks, and found that current- and voltage total harmonic distortion (THD) increases under conditions of increasing PV penetration. Furthermore, their work noted a significant increase in harmonic currents at the distribution transformer, leading to overloading and heating. Lewis [54] studied PV integration on distribution networks in a region in Australia, and found that PV system integration in the studied areas caused increased levels of current harmonic distortion on the networks. Lewis also suggests that inverter harmonics are adding, and goes on to predict that higher PV penetration levels will introduce higher harmonic values. Poosri & Charoenlarnopparut [57] investigated the harmonic impacts of PV on a residential LV network in Thailand. In the study, increased PV penetration leads to increased THD of bus voltages on the network, and it is shown that the voltage THD exceeds regulatory limits when the installed PV capacity on the networks exceeds 60% of the MV/LV transformer rated capacity.

The NRS harmonics specifications applicable to distribution system operation in South Africa, is shown in table 3.5. In addition to the requirements stipulated in table 3.5, it is also required that the supply voltage THD of all harmonics up to order 40, may not exceed 8 % [44].

**Table 3.5:** NRS 048-2 Harmonics Specifications [44]

Odd Harmonics				Even Harmonics	
Multiples of 3		Not Multiples of 3			
Order (n)	Magnitude (%)	Order (n)	Magnitude (%)	Order (n)	Magnitude (%)
3	5	5	6	2	2
9	1.5	7	5	4	1
15	0.5	11	3.5	6	0.5
21	0.3	13	3	8	0.5
$21 \leq n \leq 45$	0.2	$17 \leq n \leq 49$	$(2.27*(17/n))$ -0.27	$10 \leq n \leq 50$	$(0.25*(10/n))$ +0.25

### 3.5.9 System Frequency

The advent of high penetration levels of DG into distribution systems could bring about frequency stability issues. The balance between load and generation is important for the maintenance of system frequency. With increased PV generation, imbalance between load and generation can become a control issue. Load-generation imbalance can lead to changes in the network frequency [58]. Pourmousavi et al. [59] studied the frequency impacts of high PV penetration on a distribution feeder. It was found that high PV penetration levels caused the system frequency to be in violation of regulatory limits. The effects of PV systems on system frequency was also found to be more detrimental for concentrated PV, as opposed to PV distributed over a wider area, for the same high penetration level.

The displacement of centralised generation (with large synchronous generators) through increased PV penetration levels, will reduce system inertia, and the Rate of Change of Frequency (RoCoF) following a contingency event will increase. [60]

Yan et al. [61] studied the effects of a high penetration of wind and PV renewable generation on the frequency response of a network resembling the South Australia network. Due to the high penetration of DG, there is a concern that after a contingency, the system will experience difficulty with frequency regulation, which could result in more severe frequency deviations. This could cause PV generators to trip, due to many of the PV systems in South Australia having a default protection setting that disconnects the PV generator under conditions of under-frequency. Their study shows that low inertia and secondary PV tripping can adversely affect frequency regulation and system stability.

The NRS frequency specifications applicable to distribution system operation in South Africa, is shown in table 3.6.

**Table 3.6:** NRS 048-2 Frequency Specifications [44]

Network Type	Compatibility Level	Maximum Deviation Limit
Grid	$\pm 2\%$ ( $\pm 1$ Hz)	$\pm 2,5\%$ ( $\pm 1,25$ Hz)
Island	$\pm 2,5\%$ ( $\pm 1,25$ Hz)	$\pm 5\%$ ( $\pm 2,5$ Hz)

### 3.5.10 Interconnected Networks

Several technical effects of DG on distribution networks have been introduced. In practical distribution networks, the LV systems are interconnected to MV systems, which are in turn interconnected to HV systems. When determining allowable PV penetration levels for a practical network, the interconnected network also needs to be considered as a whole.

As an example, a scenario can be considered where an MV feeder supplies several LV networks (a typical practical scenario). DG may be interconnected on each LV network, and each LV network may be studied independently to determine allowable DG hosting capacity. In practice, however, the LV networks are also interconnected to each other via the MV feeder. This means that mutual interaction between LV networks, via the MV network, can take place. As an example, reverse power may flow from one LV network to an adjacent LV network via the MV network. Effects such as voltage rise and reverse power flow may propagate through networks and lead to problems on upstream networks. The cumulative effect of downstream DG penetration on upstream networks needs to be a focus point in future work. This includes interaction between different voltage-level networks in distribution networks, as well as the interaction between the distribution- and transmission networks in the power system.

### 3.5.11 Summary

The review of other worldwide PV penetration- and DG integration studies provides the necessary understanding of the technical effects of DG on distribution networks. The extent to which these technical issues may occur, are dependent on a number of variables:

1. The size of an individual DG system [62],
2. The location of DG on the network [62],
3. The cumulative capacity of DG systems on the network [37],
4. The electrical characteristics of the network [63],
5. The topology of the network [64],
6. The power factor of DG [62].

The review did not attempt to focus on the quantification of acceptable PV penetration limits. The reason for this is that the results of acceptable PV penetration levels differ vastly across sources. Different authors follow different calculation methodologies, provide different quantitative definitions of PV penetration, and use different reference points in networks with which to quantify PV penetration. Attempting to quantify acceptable PV penetration levels from existing studies, is meaningless if there is not a consistent base of comparison. In the lack of proper national legislation with regards to grid-connected PV installations in South Africa, CCT has aligned with the NRS 097-2-3 specification in determining allowable PV penetration limits. The NRS 097-2-3 maximum individual generation limits on shared LV feeders is shown in table 3.7.

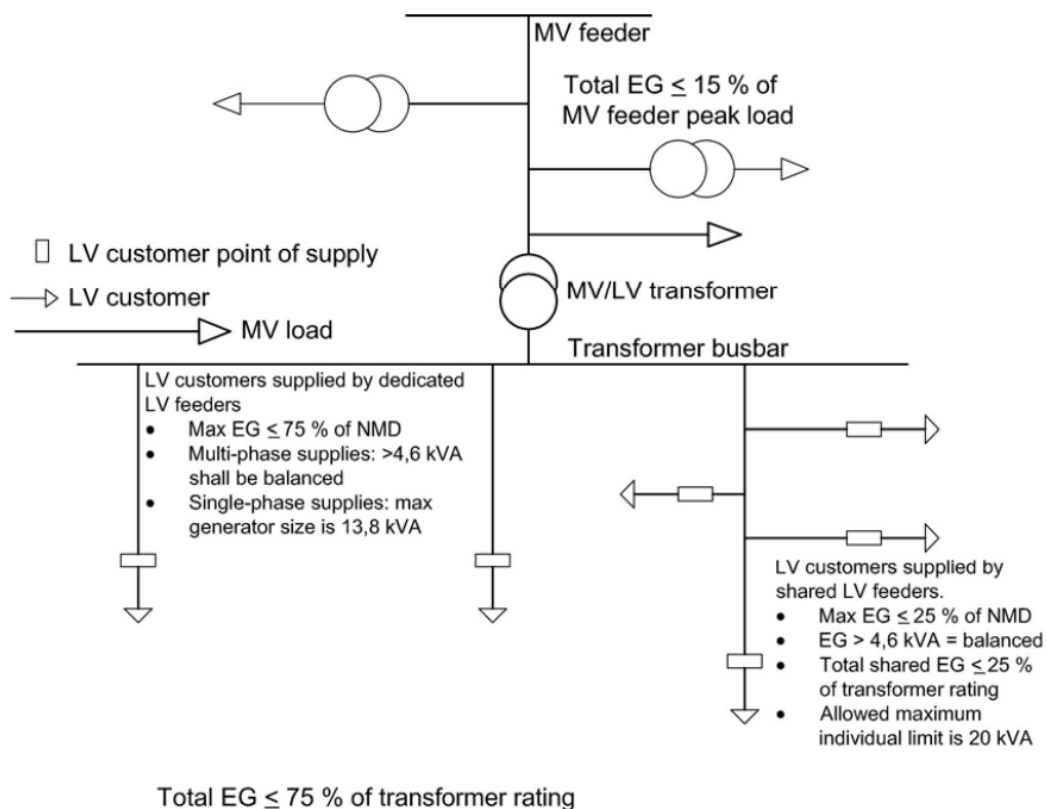
**Table 3.7:** Individual Generation Limits for Shared LV Feeders [65]

Total Phases	Circuit-breaker Size	NMD (kVA)	Generation Limit (kVA)
1	20 A	4,6	1,2
1	60 A	13,8	3,68
1	80 A	18,4	4,6
3	60 A & 80 A	41,4	13,8

In addition to table 3.7, the following requirements are also stipulated by NRS 097-2-3 [65]:

- In shared- and dedicated LV feeders, any generators that exceed 4.6 kVA should be balanced across phases.
- If a customer's supply in a shared LV feeder exceeds the values in table 3.7, the maximum generation will be capped to 25% of the customer's notified maximum demand (NMD), and if this value exceeds 20 kVA, a maximum generation limit of 20 kVA will apply.
- Generation on a dedicated LV feeder is limited to 75% of the customer NMD.
- Generation on shared LV feeders should be limited to 25% of the MV/LV transformer rating.
- The total combined generation on shared- and dedicated LV feeders should be limited to 75% of the MV/LV transformer rating.
- The total generation on an MV feeder should be limited to 15% of the peak load of the feeder.

A summary of all the NRS 097-2-3 PV penetration specifications is provided in figure 3.17:

**Figure 3.17:** Summary of NRS 097-2-3 PV Penetration Specifications [65]

In a study of harmonic issues associated with PV penetration, Dartawan et al. [66] points out that the maximum allowable PV penetration is significantly influenced by the regulatory standards adopted by the utility. This is an important issue that extends beyond the scope of harmonics. The uptake of PV (or any DG) may be significantly limited by operational limits adopted by the utility. As a closing remark, it is pointed out that the revision of standards (previously developed for passive networks) is appropriate in the presence of active networks with DG, in order not to impose possibly unnecessary restrictions to the uptake of DG.



# Chapter 4

## Modelling and Simulation Methodology

### 4.1 Introduction

This chapter serves to provide information on the modelling- and simulation methodology that is followed to model the power supply from rooftop PV systems and to investigate voltage rise and equipment overload due to distributed PV generation on electrical distribution networks. This chapter first provides an overview of the residential-, commercial- and industrial distribution networks that are being investigated. This is followed by a discussion on the modelling methodology, which provides insight into the way in which the topology, load and generation of the networks are modelled. Finally, the simulation methodology is discussed, providing insight into the way in which the technical effects of distributed PV generation are simulated, as well as how PV penetration limits are determined via simulation. All network- and software models are developed using Digsilent Powerfactory power systems simulation software. It must be noted that for all three distribution networks, due to confidentiality, pseudonyms are used for all substation-, feeder-, transformer-, and node names.

### 4.2 Networks Overview

Three different distribution networks with different customer types are investigated - a residential-, a commercial-, and an industrial network. All three networks are located in Cape Town, South Africa. The networks were identified by CCT and Eskom as networks of interest, which could see high PV uptake in the future.

The residential network is owned and operated by CCT. It is located on the Atlantic Seaboard, southwest of Cape Town City Centre, and spans an area of about 0,5 km<sup>2</sup> [67]. It is an upmarket residential suburb, listed as one of the most expensive suburbs in South Africa [68]. The residential network area is shown in figure 4.1.



**Figure 4.1:** Residential Network Area [69]

The commercial network is also owned and operated by CCT. It is located northeast of Cape Town City Centre, and spans an area of about  $2,6 \text{ km}^2$  [67]. It is a mixed-use area, comprised of commercial activities in the form of office space and retail outlets, as well as residence and entertainment. A clear-cut commercial-only network section, highlighted in red in figure 4.2, is isolated in this area for commercial network study purposes.



**Figure 4.2:** Commercial Network Area [69]

The industrial network is owned and operated by Eskom. It is located northeast of Cape Town City Centre, in close proximity of the commercial network area, and spans an area of about  $3,3 \text{ km}^2$  [67]. It is an industrial area that hosts various industrial activities. A clear-cut network section, highlighted in red in figure 4.3, is isolated in this area for industrial

network study purposes.

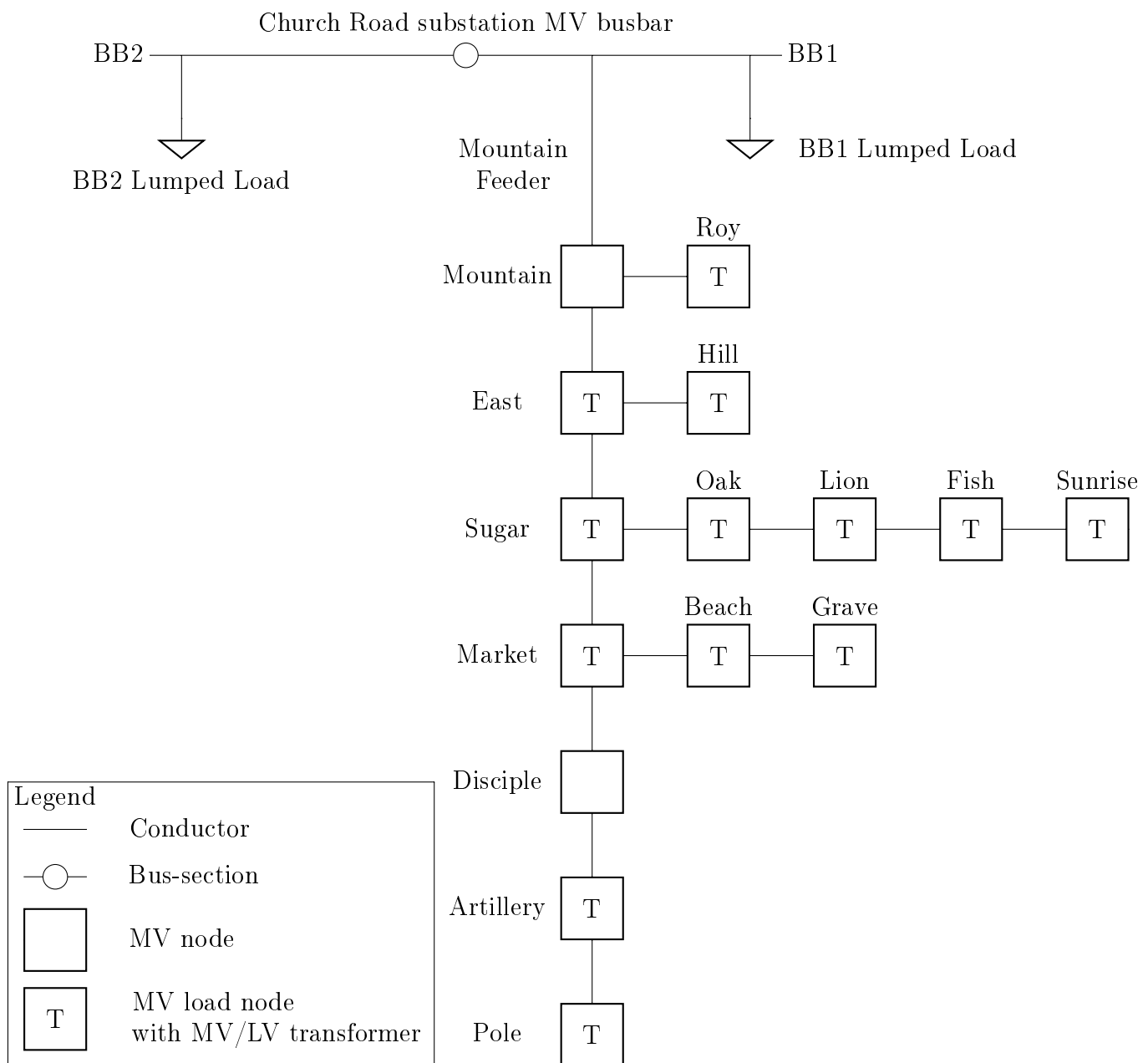


Figure 4.3: Industrial Network Area [69]

## 4.3 Modelling Methodology

### 4.3.1 Network Topology Modelling

The residential network is supplied via the nearby Church Road HV/MV distribution substation, where a 66 kV nominal HV system feeds an 11.66 kV nominal MV system. The HV network is modelled as an external grid (by its Thévenin equivalent), and connected to the substation MV busbars. The MV busbar at Church Road substation is divided into two bus-sections. Each bus-section is supplied via a 40 MVA 66/11.66 kV transformer. The greater area in which the residential network is located, is fed from the Mountain feeder, located on bus-section 1 of Church Road substation. Bus-section 1 supplies a total of 5 MV feeders and 1 local MV/LV transformer, and bus-section 2 supplies a total of 6 MV feeders and one local MV/LV transformer. Since only the Mountain feeder feeds the residential area, this is the only feeder that is graphically represented in the network model - the rest of the feeders are lumped together, and included in the model as lumped MV loads on bus-section 1, and bus-section 2, respectively. The complete downstream MV network that is fed via the Mountain feeder, is modelled graphically. The Mountain feeder topology is an MV radial system, as discussed in subsection 3.4.3.1. An SLD for the residential MV network is shown in figure 4.4. Information on the residential network MV cable composition, -MV cable characteristics, and -transformer ratings can be found in appendix A.1 - appendix A.3.



**Figure 4.4:** Residential MV Network SLD

GIS (Geographic Information System) software analysis of the MV network, via Arcgis, shows that many of the MV cables are segmented cables - they are made up of different conductors connected in series to form a composite feeder. The Mountain feeder supplies an MV network with 13 MV/LV transformers. Seven of the 13 MV/LV transformers that are supplied by the Mountain MV feeder, are located in the residential area (Sunrise, Fish, Lion, Oak, Market, Beach, Grave). The LV network is only graphically modelled in the residential area, since distributed PV generation is only connected within the residential area - for the 6 MV/LV transformers that are not in the residential area (Roy, East, Hill, Sugar, Artillery, Pole), the complete LV network of that particular MV/LV transformer is represented by a single LV load on the LV busbar of that transformer. More discussion on the load modelling will follow in subsection 4.3.2. The 7 transformers in the residential area each supply its own separate radial LV network. Each of the 7 LV networks is a common secondary main system, as discussed in subsection 3.4.4.2.

No official SLDs are available for the 7 LV networks. Information on the LV networks is particularly hard to source, since record keeping practices for LV networks are not in place. This is supported by Carter-Brown [25] who comments on South African LV distribution networks as being managed in a "fit-and-forget" manner, resulting in poor information and visibility on LV networks. Network information for the LV networks is sourced from hand-drawings and network information contained in GIS software. GIS information proves to provide the most useful and complete information for modelling purposes. The residential LV networks, derived from GIS information, is shown in figure 4.5, where the 7 LV networks are shown in different colours. The black lines are MV feeders that supply the LV networks. Note that cables are not shown according to scale, but rather as a direct link between nodes. Table 4.1 provides an overview of the 7 residential LV networks. SLDs, derived and compiled from GIS information, for each of the 7 residential LV networks are provided in figure A.2 to figure A.8 in appendix A.1. Information on the residential network LV cable composition and LV cable characteristics can be found in appendix A.1 - appendix A.2.

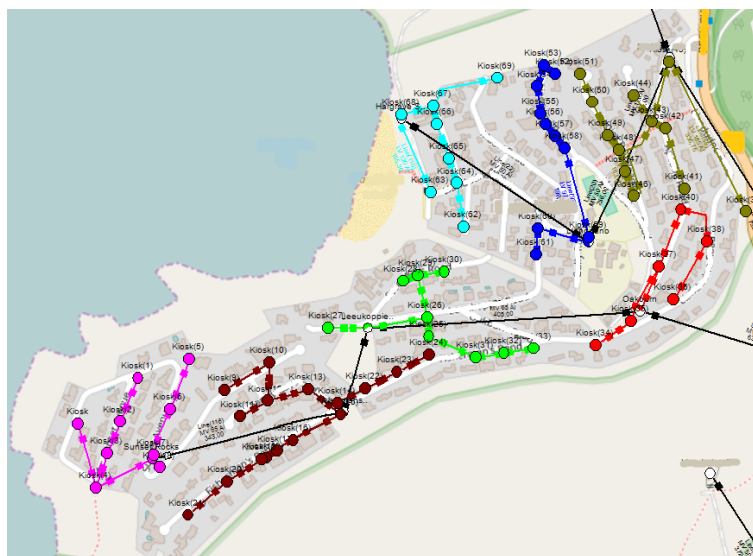


**Figure 4.5:** Residential LV Networks derived from [70]

**Table 4.1:** Residential LV Networks Overview

Colour	LV Network	Total Customers
Pink	Sunrise	36
Maroon	Fish	55
Green	Lion	45
Red	Oak	30
Gold	Market	46
Dark Blue	Beach	53
Light Blue	Grave	44

The 7 residential LV networks (Sunrise, Fish, Lion, Oak, Market, Beach, Grave) are each radially supplied via their own 11/0.4 kV MV/LV transformer, ranging in size from 315 kVA to 800 kVA. The LV networks are modelled up to the point of common coupling (PCC), i.e. the points on the network where more than one customer is connected. The common coupling point for customers on an LV network is either an LV distribution kiosk (DK) or an LV metering kiosk (MK). DKs and MKs operate independently, and a customer is supplied

by either a DK or an MK. DKs typically house 9 circuit breakers, while an MK typically houses 9 circuit breakers and 9 accompanying electromechanical meters. If a customer is supplied via a DK, the metering equipment will be located at the customer's premises, and not in the LV kiosk, as is the case with an MK [70]. DKs and MKs perform essentially the same function, acting as a common connection supply point for customers. For this reason, a DK and an MK are treated the same for simulation purposes, and both are referred to under the collective term of *LV kiosks*. The LV network modelling is done up to each LV kiosk. LV kiosks are placed at their exact geographical locations. Information is not available as to which properties are connected to which LV kiosks, so by doing the modelling geographically, it is easier to make reasonable assumptions as to which houses are connected to which LV kiosks. The LV kiosk is the first point in the network where PV generation aggregation occurs, so it is useful to model the system from this point in order to observe the influences of distributed PV generation on all parts of the LV networks.

Although three-phase, four-wire Y-connected systems are the standard for South African LV distribution systems [21], customers are predominantly connected as single-phase loads, as reported by Moodley et al. [71]. The LV networks are modelled as three-phase, four-wire Y-connected systems (corresponding to A-, B- and C-phase conductors and a neutral), with the LV customers modelled as single-phase customers. In addition to information not being available as to which properties are connected to which LV kiosks, no information is available as to the phase designation of the properties. In this regard, reasonable assumptions are made. Properties are manually assigned to a particular phase, with the objective of trying to balance the amount of customers across phases (as is done in practice). The phase allocation of properties is shown in table A.1 in appendix A.1. An example of the LV kiosks is shown in figure 4.6, where the kiosks are numbered and shown as black dots. The red, yellow and blue dots correspond to the A-, B- and C-phase designation of the different properties.



**Figure 4.6:** Example of Residential Network LV Kiosks

The commercial network is supplied via Metropolitan HV/MV distribution substation, where a 132 kV nominal HV system feeds an 11.66 kV nominal MV system. The HV network is modelled as an external grid (by its Thévenin equivalent), and connected to the substation MV busbars. The MV busbar at Metropolitan substation is divided into two bus-sections. Each bus-section is supplied via a 50 MVA 132/11.66 kV transformer. Bus-section 2 supplies the network section under study via three feeders (Office, Palace and Bird), all configured in a loop. The network configuration therefore corresponds to an MV loop system, as discussed in subsection 3.4.3.2. This three-feeder group topology is a standard MV topology, aimed at improving network reliability [70]. An SLD for the commercial MV network is shown in figure 4.7. Information on the commercial network MV cable composition, -MV cable characteristics, and -transformer ratings can be found in appendix B.1 - appendix B.3.

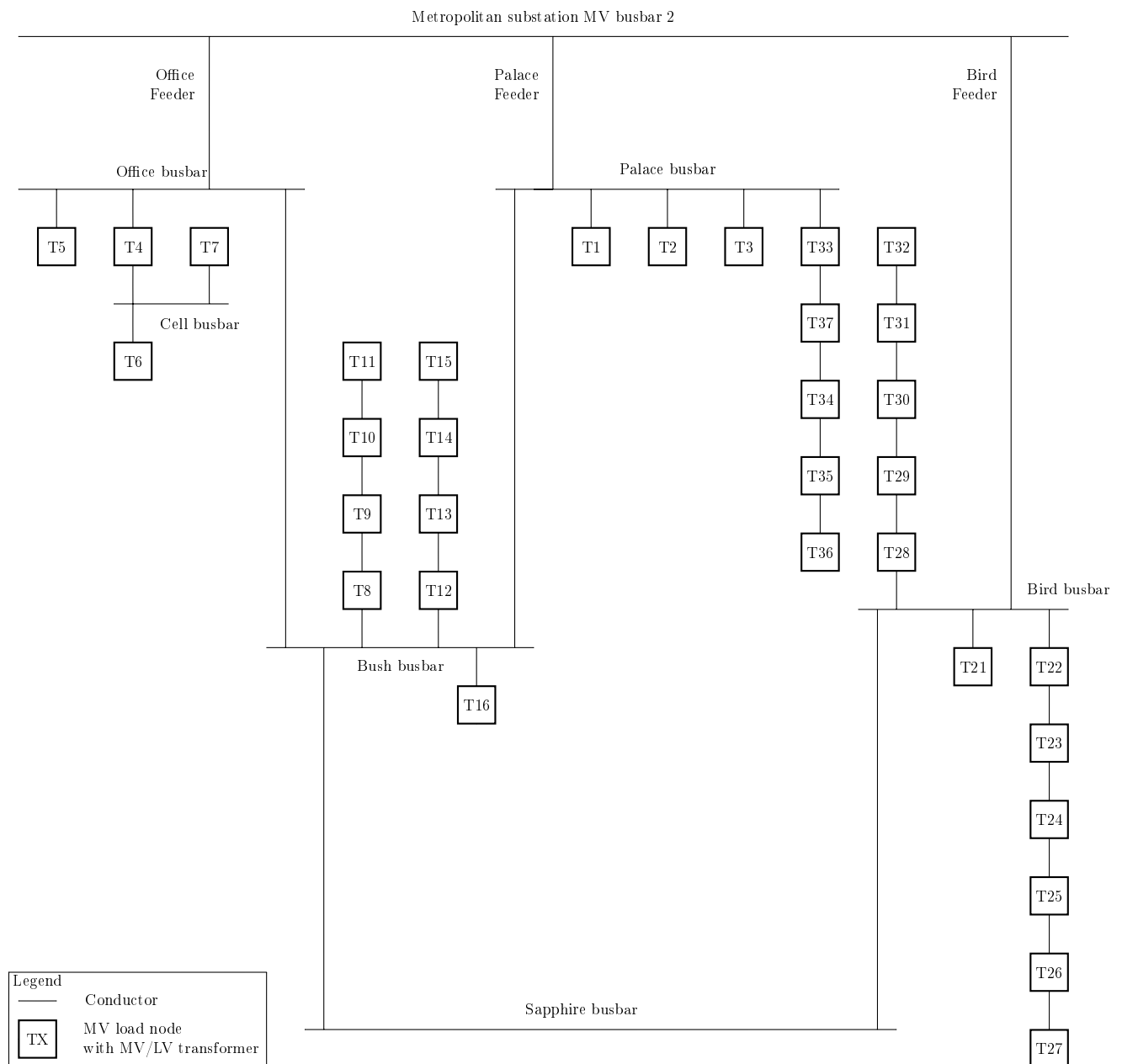


**Figure 4.7:** Commercial MV Network SLD

The three feeders (Office, Palace and Bird) supply a network with 33 MV/LV transformers. The 33 MV/LV transformers range in size from 315 kVA to 1.6 MVA. Some of the

MV/LV transformers are dedicated transformers, where a customer is supplied by their own MV/LV transformer. The individual MV/LV transformer per customer system is typically used where a large LV load is present, which is typical of a commercial network like this, where an office block may have its own transformer. Some of the transformers, are however, not dedicated transformers, but due to limited LV GIS data, only few can be identified[70]. For this reason, no LV networks are modelled, and all LV loads are directly connected to the LV busbars of the MV/LV transformers, corresponding to the LV system discussed in subsection 3.4.4.1. In a situation where more than one customer is connected to an MV/LV transformer, the loads are lumped together and presented as one LV load (the same holds true for PV generators). The MV network is, like in the residential area, modelled up to the PCCs. The PCCs are the LV busbars of the MV/LV transformers.

The industrial network is supplied via South HV/MV distribution substation, where a 66 kV nominal HV system feeds an 11 kV nominal MV system. The HV network is modelled as an external grid (by its Thévenin equivalent), and connected to the substation MV busbars. The MV network consists of a primary MV network that feeds secondary MV networks. The primary network is operated as an MV loop, as discussed in subsection 3.4.3.2. The primary MV network is interconnected under normal operating conditions. Two Eskom switching stations are supplied via the primary MV network. Switching station A is supplied from South substation via one primary MV feeder, whilst switching station B is supplied from South substation via a second primary MV feeder. Furthermore, there is an interconnected feed between the two switching stations, which creates the loop on the primary MV network. The secondary MV networks are then supplied from the primary switching stations, via radial secondary MV feeders. The secondary MV network therefore corresponds to an MV radial system, as discussed in subsection 3.4.3.1. There are normally open tie points on the secondary MV networks, which indicate that they are radially operated under normal operating conditions, but can also be operated as a loop. An SLD for the industrial MV network is shown in figure 4.8. Information on the industrial network MV cable composition, -MV cable characteristics, and -transformer ratings can be found in appendix C.1 - appendix C.3.



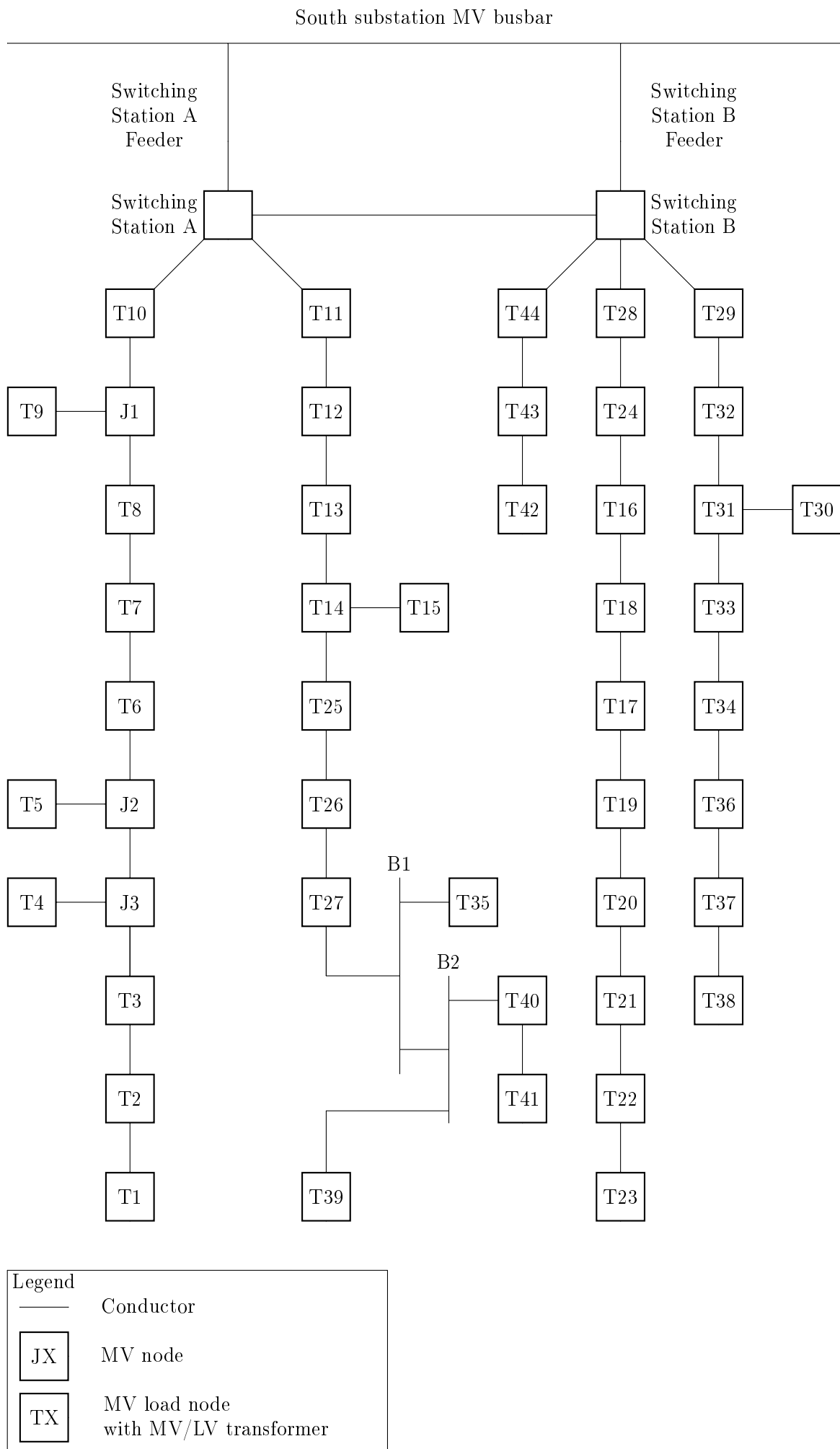


Figure 4.8: Industrial MV Network SLD

The industrial secondary MV networks supply a total of 44 load nodes, of which 40 are MV/LV transformers. The remaining 4 load nodes are customers with MV supply points. As in the commercial network, the PCCs are the LV busbars of the MV/LV transformers (or the MV supply point in the case of MV loads). No LV networks are modelled, and all LV loads are directly connected to the LV busbars of the MV/LV transformers, corresponding to the individual MV/LV transformer per customer LV system, as discussed in subsection 3.4.4.1. In a situation where more than one customer is connected to an MV/LV transformer, all customers are represented by one lumped LV load (the same holds true for PV generators).

A summary of the residential-, commercial- and industrial network characteristics is provided in table 4.2.

**Table 4.2:** Summary of Network Characteristics

Network	Nominal Voltage (kV)	Network Type	Transformer/ Supply Point Capacity (kVA)[70]
Sunrise LV	0.4	CLVMS*	500
Fish LV	0.4	CLVMS*	500
Lion LV	0.4	CLVMS*	500
Oak LV	0.4	CLVMS*	315
Market LV	0.4	CLVMS*	500
Beach LV	0.4	CLVMS*	800
Grave LV	0.4	CLVMS*	315
Residential MV	11.66	MV Radial	4950 (sum total)
Commercial MV	11.66	MV Loop	29 000 (sum total)
Industrial MV	11	MV Loop (primary) MV Radial (secondary)	24 880 (sum total)

\*Common LV Main

### 4.3.2 Network Load Modelling

The only measured load data for a distribution network that is typically available locally, is the load measured at the HV/MV distribution substation that supplies the area. The highest resolution in which this load data is typically available, is 30-minute intervals. Half-hourly average current measurements for the year 2016 (most recent full year at the commencement of the study) is available for the Church Road HV/MV substation feeders. The residential network is supplied from Church Road substation via the Mountain MV feeder, as discussed in subsection 4.3.1. No load data is available downstream in the network, and only the total load current of the Mountain MV feeder is available. Information on the load currents of individual MV/LV transformers, and information on individual property LV load currents, is therefore not available. This necessitates load-scaling techniques in order to represent downstream load currents.

As discussed in subsection 4.3.1, the residential network is situated in a greater geographical area that is solely supplied by the Mountain MV feeder. This greater geographical area has a total MV/LV transformer capacity of 4.95 MVA (13 transformers), of which 3.43 MVA (7 transformers - Sunrise, Fish, Lion, Oak, Market, Beach, Grave) are located within the residential area. The first load-scaling technique that is applied, is MV load-scaling. The load current of the Mountain MV feeder is divided amongst the 13 MV/LV transformers in

the area, according to the capacity ratings of these transformers. The 6 MV/LV transformers that are not in the residential area (Roy, East, Hill, Sugar, Artillery, Pole), will each carry a portion of the measured load current for the Mountain feeder, proportionate to the capacity rating of the MV/LV transformer. The combined residential area carries a load proportionate to the sum total of the capacity ratings of the 7 transformers (Sunrise, Fish, Lion, Oak, Market, Beach, Grave) - each of these 7 individual transformer does not carry a load proportional to its capacity rating - more load scaling techniques will soon follow. The scaling of the Mountain MV feeder load current according to the transformer ratings, is in accordance with an accepted technique that is applied in industry [70]. According to this MV load-scaling technique, the residential area will comprise roughly 70 % of the total load current that is supplied by the Mountain MV feeder.

For the 6 MV/LV transformers that are not in the residential area (Roy, East, Hill, Sugar, Artillery, Pole), the load current of that particular MV/LV transformer is converted to the LV side and a single LV load current is used to represent the entire LV network of that MV/LV transformer. The complete LV network is only graphically modelled in the residential area (Sunrise, Fish, Lion, Oak, Market, Beach, Grave), since distributed PV generation is only connected within this area. Within the residential area, a further LV load-scaling technique is applied to scale the load current down further so that the LV load current of each property can be represented. The sum total of the MV load current of the 7 residential transformers (70 % of the total load current of the Mountain MV feeder), is first converted to an LV load current. This sum total LV load current is then divided amongst the properties in the residential area according to floor space, by means of property size information obtained from GIS software [72]. Each property then constitutes a portion of the total residential area LV load current, proportionate to its floor space. The technique of scaling the total load current for the residential area according to floor space, in order to represent the load current of each individual property, is inspired by the work of Dekehah and Heunis [73]. Work done by the aforementioned concluded that for higher income electricity consumers (a criteria that this residential area satisfies), floor space appears to have a significant impact, and a linear increase in electricity consumption is noticed as floor space is increased. The load currents for all the properties that are connected to a specific kiosk, are lumped together, according to phase allocation. A lumped A-phase load current, a lumped B-phase load current, and a lumped C-phase load current is therefore modelled at each kiosk, representing all the properties connected to that kiosk. In the absence of data, it is decided to model all load currents at unity power factor. An example of the property size data used is shown in figure 4.9, where the building footprint sizes have been omitted for confidentiality purposes.

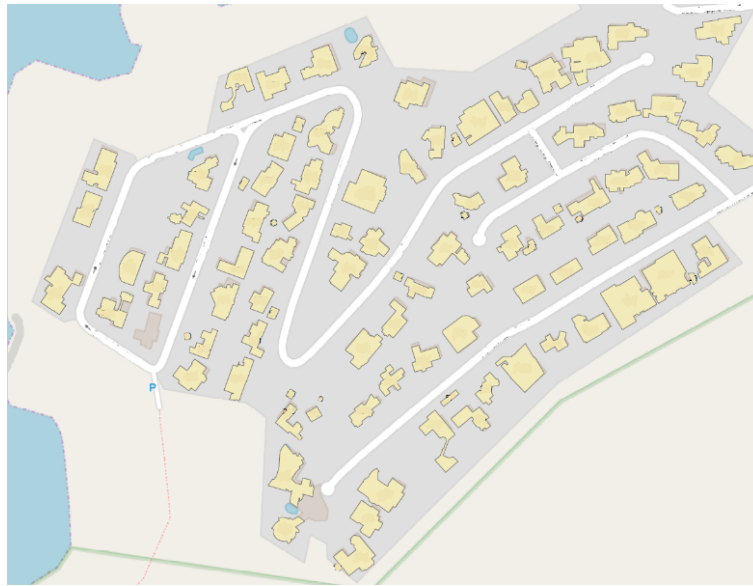


**Figure 4.9:** Example of Residential Area Building Footprint Sizes [72]

Regarding the commercial network, half-hourly average apparent power measurements for the year 2016 is available for the Metropolitan HV/MV substation feeders. No downstream load data is available. The floor space scaling technique is also employed in the commercial network, according to building footprint information provided by CCT [72]. In a commercial office building, the load can be expected to scale according to floor space, since loads are mostly comprised of lighting, office equipment and air-conditioning. In the residential area, it was sufficient to only consider the building footprint size. In the commercial area, however, every building footprint size is multiplied with the amount of storeys, in order to accurately represent the total floor space, since the majority of these commercial buildings are multi-storey. The total load for the commercial network is divided amongst the MV/LV transformers according to the total floorspace of the properties connected to that MV/LV transformer. Each property then constitutes a portion of the total commercial area load, proportionate to its floor space. Each load is modelled as a balanced three-phase LV apparent power load on the LV busbar of the respective MV/LV transformers. In a situation where more than one customer is connected to an MV/LV transformer, the loads are lumped together and presented as one balanced three-phase LV apparent power load. The balanced three-phase apparent power loads are modelled with a 0,88 lagging power factor, in accordance with load information provided by CoCT [70].

Regarding the industrial network, half-hourly average apparent power measurements for the year 2016 is available for the South HV/MV substation feeders. The loads in industrial buildings do not necessarily scale according to floor space, as it depends on the type of industry and the machinery or processes used. The transformer capacity rating scaling technique is therefore again employed, and extended to include the 4 MV loads. The total load for the industrial network is divided amongst the MV/LV transformers, and the 4 MV loads, according to transformer capacity ratings and the MV load supply point capacities. The 4 MV loads are directly connected to MV load nodes, modelled as balanced three-phase MV apparent power loads, whereas the rest of the loads are represented as balanced three-phase LV apparent power loads on the LV busbars of the respective MV/LV transformers. In a situation where more than one customer is connected to an MV/LV transformer, the loads are lumped together and presented as one balanced three-phase LV apparent power load. The balanced three-phase apparent power loads are modelled with a 0,9 lagging power

factor, in accordance with load information provided by Eskom [28].

The residential-, commercial- and industrial load data that is used, and divided amongst load nodes according to the discussed load modelling procedures, will be introduced in section 4.4, when the simulation methodology is discussed.

### 4.3.3 Network Generation Modelling

#### 4.3.3.1 Solar Panel Hosting Capacity

To determine the maximum solar panel hosting capacity of the areas under study, GIS software is used. With the help of tools contained in ArcGIS software, roofs that are eligible for solar panel installations are identified, and the area thereof measured, by means of a polygon construction tool. A polygon is drawn on the eligible roof space, so that the area thereof, and hence the solar panel hosting capacity, can be determined. The geographical direction that the roof is facing is also an attribute that is considered. After the polygons are drawn, a complete picture is available as to the total eligible roof space (with corresponding roof direction) in the area. In this project, roofs that face north, east, west, northeast, northwest, and southwest, as well as flat roofs, are considered as potential solar panel hosts.

In the residential-, commercial- and industrial area, existing installations are part of a minority and treated as if they are absent (properties with existing installations are still analysed to determine the maximum hosting capacity). There are over 300 properties in the residential area, and in 2017, only 7 rooftop PV installations could be observed in the area via Google Earth images [67]. The same holds true for the commercial- and the industrial area, where, in 2017, only 3 and 0 PV installations were observed respectively via Google Earth images [67].

Examples of the polygons that indicate potential solar panel hosts are shown in figure 4.10 - figure 4.12 for the residential-, commercial- and industrial areas respectively. The different coloured polygons indicate the different directions in which the roofs are facing. A summary of the available roof space for solar PV installations in all the areas is shown in Table 4.3.



**Figure 4.10:** Example of Polygons Indicating Roof Space with PV Potential in Residential Area



**Figure 4.11:** Example of Polygons Indicating Roof Space with PV Potential in Commercial Area

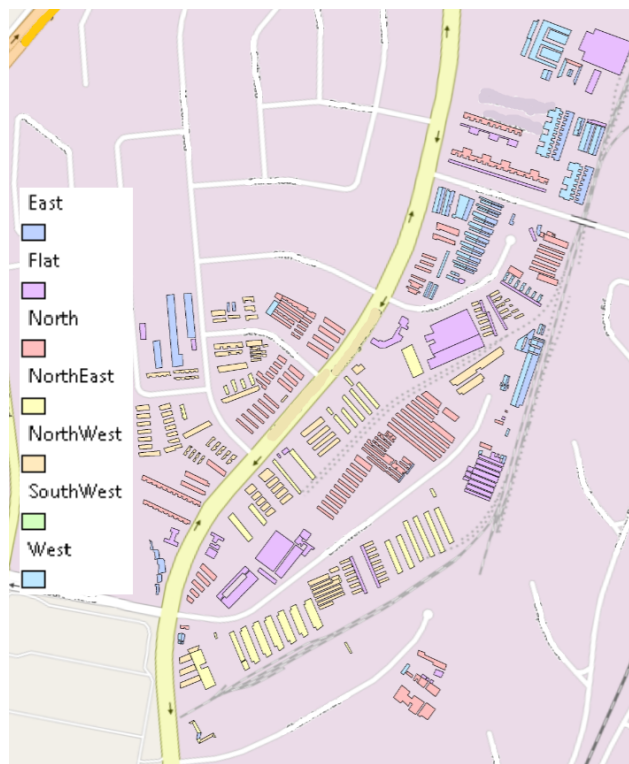


**Figure 4.12:** Example of Polygons Indicating Roof Space with PV Potential in Industrial Area

**Table 4.3:** Available Roof Space for PV Installations

Network	Direction	Available Roof Space (m <sup>2</sup> )	% of Total of Area
Residential	North	5703.1	15 %
	Northeast	2433.1	6.4 %
	Northwest	5349.1	14.1 %
	East	2386.9	6.3 %
	West	5039.6	13.3 %
	Southwest	3931.6	10.4 %
	Flat	13090.6	34.5 %
Commercial	North	6354.9	12,5 %
	Northeast	8004.4	15,7 %
	Northwest	11548.2	22,6 %
	East	2814.1	5,5 %
	West	5476	10,7 %
	Southwest	1353.4	2,7 %
	Flat	15445.9	30,3 %
Industrial	North	32467.8	23,1 %
	Northeast	20322.7	14,5 %
	Northwest	22469.2	16 %
	East	15006.7	10,7 %
	West	16986.7	12,1 %
	Southwest	0	0 %
	Flat	33318.8	23,7 %

#### 4.3.3.2 Solar Radiation Data and Terrain Horizon

Hourly solar radiation data for 2016 for the areas under study is obtained via the HelioClim-3 satellite-derived solar radiation database from SoDa. The terrain horizon for the areas under study is obtained via pvPlanner software from Solargis. This is to take into account the effects of far shading on the area due to natural obstructions such as mountains. Only horizon shading is taken into account in the simulations - the effects of near-shading is not considered (however, when the polygons are drawn in ArcGIS, roofs are excluded if it is apparent that the roof has permanent near-shading problems).

The residential area is built on mountainous terrain, and because of this, horizon shading profiles differ across the area. Even though the residential area constitutes a small area, situations arise when one side of the residential area is shaded at a particular time, whilst another side is not. Because of this, PV generation profiles may differ for two identical systems that are located in different parts of the residential area. For this reason, terrain horizons are obtained in the vicinity of each MV/LV transformer in the residential area, so that the properties connected to that transformer, share a horizon shading profile common to that specific LV network. The commercial- and industrial areas are located on flat terrain within a 3 km radius of each other, and therefore have similar terrain horizons. The terrain horizon- and sunpath diagrams are shown in figure 4.13 - figure 4.15 for the residential-, commercial- and industrial area respectively.

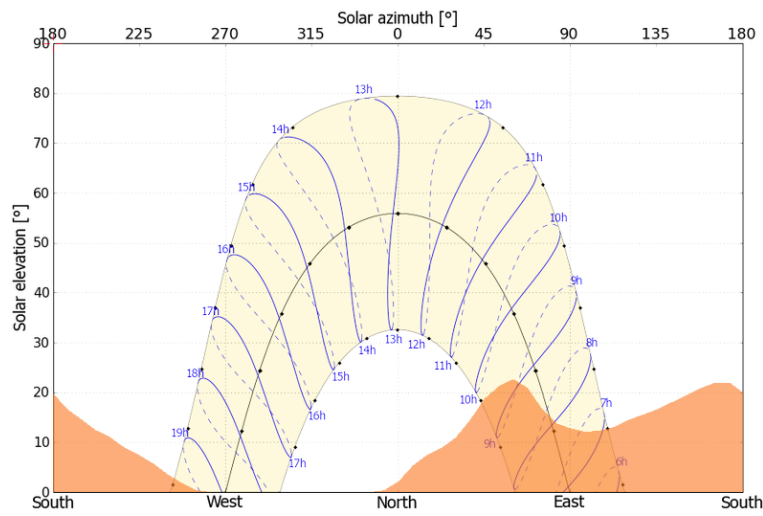


Figure 4.13: Residential Area Horizon- and Sunpath Diagram [74]

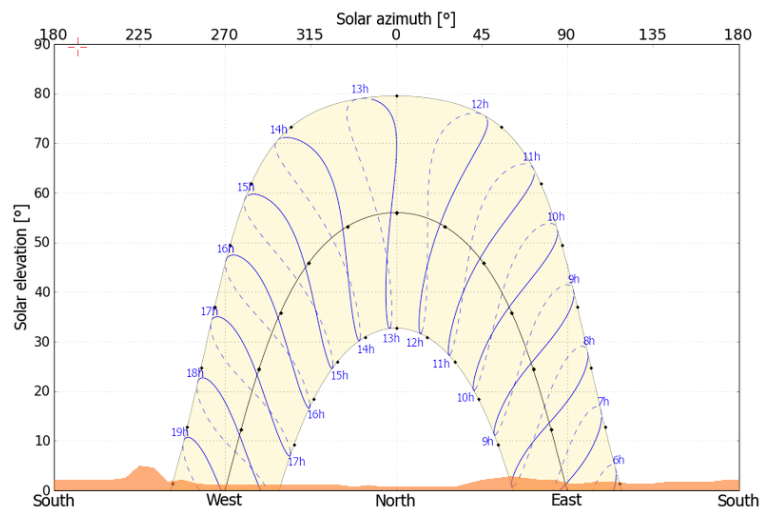


Figure 4.14: Commercial Area Horizon- and Sunpath Diagram [74]

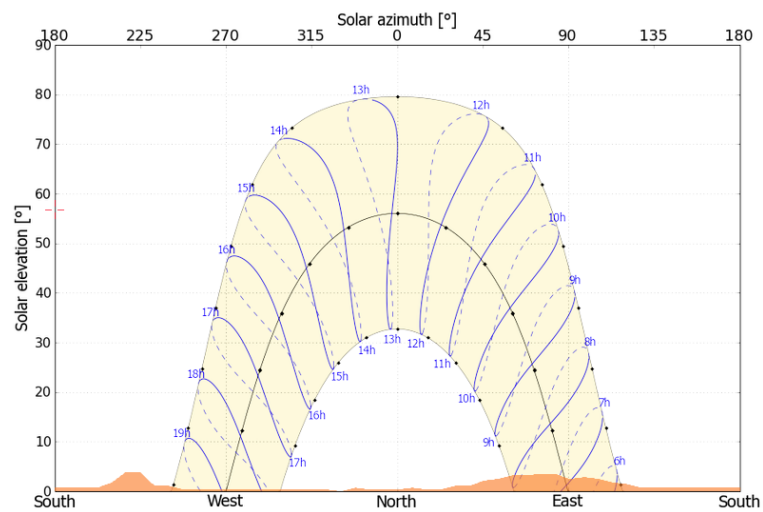


Figure 4.15: Industrial Area Horizon- and Sunpath Diagram [74]



### 4.3.3.3 Generation Profile Simulation

After solar radiation- and terrain horizon data is obtained, a power generation profile for each individual PV system is found. Since the residential area comprises over 300 properties, and due to the absence of such data, actual individual roof tilt angles are not considered. A tilt angle of  $26^\circ$  is assumed for residential tilted roofs, since this is the advised pitch angle of a tile-covered roof truss, according to The South African National Standard for Roofs [75]. For the commercial- and industrial areas, a tilt angle of  $30^\circ$  degrees is assumed for tilted roofs. In all networks, a tilt angle of  $0^\circ$  is used for flat roofs. The reference system for simulations for the three networks is shown in table 4.4. The system used for the residential area is nearly identical to the system used for the commercial- and industrial area, with the difference being the tilt angle for tilted roofs, and a slight change in PV module model.

**Table 4.4:** Reference PV System

	<b>Residential</b>	<b>Commercial and Industrial</b>
<b>PV Module</b>	Yingli Solar YL290D-30b (290 W)	Yingli Solar YL290P-35b (290 W)
<b>Inverter</b>	SMA Sunny Boy 3000TL-21 (3 kW)	SMA Sunny Boy 3000TL-21 (3 kW)
<b>System Size</b>	2.9 kW	2.9 kW
<b>Tilt Angle</b>	$26^\circ$ assumed for tilted roofs; $0^\circ$ for flat roofs	$30^\circ$ assumed for tilted roofs; $0^\circ$ for flat roofs

The 2016 solar radiation data from SoDa, and the terrain horizon data from pvPlanner, is imported into PVsyst software. By means of PVsyst simulations, an hourly 2016 PV generation profile is obtained for all of the reference systems. The following simulations, for the residential-, commercial- and industrial area, are performed:

- Residential 2.9 kW  $26^\circ$ -tilt reference system facing north, east, west, northeast, northwest, southwest.
- Flat installed 2.9 kW residential reference system.
- Commercial/industrial 2.9 kW  $30^\circ$ -tilt reference system facing north, east, west, northeast, northwest, southwest.
- Flat installed 2.9 kW commercial/industrial reference system.

The data obtained from the polygon construction (discussed in subsection 4.3.3.1) by means of ArcGIS, makes it possible to determine the maximum PV system size in  $\text{m}^2$  that each property is able to host. This total system size can be made up of a combination of north/east/west/northeast/northwest/southwest/flat subsystems. Using the knowledge that the 290 W reference PV modules have a surface area of  $1.6368 \text{ m}^2$ , each subsystem's size in  $\text{m}^2$  can be converted to kW. Each subsystem size in kW can be used to derive a scaling factor (where scaling factor = subsystem size in kW  $\div$  2.9 kW) to multiply with the corresponding north/east/west/northeast/northwest/southwest/flat 2.9 kW reference system generation profile, in order to determine a generation profile for that particular subsystem. The generation profiles for all of the subsystems can then be added up, to yield a generation profile for the total system. The outcome of the calculation is the maximum PV generation profile that each property can possibly yield, with the maximum size PV system that can be installed at that property.

In subsection 4.3.2 it was mentioned that the resolution of the available load data is 30-minute intervals, whilst the resolution of the available generation data is 60-minute intervals. A mismatch in resolution therefore exists between the load and generation data. As will be shown in subsection 4.4.3.2, the Digsilent Powerfactory simulations will be performed at 30-minute intervals. Digsilent Powerfactory has built-in interpolation functionalities, in order to generate intermediate 30-minute data points for the hourly generation data, in order to make the resolution match. However, in order to reduce computation time, this process is manually executed on the generation data in order to convert the hourly generation data to 30-minute interval data. Linear interpolation is used for this purpose.

All PV systems are assumed to be operating at unity power factor, and are modelled as negative active power loads (negative load corresponds to generation). The PV systems for the residential network are modelled as single-phase PV systems, due to the single-phase connection topology. The PV system that a particular residential property can host, is connected to the same phase that the load of that property is connected to. Since the commercial- and industrial network assumes balanced three-phase loads, PV systems are also modelled as balanced three-phase PV systems. The PV system that a particular industrial- or commercial property can host, is connected to the same transformer LV busbar that the load of that property is connected to. In a situation where more than one customer is connected to an MV/LV transformer, the PV systems are lumped together and presented as one PV system. For the industrial network MV loads, the PV systems are connected to the same MV supply point as the MV load.

## 4.4 Simulation Methodology

### 4.4.1 Simulation Data

The discussion in subsection 3.5.2 provided an explanation of the way in which distributed PV generation may cause reverse power flow. Equation (4.1) (identical to equation (3.9)) shows how reverse power flow occurs when a negative mismatch exists between load and generation:

$$\textit{Net Load} = \textit{Load} - \textit{Generation} \quad (4.1)$$

When the generation on a feeder exceeds the load on a feeder, the net load becomes negative, which corresponds to reverse power flow. The question of determining how much distributed PV generation a network can accommodate, due to the constraints of voltage rise and equipment overload, becomes a question of identifying the allowable PV penetration levels whereby worst-case reverse power flow will still result in a network that is operating within regulatory limits. In guiding the understanding of the occurrence of maximum reverse power flow, it is useful to first consider the global irradiation for Cape Town. Figure 4.16 shows the global irradiance per month, consisting of reflected-, diffuse- and direct irradiance, for Cape Town.

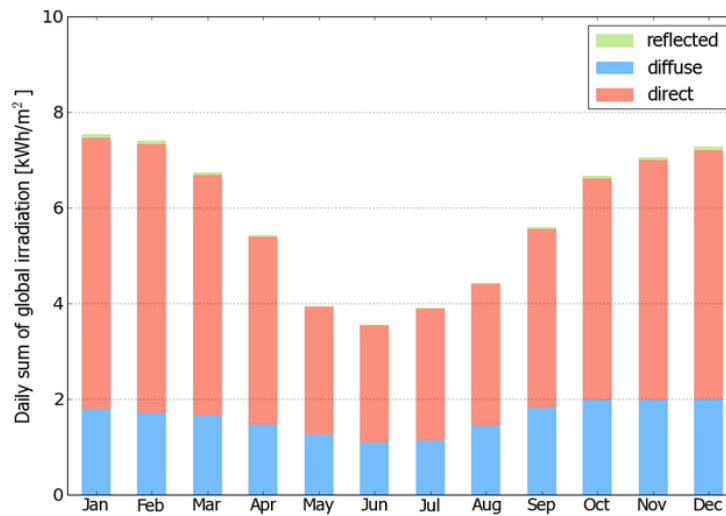


Figure 4.16: Cape Town Global Irradiation [74]

The data clearly shows that the global irradiation for the summer months far exceed the global irradiation for winter months, which in turn corresponds to higher PV output. In the process of determining the maximum allowable levels of PV penetration that will not result in network violations, it is not necessary to consider non-critical time periods such as winter. Rather, the critical time that needs to be considered, is the period around midday (around 11h00 - 14h00) in summer - corresponding to maximum PV output. It can be seen that January and December will correspond to the highest PV output months, which intuitively suggests that these will be the constraining months in terms of maximum allowable PV penetration. However, in accordance with equation (4.1), the deciding factor is the net load, which suggests that the generation data can't be solely used as indicator - monthly loads also need to be considered. For completeness, the load- and generation data for the first three months (January - March) and the last three months (October - November) of the year 2016 is analysed, since these will be 6 highest yielding months in terms of PV output. The load data (as provided by CCT and Eskom) and generation data (obtained via simulation) for the residential-, commercial- and industrial networks, is assessed at every 30-minute interval for the first three months (January - March) and the last three months (October - November) of 2016. From the data of each month, load- and generation profiles for a hypothetical 24-hour day are derived for each month. For the load data, a 24-hour profile of minimum- and average load is derived for each month, and for the generation data, a 24-hour profile of maximum- and average generation is derived for each month, according to the following procedure:

**Minimum load:** For a 24-hour profile of minimum load, the load value for each 30-minute interval is obtained by taking the minimum load value at that time interval for all days of that month.

**Average load:** For a 24-hour profile of average load, the load value for each 30-minute interval is obtained by taking the average of all the load values at that time interval for all days of that month.

**Maximum generation:** For a 24-hour profile of maximum generation, the power value for each 30-minute interval is obtained by taking the maximum power value at that time interval for all days of that month.

Average generation: For a 24-hour profile of average generation, the power value for each 30-minute interval is obtained by taking the average of all the power values at that time interval for all days of that month.

The profiles of average loads and average generation are to provide a basis of comparison for the profiles of minimum loads and maximum generation, whereas the profiles of minimum loads and and maximum generation provide a basis upon which the worst-case reverse power flow can be assessed. For this scenario, equation 4.1 can be adjusted to equation (4.2):

$$\text{Maximum Negative Net Load} = \text{Minimum Load} - \text{Maximum Generation} \quad (4.2)$$

#### 4.4.1.1 Minimum Load

Figure 4.17 - Figure 4.19 show the average and minimum 24-hour total load profiles for the entire residential-, entire commercial- and entire industrial area. The load profiles for each entire area, is constituted by the sum total of the generation profiles of all the individual loads in the area. It is observed that December has the lowest minimum load profile for the 11h00 -14h00 time period of interest, for the residential- and industrial network. For the commercial network, December has the lowest minimum load profile profile for the 12h30 - 14h00 period (and amongst the lowest for 11h00 - 12h30).

The residential load profiles have clearly discernible morning and evening peaks (Note the residential network load is presented in this section using active power, for illustrative purposes, and the actual loads are modelled using current loads, as discussed in subsection 4.3.2). Between the morning and evening peaks, a sag in the residential load profile is observed. From the profiles of average loads for the commercial network, the onset of commercial activity at the start of a workday is clearly visible - the load profile ramps up, reaches a plateau, and ramps down at the end of a work day. When considering the profiles of minimum loads for the commercial network, the entire profile flattens out somewhat, and the increment in daytime load is not as prominent. Intuitively, these minimum load profiles will correspond to weekends or public holidays (December has 4 public holidays in South Africa, the most of any month [76]), when most commercial activity ceases. This provides a clear basis for understanding that a weekend day/public holiday in December will provide a typical worst-case reverse power flow scenario for the commercial network. As an example, consider a sunny Sunday afternoon/public holiday in December. PV generators are generating maximum output, whilst most commercial buildings are closed. This scenario provides the biggest mismatch between load and generation. From the profiles of average loads for the industrial network, the onset of industrial activity at the start of a workday is clearly visible - the load profile ramps up, reaches a plateau, and ramps down at the end of a work day. When considering the profiles of minimum loads for the industrial network, the entire profile flattens out. Just like in the commercial area, these minimum load profiles will correspond to weekends/public holidays, when most industrial activity ceases. This provides a clear basis for understanding that a weekend day/public holiday in December will provide a typical worst-case reverse power flow scenario for the industrial network, as has been explained for the commercial network.

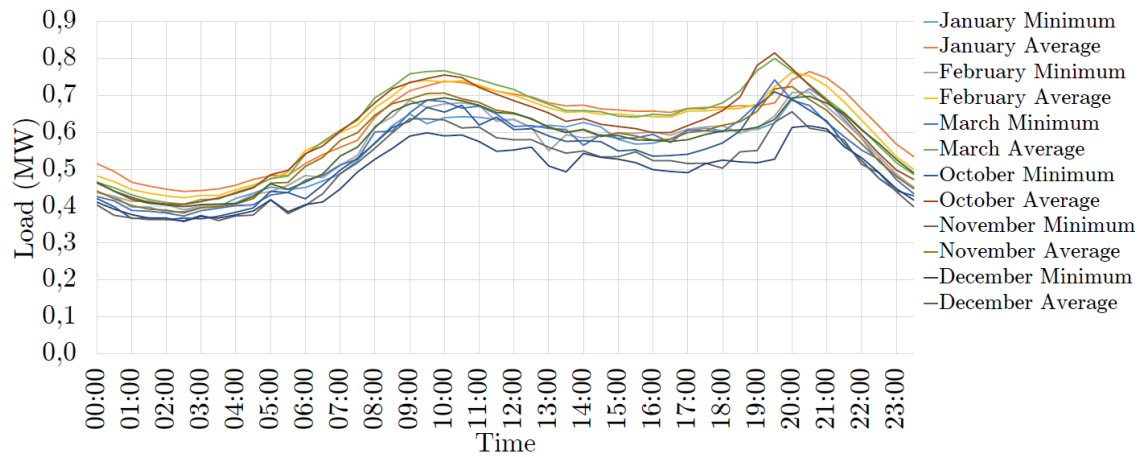


Figure 4.17: Residential Area Total Daily Load Profile derived from [70]

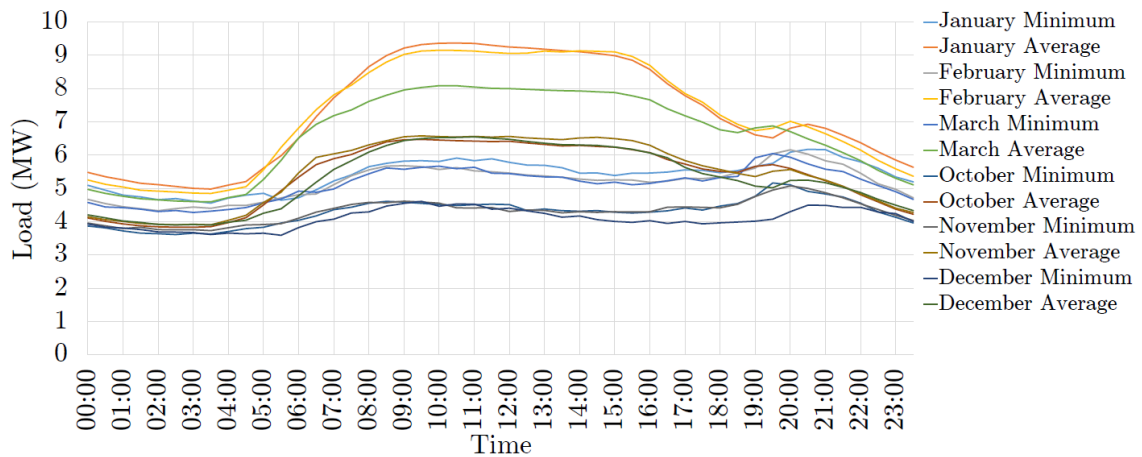


Figure 4.18: Commercial Area Total Daily Load Profile derived from [70]

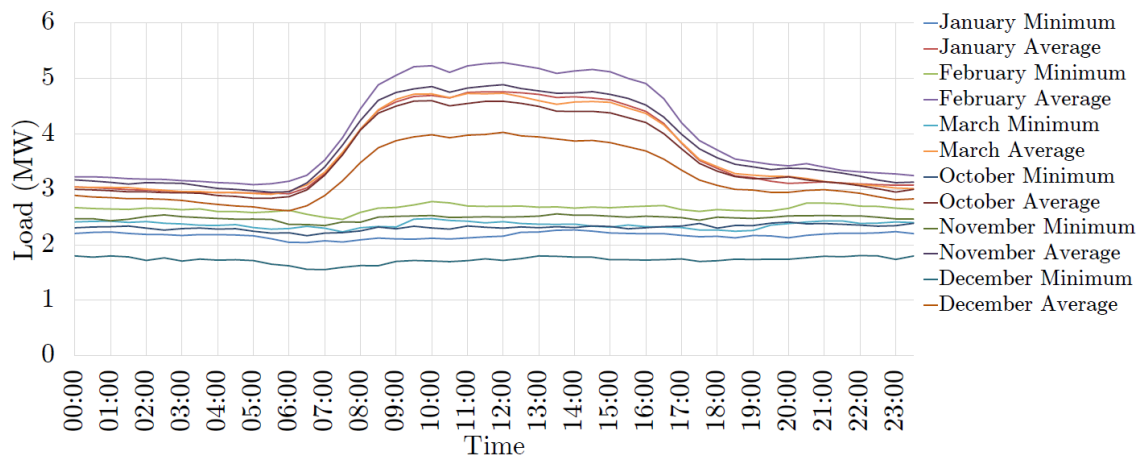
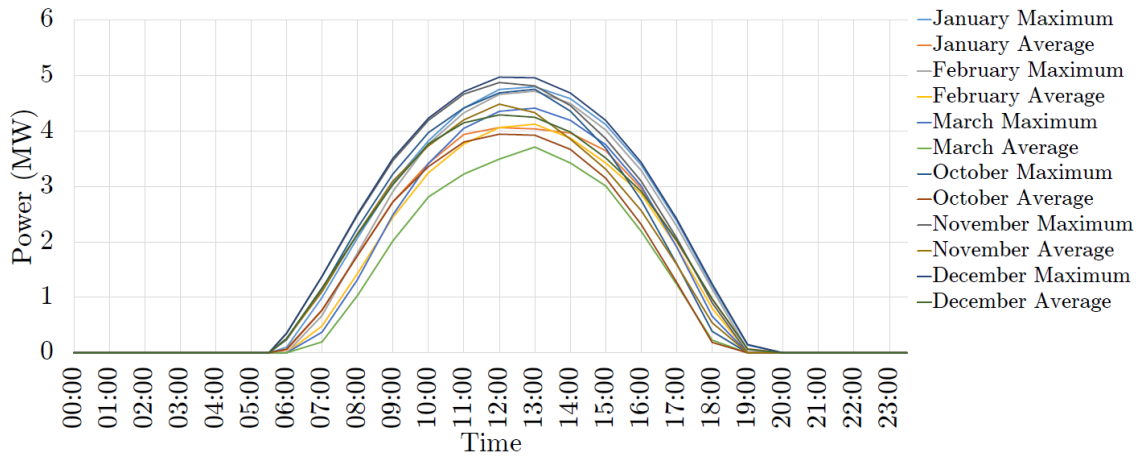


Figure 4.19: Industrial Area Total Daily Load Profile derived from [28]

#### 4.4.1.2 Maximum Generation

Figure 4.20 - Figure 4.22 show the average and maximum 24-hour total generation profiles for the entire residential-, entire commercial- and entire industrial area, where all PV-eligible roofspace is utilised. The generation profiles for each entire area, is constituted by the sum total of the generation profiles of all the individual PV systems in the area. It is observed that December has the highest maximum generation profile for the 11h00 -14h00 time period of interest, for all three networks.



**Figure 4.20:** Residential Area Total Daily PV Generation Profile Utilising Maximum PV-eligible Roofspace

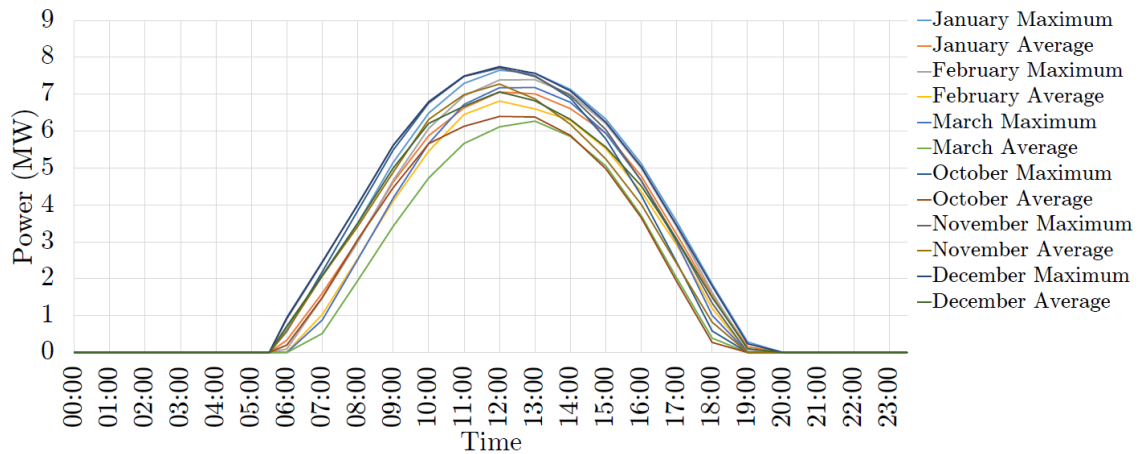


**Figure 4.21:** Commercial Area Total Daily PV Generation Profile Utilising Maximum PV-eligible Roofspace

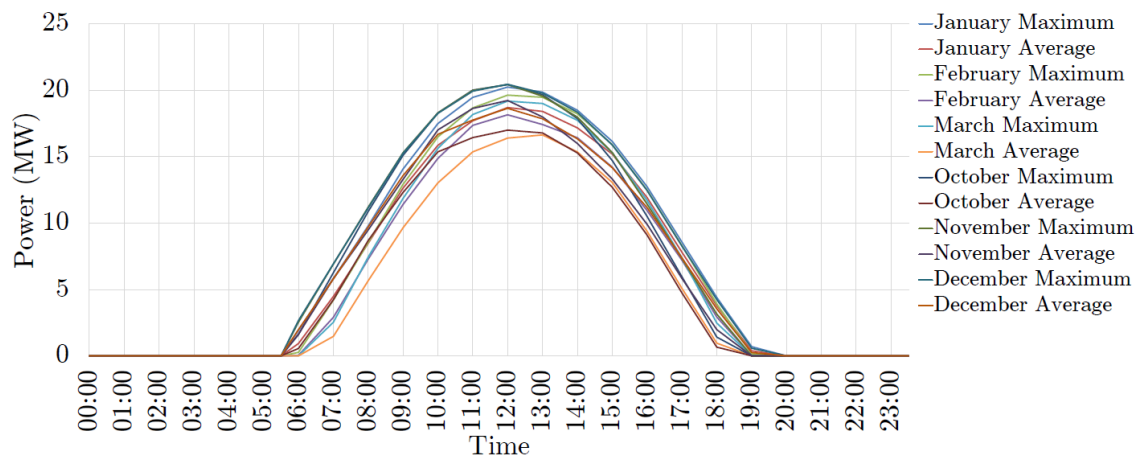


**Figure 4.22:** Industrial Area Total Daily PV Generation Profile Utilising Maximum PV-eligible Roofspace

#### 4.4.1.3 Summary

Figure 4.23 - Figure 4.25 show, for illustrative purposes, the resultant 24-hour total net load profiles (commonly referred to in literature as *duck curves*) for varying levels (as a % of maximum possible PV) of PV installations for the entire residential-, entire commercial- and entire industrial area. These net load profiles are obtained by using the derived 24-hour December profiles for minimum load and maximum generation. It is observed that 11h00 - 14h00 constitutes the time period of most concern (in terms of reverse power flow), corresponding to the midday period of maximum generation.

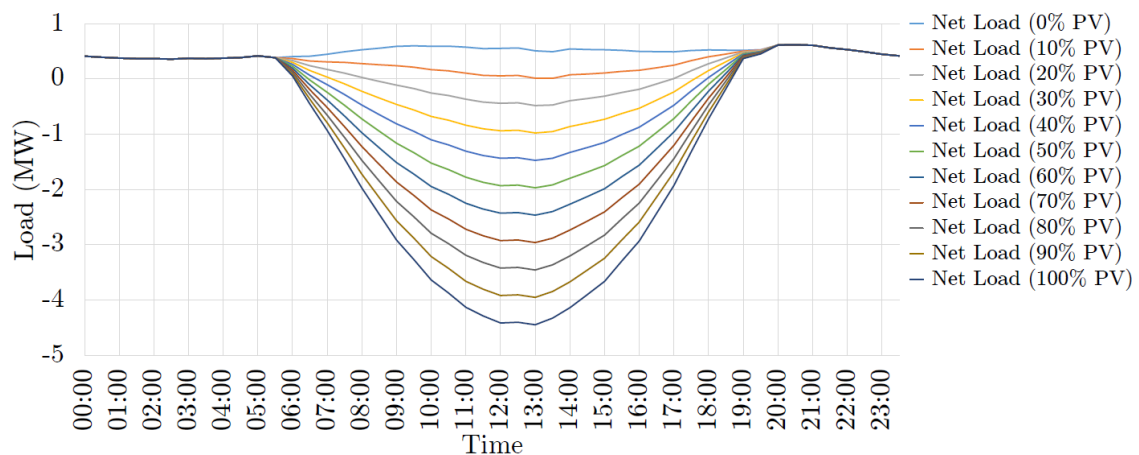


**Figure 4.23:** Residential Area Total Daily Net Load Profiles with Varying PV Generation

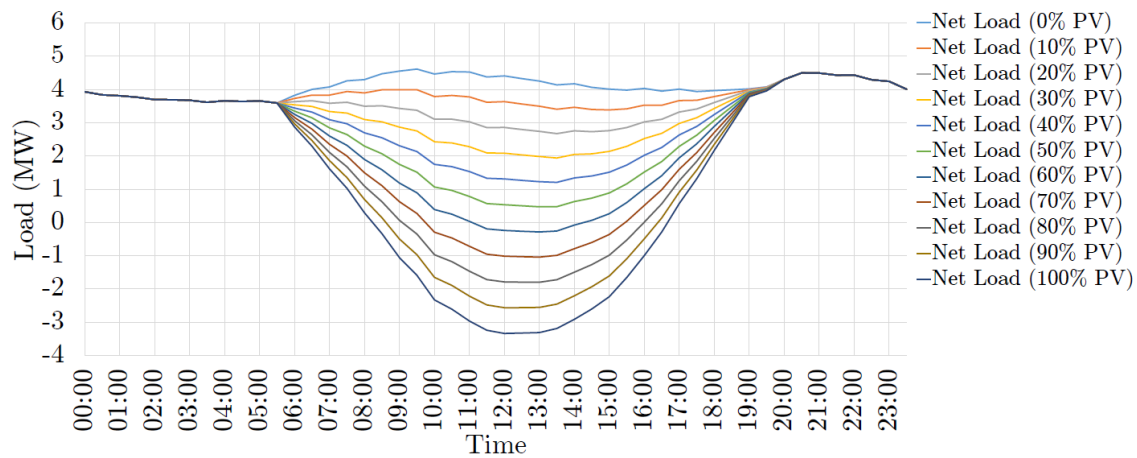


**Figure 4.24:** Commercial Area Total Daily Net Load Profiles with Varying PV Generation

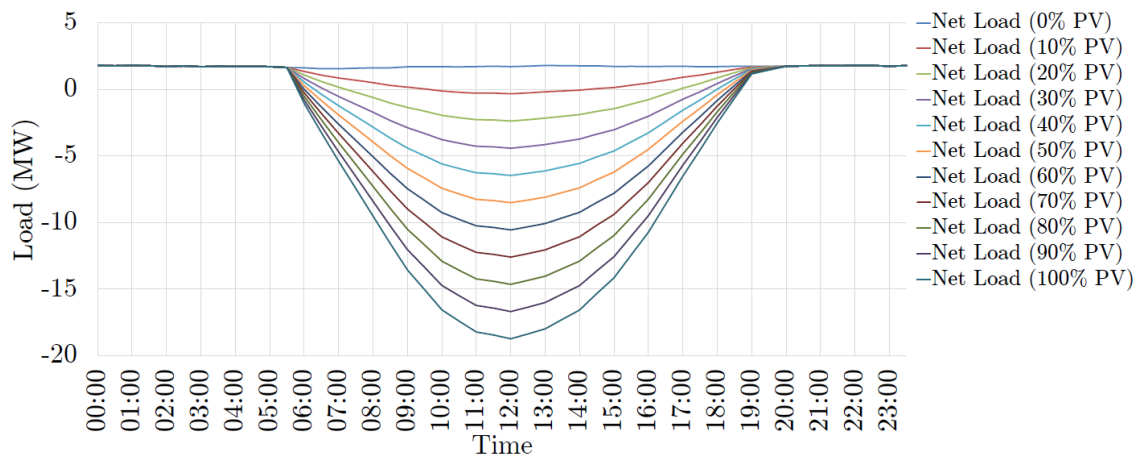


**Figure 4.25:** Industrial Area Total Daily Net Load Profiles with Varying PV Generation

Analysis of the load- and generation data for the year 2016 confirms that the month of December provides the scenarios of interest for determining allowable PV penetration levels, when considering network conditions under coincidence of minimum load and maximum generation. The derived December load- and generation data is therefore used to determine acceptable PV penetration levels in the residential-, commercial- and industrial area (more discussion in this regard follows in subsection 4.4.3.2).

The approach of using the worst-case scenarios of minimum load coinciding with maximum generation, can be described as a conservative approach. This is, however, the intention of the simulation methodology. It is useful from the perspective of the utility to know the resultant network conditions that could arise when these scenarios occur under different levels of PV penetration. Even under worst-case operating conditions, a distribution network still has to operate within regulatory limits, therefore this approach aids in understanding the extent to which utilities need to limit PV uptake in order to secure reliable operation of the networks.



## 4.4.2 Software Development

The network topologies, loads, and generators are modelled in Digsilent Powerfactory according to the methodologies outlined in subsection 4.3.1, - 4.3.2, and - 4.3.3, with the simulation data as discussed in subsection 4.4.1. Digsilent Powerfactory can perform many tasks using built-in methods and functionalities. The simulation procedures that is to be applied to the networks, however, require functionality extending beyond the scope and capabilities of standard Powerfactory features. Powerfactory allows the user to extend the functionality of the program by making it possible to automate Powerfactory tasks using Python or Digsilent Programming Language (DPL). DPL is used in this study as programming language to develop software to automate the simulation process. DPL is based on a C-like syntax. Powerfactory content is organised in an object-oriented manner, and objects, elements contained within objects, and their parameters can be accessed via DPL. Decision- and flow commands, mathematical expressions, user-defined methods and -variables, and object-oriented interfacing are all functionalities provided by DPL in order to set up an interface for the automation of tasks in Powerfactory. [77, 78]

## 4.4.3 PV Penetration Definition

In this project, PV Penetration is quantified by equation (4.3):

$$PV \text{ Penetration } (\%) = \frac{\text{Maximum Allowable PV (kW)}}{\text{Network MD (kVA)}} \cdot 100 \quad (4.3)$$

Maximum allowable PV refers to the maximum cumulative capacity of PV systems on the network, before a network violation (discussed in section 5.3.1) occurs. Network MD refers to the network maximum demand (MD), which is the maximum load that the network can supply before a network violation (discussed in section 4.4.3.1) occurs. Discussion of the topologies of the networks in subsection 4.3.1 has shown that the commercial- and industrial networks are only modelled up to the LV busbar of the network MV/LV transformers. The residential network, however, consists of an MV network and 7 LV networks, with all LV networks being graphically modelled. Each LV network in the residential area is first isolated and independently studied, in order to identify the PV penetration limits of each independent LV network. When an LV network is isolated, the rest of the residential network is modelled as an external grid that is connected to the MV busbar of the isolated LV network's MV/LV transformer. After studying each LV network, all LV networks are interconnected to the MV network (as it is in practice) and the residential interconnected MV/LV network is studied. The PV penetration quantity is referenced to specific points in the networks. For the simulation scenarios where the 7 residential LV networks are isolated, the network reference point is the LV busbar of the MV/LV transformer that supplies the isolated LV network. For the commercial- and the industrial network, the network reference point is the MV busbar of the HV/MV distribution substation that supplies the network. For the residential interconnected MV/LV network, *maximum allowable PV* refers to the combined cumulative capacity of PV systems on the 7 LV networks, before a network violation occurs, and *network MD* refers to the MD of the combined 7 LV networks, under interconnected conditions. Note that the *maximum allowable PV* for the interconnected MV/LV network does not necessarily correspond to the sum total of the *maximum allowable PV* for the 7 isolated LV networks, and the *network MD* for the interconnected MV/LV network does not necessarily correspond to the sum total of the network MDs for the 7 isolated LV networks, since network operational characteristics change under interconnected conditions, due to mutual interaction between LV networks and the MV network.

#### 4.4.3.1 Network MD Simulations

The Network MD is the maximum load that the network can supply before a network violation occurs. The network MD is determined for a passive network, where only loads are present in the network. The network violations that are considered in this definition for this project, are voltage violations and thermal overload. Voltage violations are assessed at every node, or terminal, in the network, whilst thermal overload is considered for all cables and transformers. Thermal overload for cables and transformers are defined as a condition where the loading exceeds 100% of the rated value of the element. Voltage violations are defined as undervoltage (voltage  $< 0.9$  p.u. and voltage  $< 0,95$  p.u.) for LV- and MV networks respectively, as per the NRS 048-2 specification [44]. The network MD violation thresholds are summarised in table 4.5.

**Table 4.5:** Network Violation Thresholds: Network MD Simulations (Passive Network)

Network	Undervoltage (p.u.) [44]	Cable Overload (%)	Transformer Overload (%)
LV	0,9	100	100
MV	0.95	100	100

An algorithm, written in DPL, is used to determine the network MD. The algorithm performs iterative load flow calculations under incremental network loading conditions, until a loading condition is reached where the first network violation occurs. The load flow calculation considers a single data point in time, and since half-hourly average load data is used, a single load-flow calculation represents the average network state for half an hour. The load flow calculation can be set up to be performed at any instance in time - the load is divided amongst the load nodes according to the procedures outlined in section 4.3.2, and therefore the load level at which the first violation occurs, will be the same regardless of the load level at which iterations are commenced. The fundamental operation of the network MD algorithm is shown in figure 4.26.

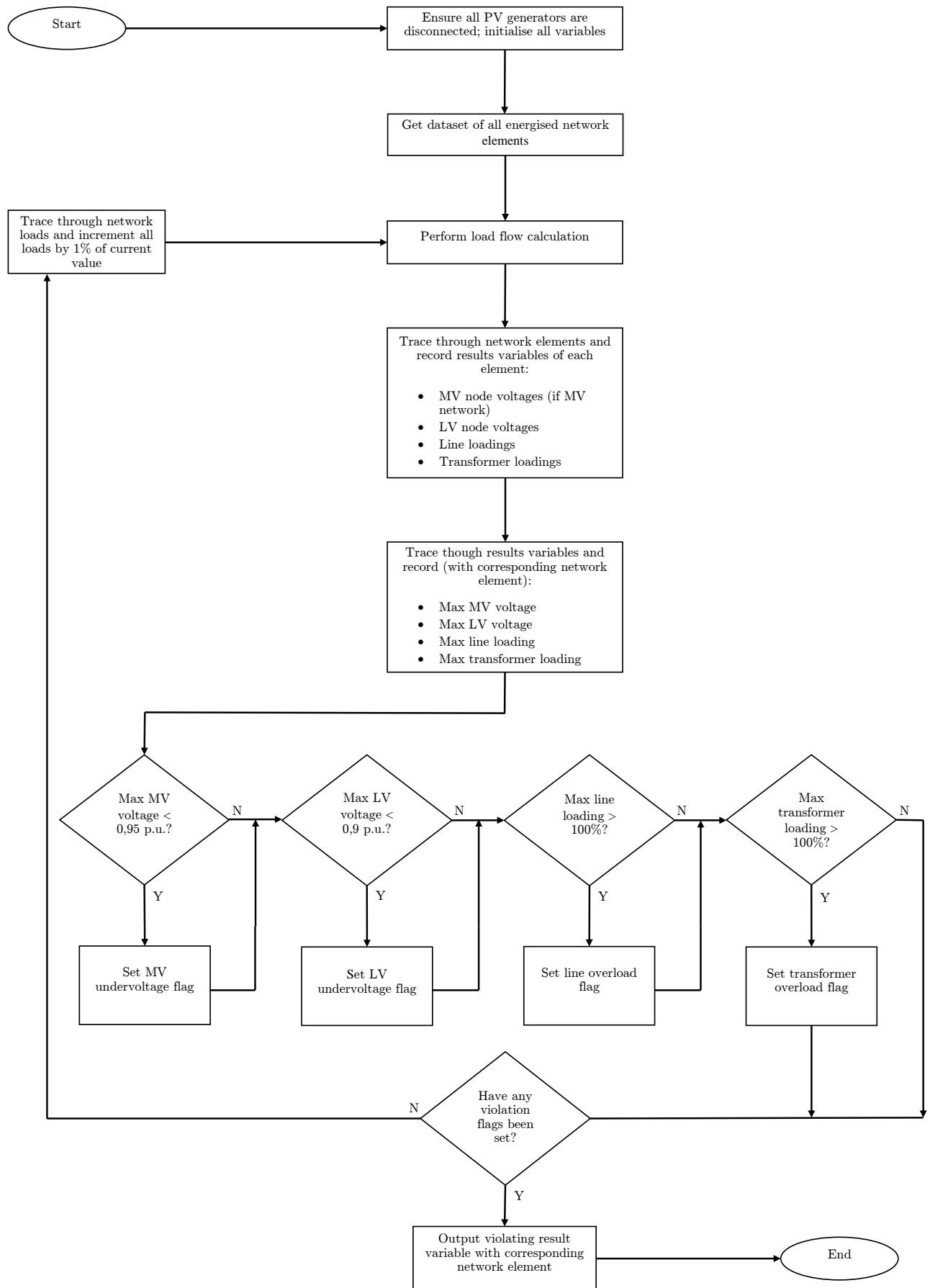


Figure 4.26: Feeder MD Algorithm Flowchart

#### 4.4.3.2 PV Placement Simulations

An algorithm, written in DPL, is used to simulate the introduction of PV generators into the existing passive network, in order to determine how the network will react under different levels of PV penetration. The algorithm performs iterative time-series quasi-dynamic simulations, recording relevant results variables after each iteration. The algorithm is based on a process whereby PV generators are randomly sized across the network, and different PV placement scenarios are tested.

The load models in Powerfactory are modelled in such a way that they are controlled by a scaling factor, which can scale the magnitude of the load by multiplying it with the scaling factor. Since all generators are modelled as negative loads, the output of a PV generator can be controlled using the scaling factor. Each generator power output profile is constrained on the lower limit by 0, corresponding to no generator installed, and on the upper limit it is constrained by the maximum size installable PV system, limited by roofspace (and corresponding orientation of panels) at that particular property, as explained in subsection 4.3.3. The random sizing of a PV system is done by assigning a random number as scaling factor. The random number is uniformly spread on the interval  $[0;1]$  with discrete steps of 0,01. This corresponds to assigning a generator anywhere from 0% to 100% of its maximum capacity, according to a uniform distribution with discrete steps of 1%. There is uncertainty about the size of the PV system that a property owner will choose to install. The maximum possible PV generation at each property, is however, known. The random sizing of PV systems, bound between practical limits for each property, allows the output results to consider the effect of the variation in this uncertain input parameter. The algorithm commences at a condition of maximum PV penetration, using 100% of PV-eligible roof space at all nodes, to include the absolute worst-case scenario in the results set. Thereafter, random PV allocation is done according to a set of rules. For balanced three-phase networks (commercial and industrial), balanced random three-phase PV allocations are done, whereas for the unbalanced networks (residential single-phase customers), random allocations are done per phase. The output results for all 100 000 PV placement scenarios are recorded, and presented in scatter plot format. More discussion on the results representation and -interpretation, along with the PV penetration network violation assessment limits, will follow in chapter 5.

Derived 24-hour December profiles for the minimum load and maximum generation of the different networks, as discussed in section 4.4.1, are utilised in the simulations. In section 4.4.1, it was shown that 11h00 - 14h00 constitutes the time period of most concern (in terms of reverse power flow), corresponding to the midday period of maximum generation. It is not necessary to consider any data points outside this time range, since the worst-case scenario will occur in this time interval. The quasi-dynamic simulation utilises 7 data points, corresponding to 11h00, 11h30, 12h00, 12h30, 13h00, 13h30 and 14h00. For each PV placement scenario, a time-series quasi-dynamic simulation is performed. The quasi-dynamic simulation performs sequential time-series load-flow calculations (at 11h00, 11h30, 12h00, 12h30, 13h00, 13h30 and 14h00), representing the average network state for each half-hourly interval, since half-hourly average load data is used. Each load-flow calculation is iteratively solved by employing the Newton-Raphson method [77].

The process of narrowing down the simulation to consider only the critical data points, streamlines the simulation process and avoids burdening the computer with unnecessary data points in an already computationally expensive simulation. As an example - each network is solved through a process of 100 000 quasi-dynamic simulation iterations (corresponding to 100 000 different PV placement scenarios) which takes approximately a day to solve under

the current simulation procedure. If, for instance, as opposed to using the 7 critical data points, it was decided to use half-hourly load data for the entire year of 2016 (unnecessarily including non-critical data points such as night-time and winter months), the same simulation would take approximately 208 days to complete. The fundamental operation of the PV penetration algorithm is shown in figure 4.27.

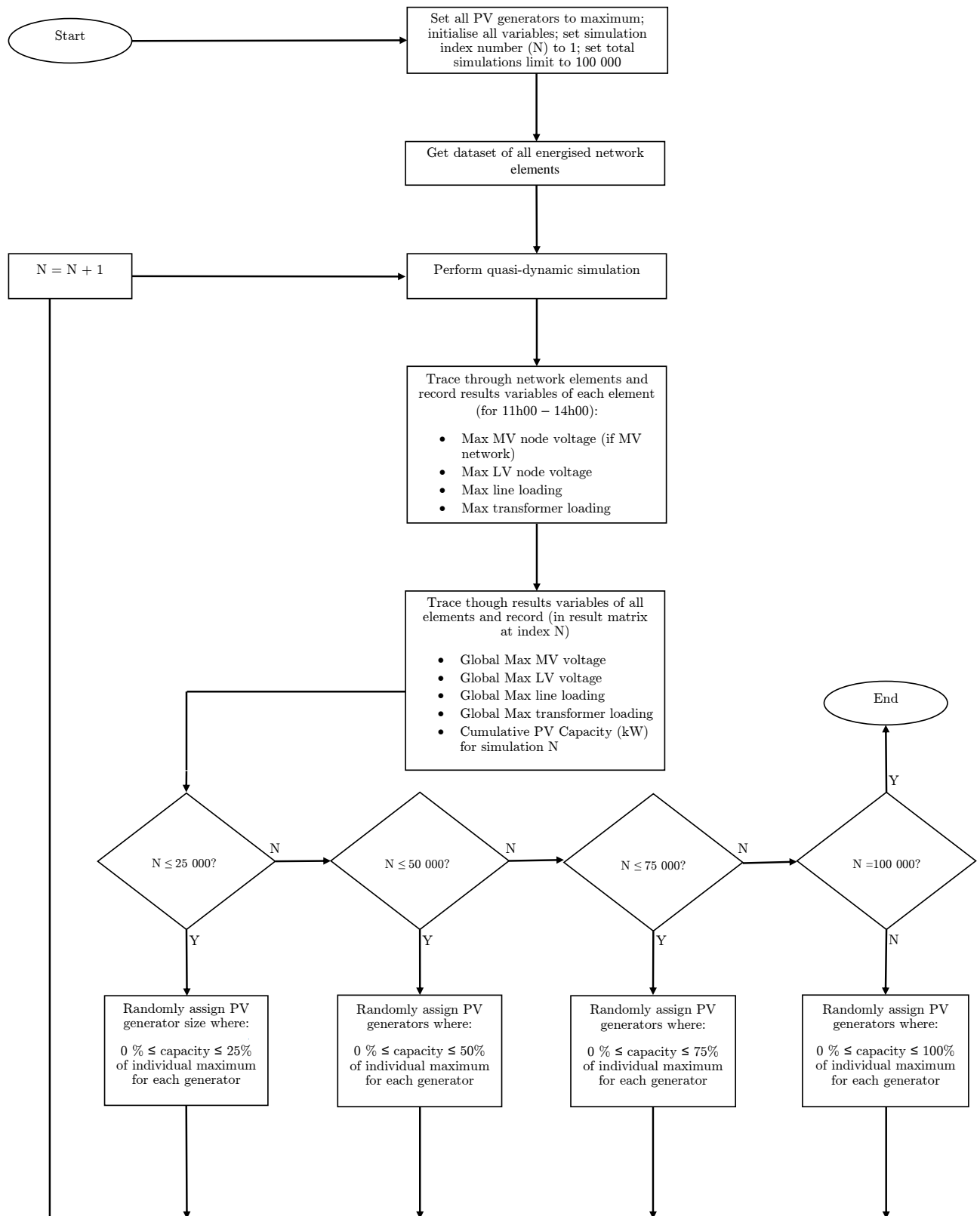


Figure 4.27: PV Placement Algorithm Flowchart

# Chapter 5

## Results

### 5.1 Introduction

This chapter provides the results obtained for the residential-, commercial- and industrial network studies. The chapter first provides results for the network MDs. Thereafter, PV penetration results are considered - an explanation of the method by which the results are analysed, is first provided, followed by results for all networks. The chapter concludes with a summary and discussion of the results.

### 5.2 Network MD Results

The results obtained by the DPL algorithm, implemented in section 4.4.3.1 to calculate the network MDs, are shown in table 5.1. It is observed that only the Sunrise Isolated LV network MD is constrained by undervoltage, whereas all other network MDs are constrained by line overload.

**Table 5.1:** Network MD Results

<b>Network</b>	<b>Network MD</b>	<b>Constraint</b>
Sunrise isolated LV	284,6 kVA	LV undervoltage
Fish isolated LV	248,5 kVA	Line overload
Lion isolated LV	193,8 kVA	Line overload
Oak isolated LV	228,7 kVA	Line overload
Market isolated LV	264 kVA	Line overload
Beach isolated LV	290,8 kVA	Line overload
Grave isolated LV	170 kVA	Line overload
Residential IC MV/LV	1,1657 MVA	Line overload
Commercial MV	12,9413 MVA	Line overload
Industrial MV	10,8018 MVA	Line overload

### 5.3 PV Penetration Results

#### 5.3.1 Results Analysis Method

The DPL algorithm, implemented in section 4.4.3.2 to perform PV placement simulations, tests 100 000 different PV placement combinations for each network. For each of the networks, the maximum voltages, maximum line loadings as well as maximum transformer

loadings are recorded for each of the 100 000 simulations. The results are presented in scatter plot format. Each dot on a scatter plot represents a PV placement combination. In the majority of results scatter plots, a positive linear relationship is discernible, i.e. as PV penetration levels increase, the maximum observed voltage/line loading/transformer loading also increases. The method of interpretation of the scatter plot, in order to determine maximum allowable PV penetration limits, depends on the data analyst. The statistical analysis of the scatter plot can be done in different ways, depending on the threshold of acceptance for maximum PV installations adopted by the analyst. In the scatter plots, the maximum observed voltage/line loading/transformer loading is presented as the y-axis variable, whereas the x-axis variable correspond to the cumulative PV capacity installed on the network. In this project, a method of piece-wise percentile analysis is used. The scatter plot x-values are binned into discrete x-value bins. The 95th percentile of the y-values contained at each x-value bin is then obtained. The 95th percentile values at the discrete x-bins are interconnected to form a continuous piece-wise 95th percentile line graph, that is then plotted in red over the scatter plot. The data binning is done according to the following procedure:

Isolated LV networks:	X values are packed into discrete 1 kW bins, i.e. x-values are rounded off to the nearest kW. The 95th percentile for the y data values contained within each 1 kW-bin is then obtained.
Interconnected MV/LV- & MV networks:	X values are packed into discrete 10 kW bins, i.e. x-values are rounded off the to the nearest 10 kW. The 95th percentile for y the data values contained within each 10 kW-bin is then obtained.

In each of the scatter plots, a black dashed horizontal threshold line is drawn on the y-axis, at the values of the network violation limits. The network violations that are considered to determine PV hosting capacity, are voltage violations and thermal overload. Voltage violations are assessed at every node, or terminal, in the network, whilst thermal overload is considered for all cables and transformers. Thermal overload for cables and transformers is defined as a condition where the loading exceeds 100% of the rated value of the element. Voltage violations are defined as overvoltage (voltage > 1,1 p.u. and voltage > 1,05 p.u.) for LV- and MV networks respectively, as per the NRS 048-2 specification [44]. The PV penetration network violation thresholds are summarised in table 5.2.

**Table 5.2:** Network Violation Thresholds: PV Penetration Simulations (Active Network)

<b>Network</b>	<b>Overvoltage (p.u.) [44]</b>	<b>Cable Overload (%)</b>	<b>Transformer Overload (%)</b>
LV	1,1	100	100
MV	1,05	100	100

The first intersection of the black dashed threshold line and the red piece-wise 95th percentile line is taken as the maximum allowable cumulative PV capacity on the network. The practical significance of this intersection point is that at this particular cumulative PV capacity, 95% of PV placement combinations resulted in scenarios that do not violate network regulatory limits. Only 5% of placements combinations at this particular PV penetration level resulted in network violations. The choice to use the 95th percentile is simply because this provides a conservative threshold of acceptance, without being overly restrictive. If, for example, the same piece-wise percentile analysis was performed with the 100th percentile used as threshold of acceptance, the acceptable PV penetration level will be restricted to the



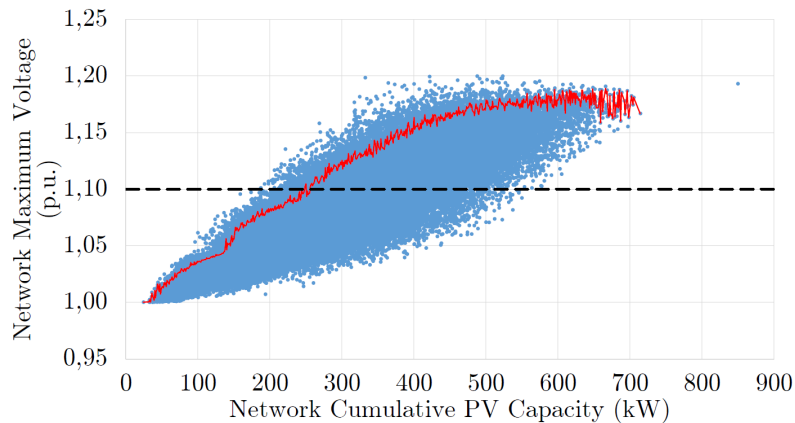
PV penetration level where the very first network violation occurs. This could result in a scenario where the maximum allowable PV capacity on the network is restricted to a value where only one simulated PV placement scenario resulted in a network violation, whereas hundreds/thousands of other placement scenarios, for the same PV penetration level, did not result in network violations. This illustrates how the acceptable PV penetration levels will vary according to the risk of network violations that is deemed acceptable by the analyst.

Since half-hourly average load data is used in the simulations, the y-axis variables (maximum observed voltage/-line loading/-transformer loading) represent the average condition observed at that node/line/transformer for that 30-minute interval. Any dots above the black threshold lines therefore represent a 30-minute average steady-state overvoltage/line overload/transformer overload. The isolated, rightmost dots on the scatter plots, provide the results for the scenarios of maximum PV installation on the networks, utilising all available PV-eligible roofspace (the red piece-wise 95th percentile line is not extended to these rightmost, isolated dots). In the scatter plots, *network cumulative PV capacity* refers to the sum total of the capacity of each PV system installed on that network. Each individual PV system's capacity is taken as the maximum output of the system's inverter.

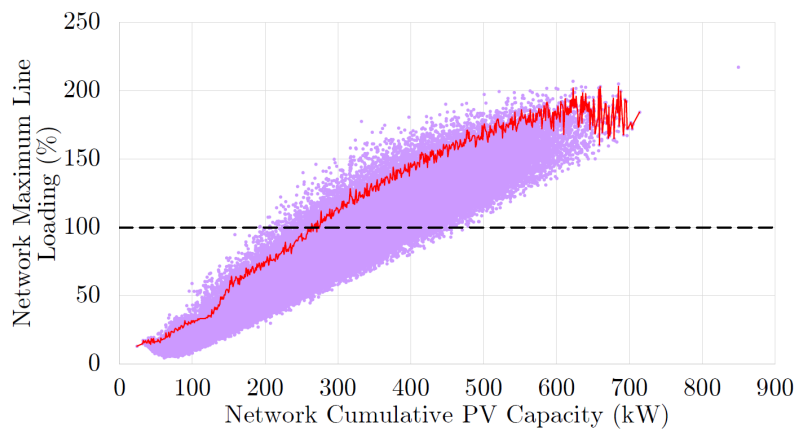
## 5.3.2 Case Study 1: Residential Network

### 5.3.2.1 Sunrise Isolated LV Network

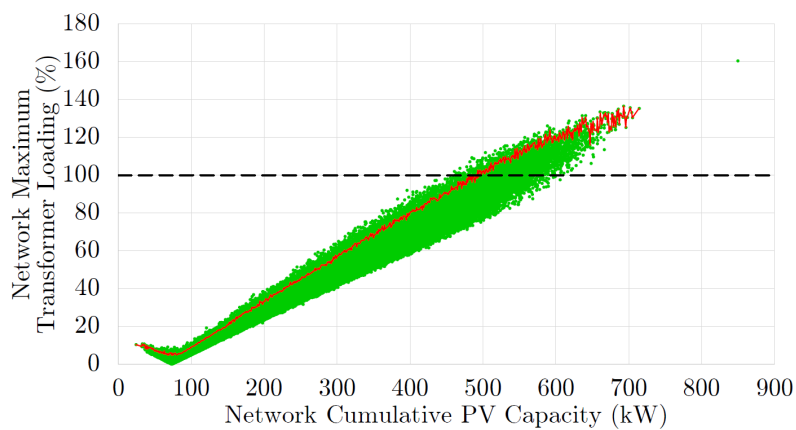
Figure 5.1 - figure 5.3 shows the voltage-, line loading- and transformer loading scatter plot results for Sunrise isolated LV network. Discussion on the results will follow in subsection 5.3.5.



**Figure 5.1:** Sunrise Isolated LV Network Maximum Voltage Results



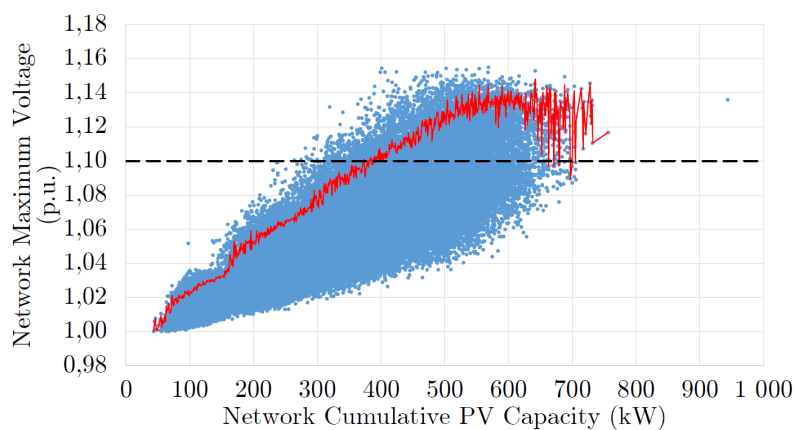
**Figure 5.2:** Sunrise Isolated LV Network Maximum Line Loading Results



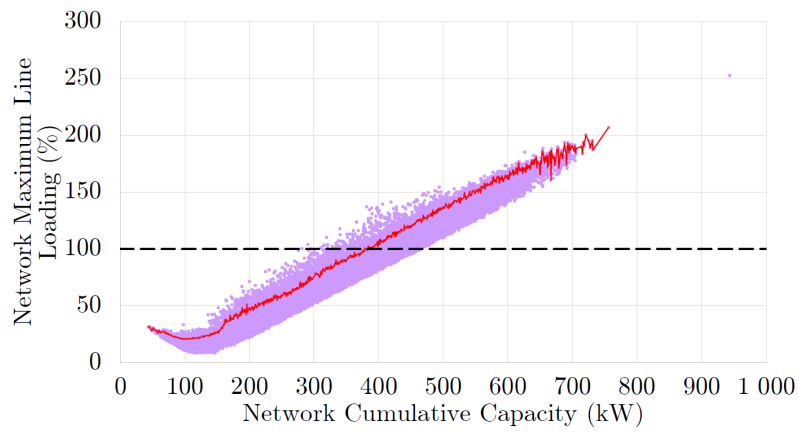
**Figure 5.3:** Sunrise Isolated LV Network Maximum Transformer Loading Results

### 5.3.2.2 Fish Isolated LV Network

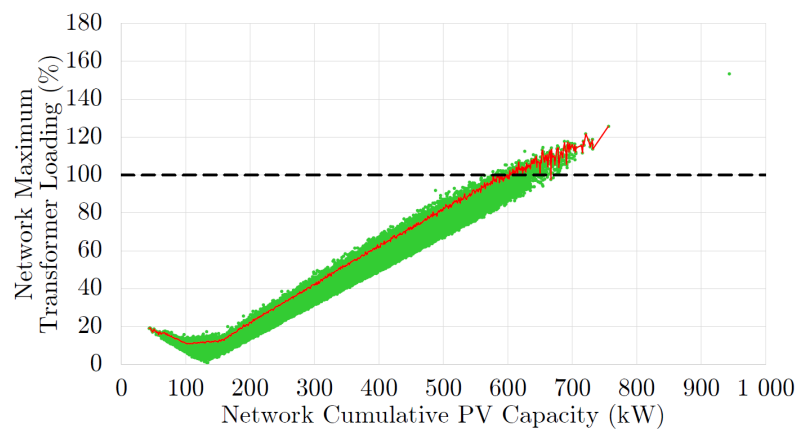
Figure 5.4 - figure 5.6 shows the voltage-, line loading- and transformer loading scatter plot results for Fish isolated LV network. Discussion on the results will follow in subsection 5.3.5.



**Figure 5.4:** Fish Isolated LV Network Maximum Voltage Results



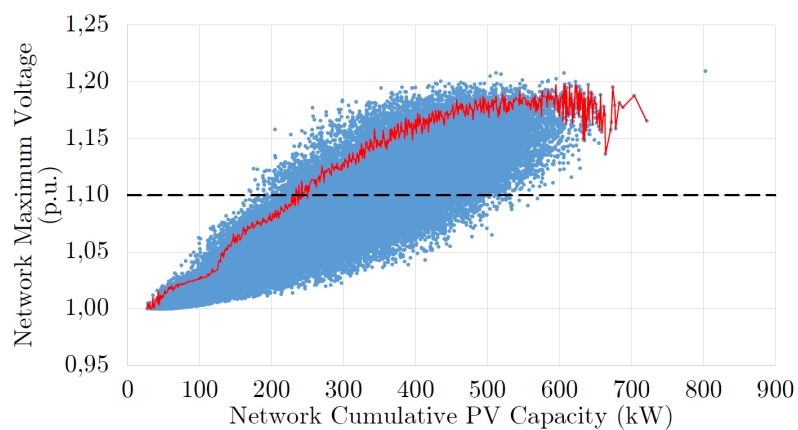
**Figure 5.5:** Fish Isolated LV Network Maximum Line Loading Results



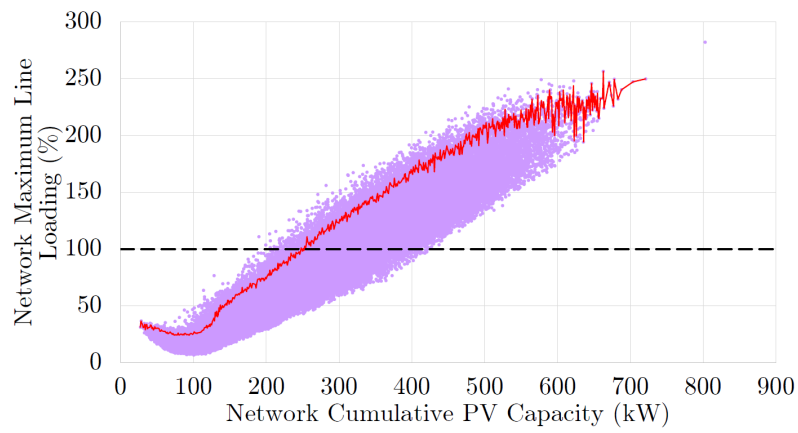
**Figure 5.6:** Fish Isolated LV Network Maximum Transformer Loading Results

### 5.3.2.3 Lion Isolated LV Network

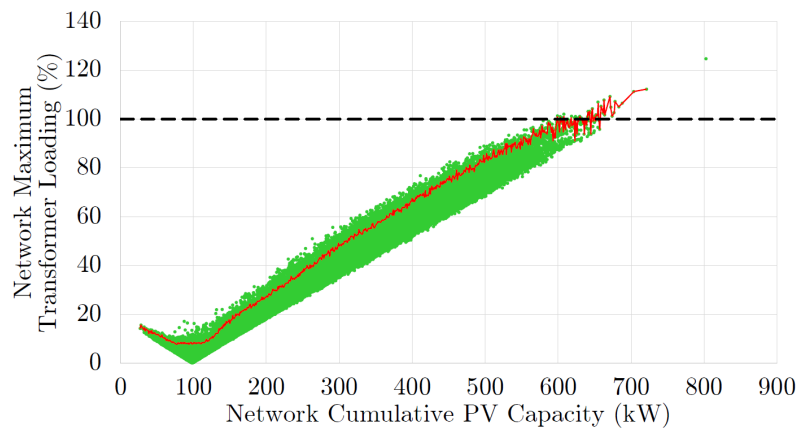
Figure 5.7 - figure 5.9 shows the voltage-, line loading- and transformer loading scatter plot results for Lion isolated LV network. Discussion on the results will follow in subsection 5.3.5.



**Figure 5.7:** Lion Isolated LV Network Maximum Voltage Results



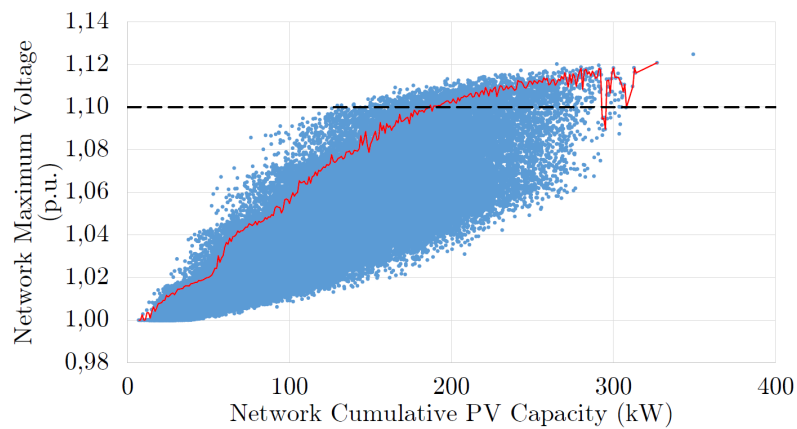
**Figure 5.8:** Lion Isolated LV Network Maximum Line Loading Results



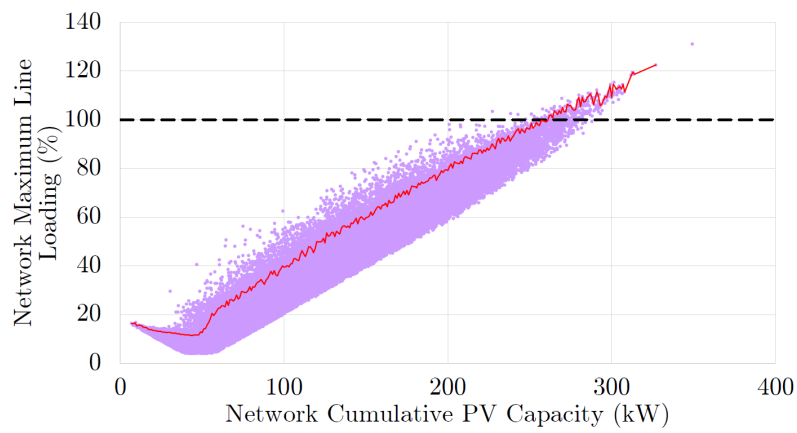
**Figure 5.9:** Lion Isolated LV Network Maximum Transformer Loading Results

### 5.3.2.4 Oak Isolated LV Network

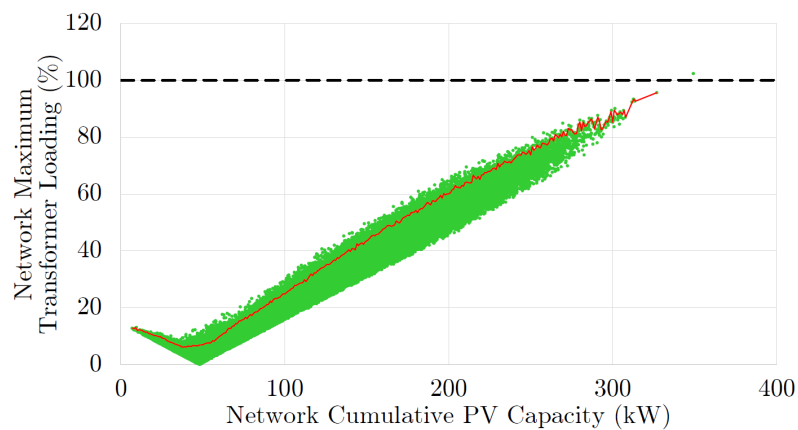
Figure 5.10 - figure 5.12 shows the voltage-, line loading- and transformer loading scatter plot results for Oak isolated LV network. Discussion on the results will follow in subsection 5.3.5.



**Figure 5.10:** Oak Isolated LV Network Maximum Voltage Results



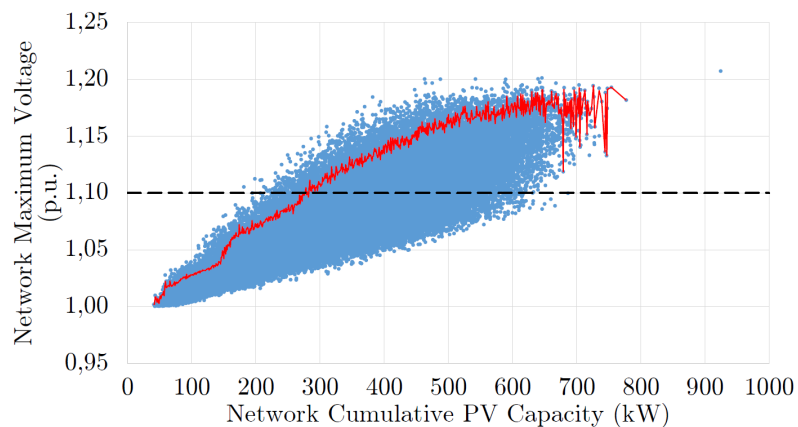
**Figure 5.11:** Oak Isolated LV Network Maximum Line Loading Results



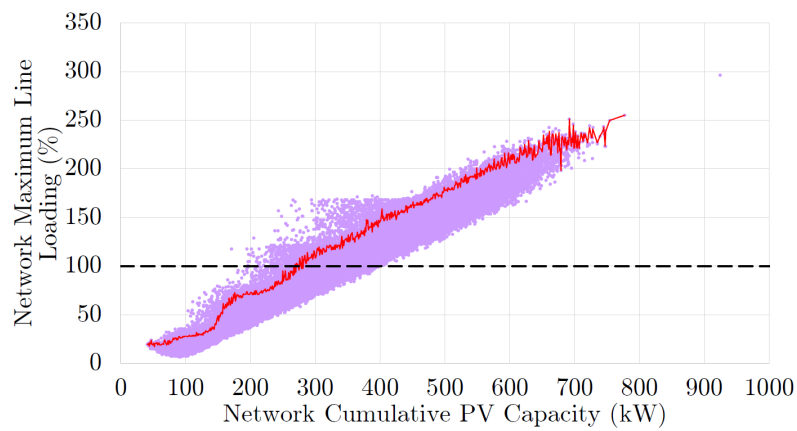
**Figure 5.12:** Oak Isolated LV Network Maximum Transformer Loading Results

### 5.3.2.5 Market Isolated LV Network

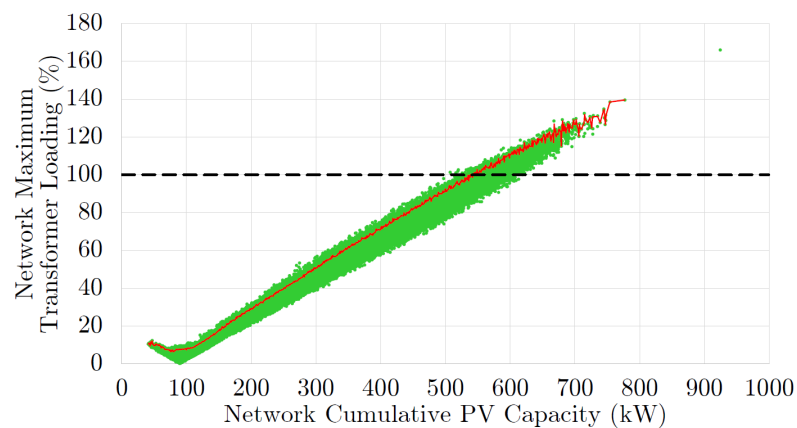
Figure 5.13 - figure 5.15 shows the voltage-, line loading- and transformer loading scatter plot results for Market isolated LV network. Discussion on the results will follow in subsection 5.3.5.



**Figure 5.13:** Market Isolated LV Network Maximum Voltage Results



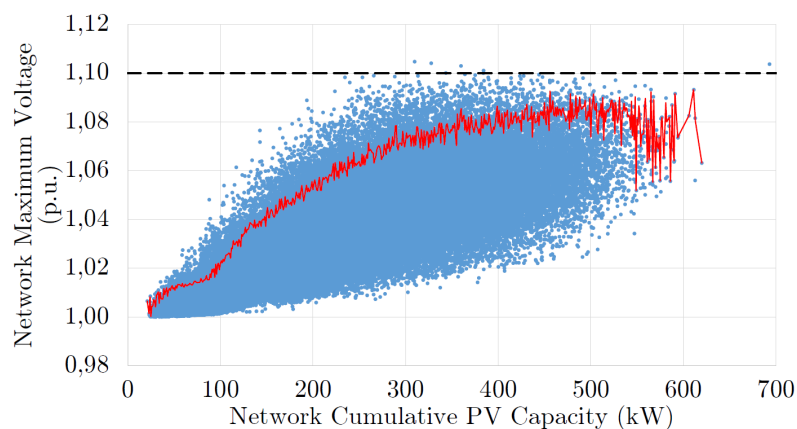
**Figure 5.14:** Market Isolated LV Network Maximum Line Loading Results



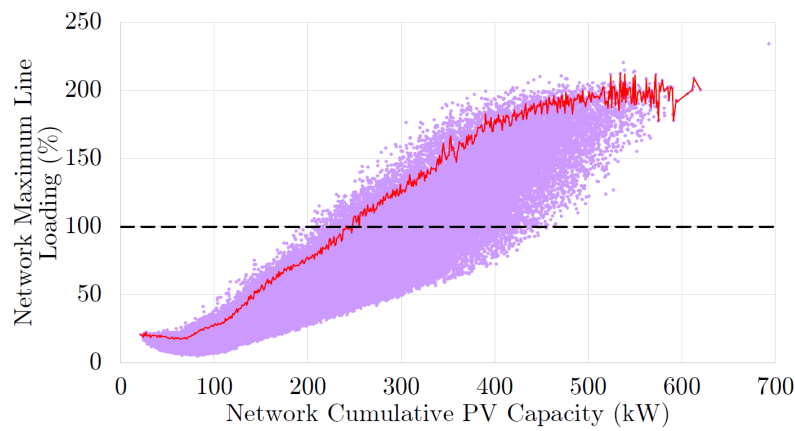
**Figure 5.15:** Market Isolated LV Network Maximum Transformer Loading Results

### 5.3.2.6 Beach Isolated LV Network

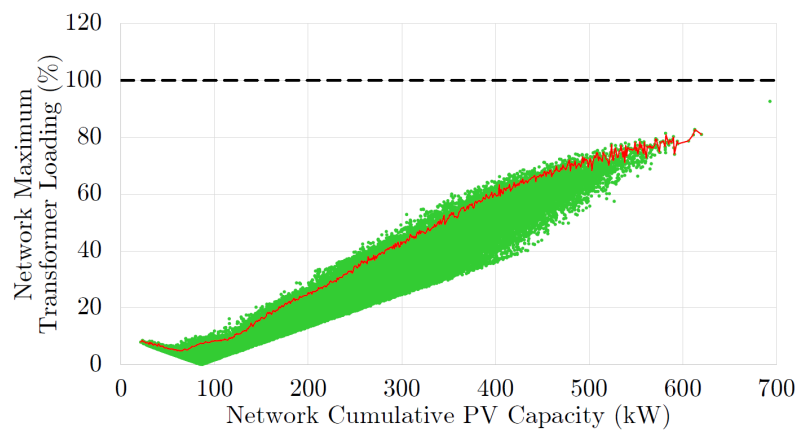
Figure 5.16 - figure 5.18 shows the voltage-, line loading- and transformer loading scatter plot results for Beach isolated LV network. Discussion on the results will follow in subsection 5.3.5.



**Figure 5.16:** Beach Isolated LV Network Maximum Voltage Results



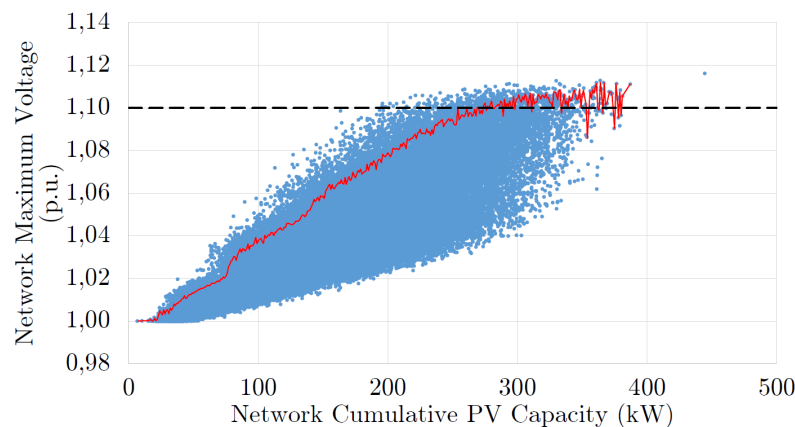
**Figure 5.17:** Beach Isolated LV Network Maximum Line Loading Results



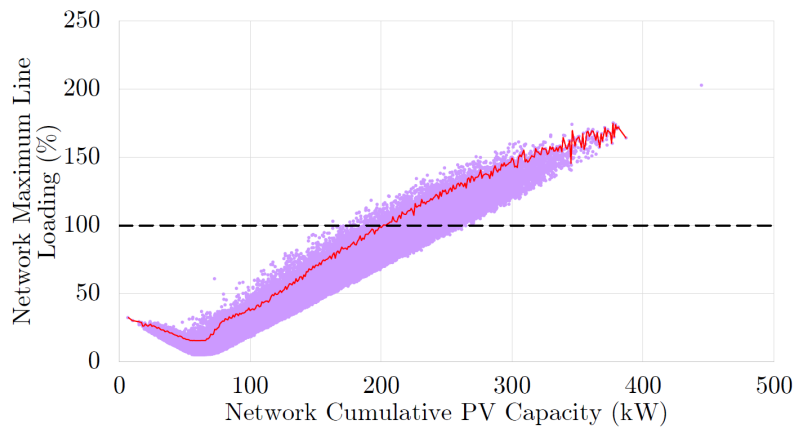
**Figure 5.18:** Beach Isolated LV Network Maximum Transformer Loading Results

### 5.3.2.7 Grave Isolated LV Network

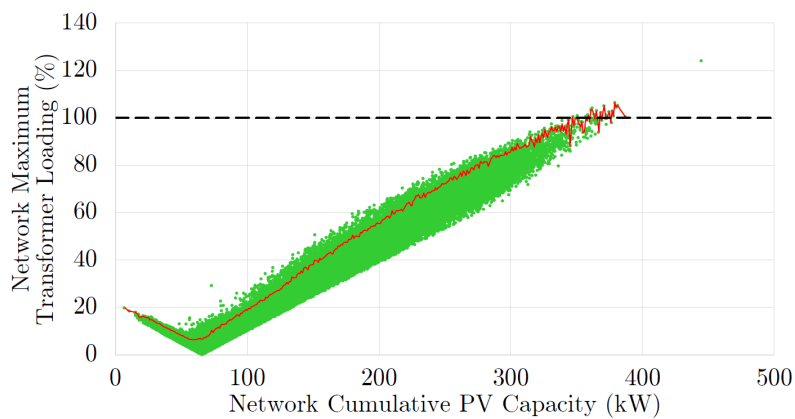
Figure 5.19 - figure 5.21 shows the voltage-, line loading- and transformer loading scatter plot results for Grave isolated LV network. Discussion on the results will follow in subsection 5.3.5.



**Figure 5.19:** Grave Isolated LV Network Maximum Voltage Results



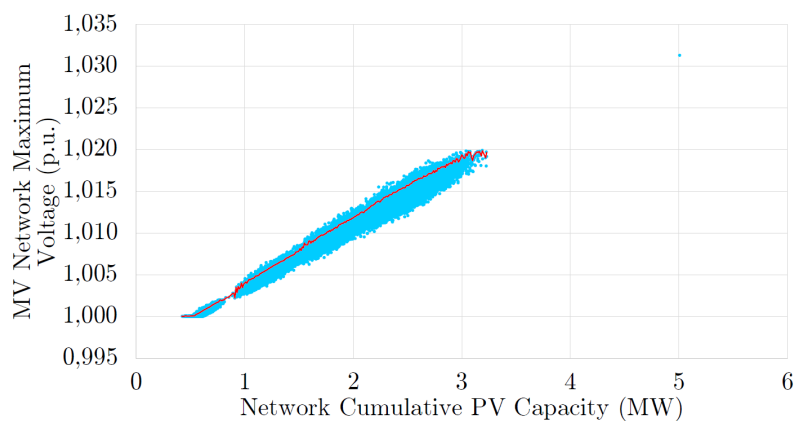
**Figure 5.20:** Grave Isolated LV Network Maximum Line Loading Results



**Figure 5.21:** Grave Isolated LV Network Maximum Transformer Loading Results

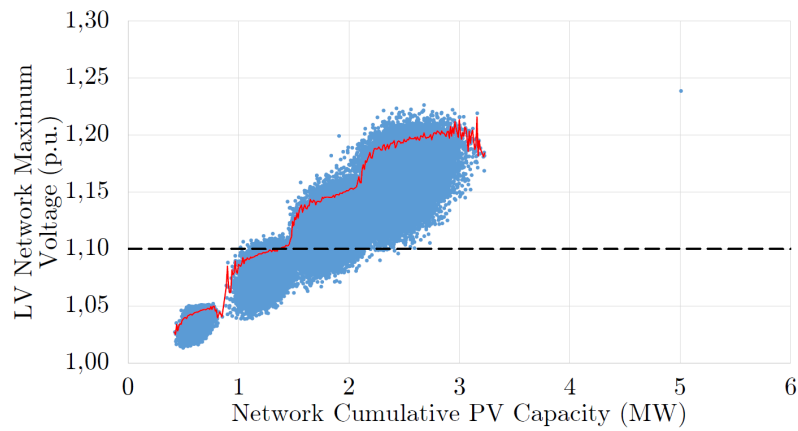
### 5.3.2.8 Residential Interconnected MV/LV Network

Figure 5.22 - figure 5.25 shows the voltage-, line loading- and transformer loading scatter plot results for the residential interconnected MV/LV network. Discussion on the results will follow in subsection 5.3.5.



**Figure 5.22:** Residential Interconnected MV/LV Network: MV Network Maximum Voltage Results





**Figure 5.23:** Residential Interconnected MV/LV Network: LV Network Maximum Voltage Results

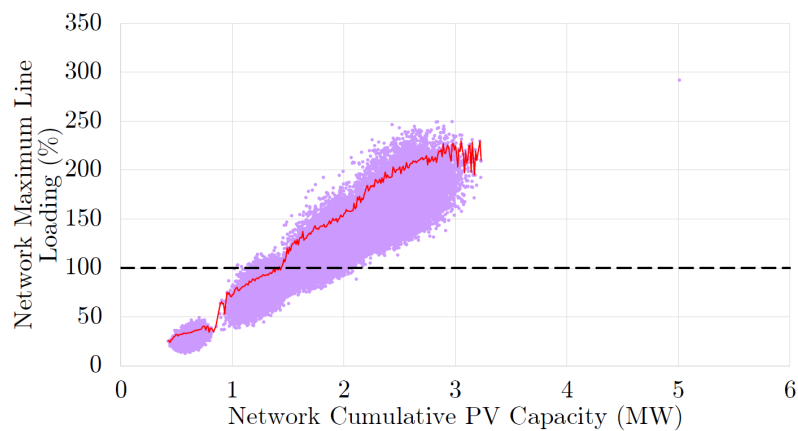


**Figure 5.24:** Residential Interconnected MV/LV Network Maximum Line Loading Results

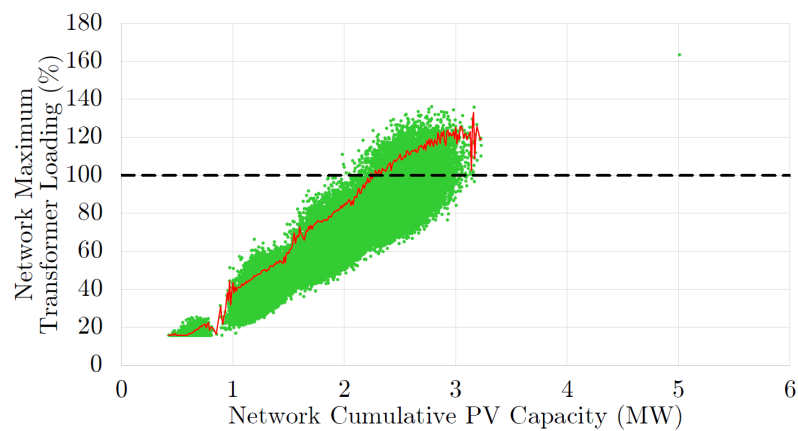


**Figure 5.25:** Residential Interconnected MV/LV Network Maximum Transformer Loading Results

### 5.3.3 Case Study 2: Commercial Network

Figure 5.26 - figure 5.28 shows the voltage-, line loading- and transformer loading scatter plot results for the commercial network. Discussion on the results will follow in subsection 5.3.5.

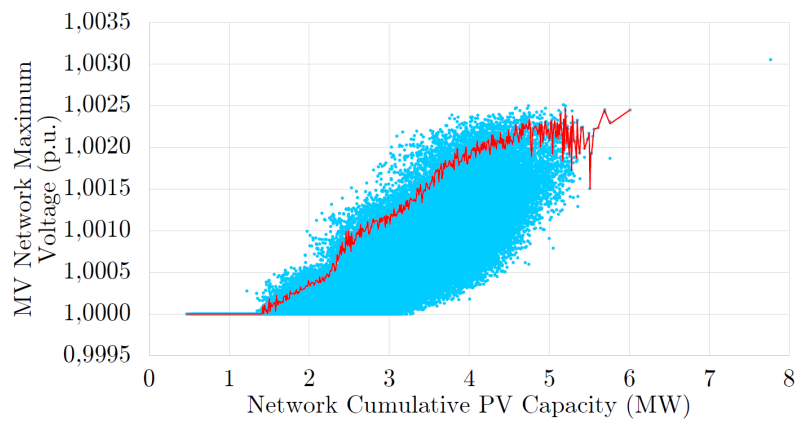


**Figure 5.26:** Commercial Network: MV Network Maximum Voltage Results

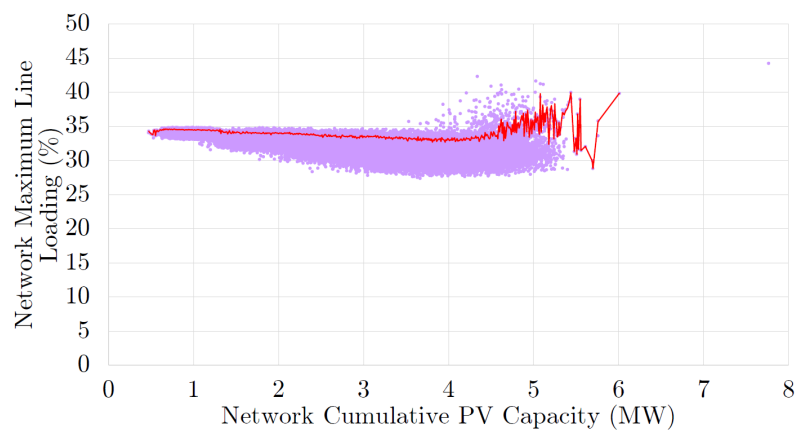


**Figure 5.27:** Commercial Network Maximum Line Loading Results

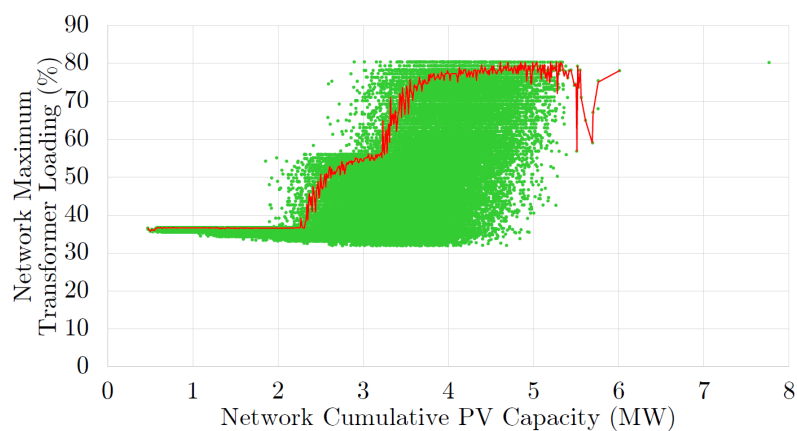


**Figure 5.28:** Commercial Network Maximum Transformer Loading Results

### 5.3.4 Case Study 3: Industrial Network

Figure 5.29 - figure 5.31 shows the voltage-, line loading- and transformer loading scatter plot results for the industrial network. Discussion on the results will follow in subsection 5.3.5.

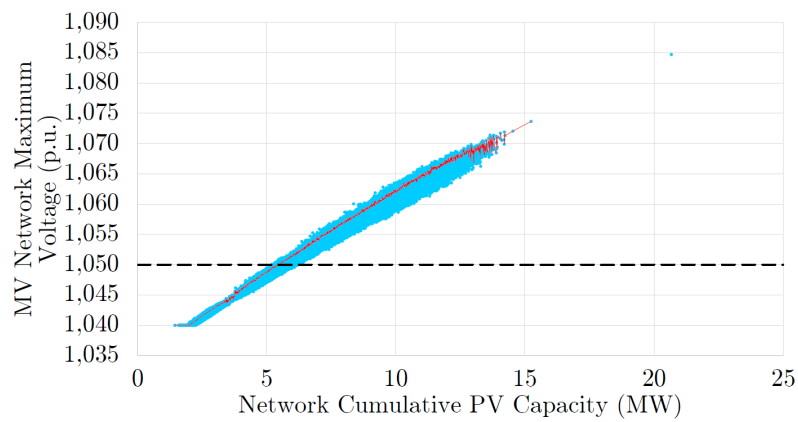


**Figure 5.29:** Industrial Network: MV Network Maximum Voltage Results

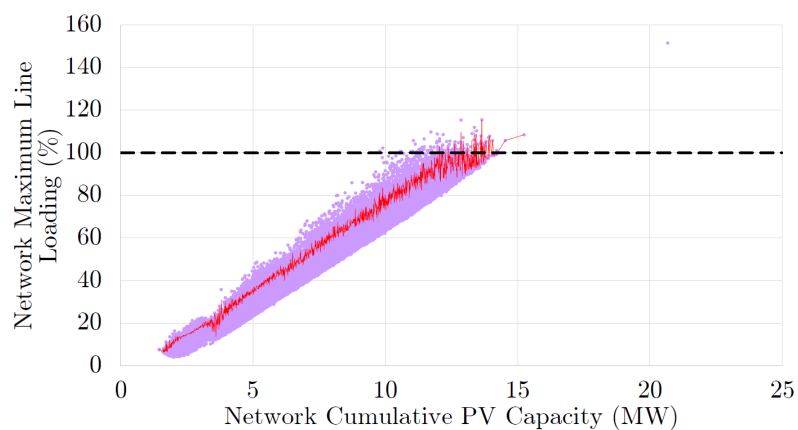


**Figure 5.30:** Industrial Network Maximum Line Loading Results

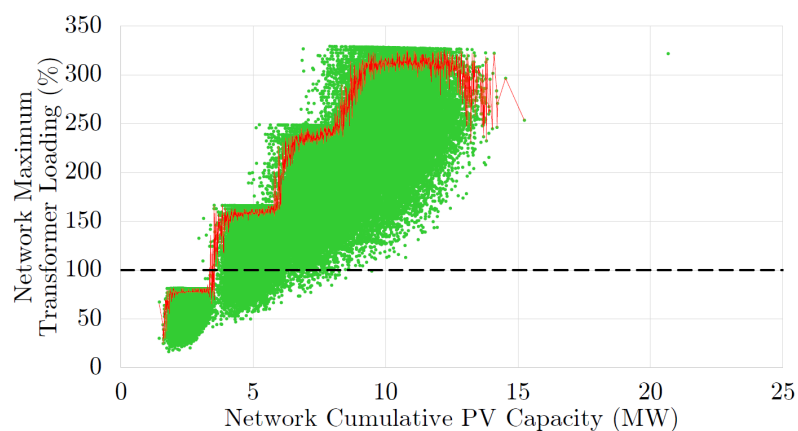


**Figure 5.31:** Industrial Network Maximum Transformer Loading Results

### 5.3.5 Results Summary and Discussion

Key results are summarised in table 5.3 - table 5.5. Table 5.3 provides information on the worst-case scenarios for each network - that is, the network conditions that could arise if all PV-eligible roofspace is used, and the maximum possible PV penetration level (as limited

by roofspace) is reached. Table 5.4 provides information the maximum allowable PV that can be installed on each network, according to each network violation, and concludes the decisive network violation that limits PV uptake for each network. Table 5.5 summarises the PV penetrations results obtained in this project, according to all the modelling-, simulation- and results analysis procedures presented in this thesis. Observations made from the results are discussed following the tables.

**Table 5.3:** PV Penetration Results for Scenarios Utilising Maximum PV-eligible Roofspace

Network	Maximum Possible PV (kW)	Maximum MV Voltage (p.u)	Maximum LV Voltage (p.u.)	Maximum Line Loading (%)	Maximum Transformer Loading (%)
Sunrise isolated LV	850	-	1,19	217	161
Fish isolated LV	944	-	1,14	252	153
Lion isolated LV	803	-	1,21	282	125
Oak isolated LV	349	-	1,12	131	102
Market isolated LV	924	-	1,21	296	166
Beach isolated LV	693	-	1,10	234	93
Grave isolated LV	445	-	1,12	203	124
Residential IC MV/LV	5008	1,03	1,23	292	163
Commercial	7767	1,00	-	44	80
Industrial	20673	1,08	-	152	322

**Table 5.4:** Maximum Allowable PV According to Each Network Violation

Network	Allowable PV (kW)				
	MV Voltage Violation	LV Voltage Violation	Line Loading Violation	Transformer Loading Violation	Decisive Network Violation
Sunrise isolated LV	-	249	264	491	LV overvoltage
Fish isolated LV	-	373	379	596	LV overvoltage
Lion isolated LV	-	234	248	599	LV overvoltage
Oak isolated LV	-	187	262	*	LV overvoltage
Market isolated LV	-	277	269	539	Line overload
Beach isolated LV	-	*	241	*	Line overload
Grave isolated LV	-	254	202	347	Line overload
Residential IC MV/LV	*	1470	1420	2240	Line overload
Commercial	*	-	*	*	None
Industrial	5420	-	12050	3350	Transformer overload

\*no threshold crossing

**Table 5.5:** Summary of PV Penetration Results

<b>Network</b>	<b>Max allowable PV (kW)</b>	<b>PV Penetration (%)</b>	<b>Constraint</b>
Sunrise isolated LV	249	87	LV overvoltage
Fish isolated LV	373	150	LV overvoltage
Lion isolated LV	234	121	LV overvoltage
Oak isolated LV	187	82	LV overvoltage
Market isolated LV	269	102	Line overload
Beach isolated LV	241	83	Line overload
Grave isolated LV	202	119	Line overload
Residential IC MV/LV	1420	122	Line overload
Commercial	7767	60	Maximum roofspace
Industrial	3350	31	Transformer overload

In subsection 3.5.3 and subsection 3.5.4, as part of the literature discussion on the technical effects of DG on electrical distribution networks, it was shown that the installation of DG can reduce line- and transformer loading (and consequently system losses). However, this happens only up to a certain point, after which the effect reverses as DG penetration levels increase. This was confirmed in the simulation results - in several scatter plots (Sunrise Isolated LV transformer-, Fish Isolated LV line-, Fish Isolated LV transformer-, Lion Isolated LV line-, Lion Isolated LV transformer-, Oak Isolated LV line-, Oak Isolated LV transformer-, Market Isolated LV transformer-, Beach Isolated LV line-, Beach Isolated LV transformer-, Grave Isolated LV line-, and Grave Isolated LV transformer loading), it is observed that initially, at low PV installation levels, the maximum line- and maximum transformer loading is reduced. This loading reduction is only observed until a certain point of PV installation levels, after which the effect reverses, and line- and transformer loadings increase again. The initial reduction in line- and transformer loading is because the load requirements of the network is partly fulfilled by the PV systems. Loads are supplied by their own PV systems, reducing conventional load demand from the substation, which consequently leads to reduced transformer- and line loading. As PV penetration levels start to increase, and surplus PV generation starts to manifest, reverse power flow (and eventually excessive reverse power flow) will increase line- and transformer loading, as well as system losses.

When considering the network MDs for the residential LV networks, it is observed that all network MDs (except for Sunrise Isolated LV) is determined by the constraint of line overload. For passive, load-only conditions, it was expected that overload problems would occur before undervoltage problems, since these are short cable circuits (it was expected that for short cables, overload would be more of a concern than undervoltage, whereas undervoltage would be more of a concern on long cables). The Sunrise Isolated LV network MD, is however constrained by undervoltage. This is most likely due to voltage imbalance, caused by the single-phase customer connections. In subsection 3.5.5, as part of the literature discussion on the technical effects of DG on electrical distribution networks, it was shown that voltage imbalance could become a significant problem when single-phase DG is installed on LV networks with single-phase customers. Table 5.5 shows that the potential uptake of 4 LV networks (Sunrise, Fish, Lion and Oak) is constrained by LV overvoltage. It is interesting to notice that the networks MDs of Fish, Lion and Oak were constrained by line overload, but their potential PV uptake is constrained by overvoltage. This shows that the introduction of PV on these networks causes unbalanced voltage rise that causes the network to violate reg-

ulatory voltage limits, before line overload occurs, as had been the constraint in the passive, load-only case. Three of the LV networks (Market, Beach and Grave), however, still have PV uptake potentials that are constrained by line overload. From table 5.4, it is observed that transformer loading is never the bottleneck to the uptake of PV for the isolated residential LV networks. Voltage- and line loading violations will occur long before the transformers are overloaded. The transformers are adequately sized to handle PV penetration levels beyond that what is possible due to voltage- and line loading violations. It must be noted that the residential LV networks differ vastly. This can be seen in total customers (ranging from 30 - 55), transformer rating (315 kVA - 800 kVA), as well as network topology and cable composition (shown in appendix A.1). The consequence is a wide spectrum of maximum allowable PV installations (187 kW - 373kW) and PV penetration levels (82% - 150%), as well as differing constraints (overvoltage and line overload) to PV uptake. No general rule of thumb dictates allowable PV penetration on the isolated LV networks. The reason for initially studying the LV networks independently, was to investigate if consistencies between results for the different LV networks existed, in order to determine if generalisations could be made for LV network PV hosting capacities. The results, however, indicate that each network should be considered on a case-to-case basis, and results cannot be generalised.

Results for the residential interconnected MV/LV network, which provides the practical operating scenario, show that line overload is the bottleneck to the PV hosting capacity for the interconnected network. When ignoring the line overload, and observing only the voltage results, it can be observed that in terms of voltages, LV voltages will be the bottleneck to the PV hosting capacity, and not MV voltages. LV voltage violations limit the allowable PV installations to 1470 kW, whereas, for even the worst-case scenario of maximum possible PV installations (5008 kW), no MV voltage violations occur. Once again, transformer overload is not the violation of concern.

Even at maximum possible PV penetration levels, as limited by PV-eligible roof space, the commercial network is still safely operating within regulatory limits. The maximum voltage rise is just over 1,003 p.u., whereas the maximum possible loading is 44% for lines, and 80% for transformers. The commercial network is the only network where the network MD exceeds the maximum possible PV installations. It is observed that there is not enough PV-eligible roof space in the commercial area to be of any concern to network operation. From a practical perspective, it can be reasoned that this is due to the multi-storey characteristics of the commercial buildings, making them dense, concentrated loads. A dense, multi-storey load will likely consume most of the PV power generated on its roof space, leaving little excess power for export to the network.

The industrial area experiences the same scenario as the residential network, where the amount of installable PV, as limited by PV-eligible roof space, far exceeds the network MD. The decisive network violation posing the bottleneck to PV uptake in the industrial area, is transformer overload. In subsection 4.3.2, it was mentioned that loads in industrial buildings do not necessarily scale according to floor space, as it depends on the type of industry and the machinery or processes used. There is not necessarily good correlation between building size and load size for an industrial area. A practical example is a situation where a large building, with plenty of roof space, such as a storage warehouse, may have a small load (compared to other industrial loads) due to the absence of electrical machines and other heavy industrial loads. Such a building will be supplied by a small transformer, but have vast amounts of roof space for PV installations (the industrial area has, at some load nodes, small 100- and 200 kVA transformers). Even in scenarios where a moderate/large size trans-

former is present, the amount of roof space, and subsequent PV generation capacity, may prove to exceed the capabilities of the transformer.

In an industrial area, PV generation needs to be sized in correlation with the building load, or in cases where a large PV system is installed with the purpose of exporting a significant amount of PV power to the network, appropriate transformer upgrades will be necessary. If transformer resizing solves the transformer overload issue, MV voltage violations will be the next issue of concern in the industrial area. This will necessitate active voltage regulation techniques, to keep the network voltage within regulatory limits. In this regard, when considering figure 5.29, it can be seen that the industrial network's MV voltage scatter plot starts at a minimum of 1,04 p.u. The reason for this is because of the default setting of the OLTC at South HV/MV distribution substation. The Eskom tap-changer in the substation is usually set to 1,05 p.u. and has a bandwidth of  $\pm 1\%$  [28]. When performing load-flow studies on passive networks, undervoltages are typically the concern, and the tap-changer position is set to 1,04 p.u. as a conservative approach [28]. In this project, the tap-changer was kept at its 1,04 p.u. position. The MV overvoltage issue, when PV generators are present, can be solved by adjusting the tap changer at South substation to the 1,00 p.u. position. Even under maximum possible PV penetration, MV overvoltage will then not be a problem anymore. If no transformer upgrades, or lowering of the substation OLTC tap position is implemented, transformer overload will limit the maximum allowable PV to 3 350 kW, whereas MV voltage violation will limit the maximum allowable PV uptake to 5 420 kW. If these two issues are solved, the industrial network hosting capacity can be increased to 12 050 kW, as limited by line overload.

Some of the results yielded rather odd-shaped scatter plots. A discussion in this regard is appropriate. Consider the LV voltage-, line loading- and transformer loading results (figure 5.23 - figure 5.25) for the residential interconnected MV/LV network. It can be seen that 4 distinct clusters (or smaller, localised scatter plots) formed in the results scatter plots. This clustering-effect can be attributed to the PV placement algorithm, discussed in subsection 4.4.3.2. The algorithm simulates 100 000 PV placement scenarios in 4 phases, where each phase consists of 25 000 simulations. In the first phase, individual PV generator capacities are restricted between 0%-25% of their individual maximum potential (as limited by roof space), in phase 2 between 0%-50%, in phase 3 between 0%-75%, and in phase 4 between 0%-100%. The localised clusters correspond to the 4 simulation phases. For the residential network, the clustering effect is only observed for the interconnected MV/LV network, where the cumulative capacity can assume a much wider range (MW-range) as opposed to the isolated LV networks (kW-range). With regards to the clustering effect, a very important observation can be made. As an example, consider figure 5.24, which shows the line loading results for the residential interconnected MV/LV network (line overload was also the decisive constraint to PV uptake in this network). For the first cluster (leftmost, 0%-25%) the red piece-wise 95th percentile line is far below the black overload threshold line. For the second cluster, the red piece-wise 95th percentile line only crosses the black overload threshold line right towards the end of the cluster. For cluster 3 and -4, the entire red piece-wise 95th percentile line is above the black overload threshold line. This observation has very important practical significance. If each individual property is limited to between 0%-25% of its maximum PV generation potential, all PV-eligible properties can partake in PV generation. If each individual property is limited to between 0%-50% of its maximum PV generation potential, the majority of PV-eligible properties can also partake in PV generation. However, once properties are allowed to move into the 0%-75% and 0%-100% ranges, all PV-eligible properties will not be able to partake in PV generation any

longer. The consequence of not restricting the generation of individual properties, is that some properties can choose to install large systems that take up disproportionate amounts of the network's allowable PV capacity. This could prevent neighbouring properties from participating in PV generation. At anticipated higher PV penetration levels in the future, this will become an important regulatory issue. Utilities will need to implement fair regulations, in order to allow all property owners a fair share of PV generation.

The industrial network transformer loading scatter plot (figure 5.31) also displays the clustering effect. It is also observed that the top of each cluster displays a flat roof. Each transformer in the industrial network has a PV system and a load connected to its LV busbar. The maximum loading of the transformer will be dependent on maximum reverse power flow, which will correspond to the largest possible PV installation (as limited by roof space) on the transformer's LV busbar. In each cluster, each transformer's PV system is randomly assigned a capacity of 0%-25%, 0%-50%, 0%-75% and 0%-100% of its maximum possible capacity. In each cluster, each PV system is simulated 25 000 times - of these 25 000 simulations, a PV system can assume the same capacity value more than once. The flat roofs of the clusters are caused by the same transformer (likely a small transformer at a property with vast amounts of roof space, as previously discussed) - the transformer reaches its maximum PV capacity (25%-, 50%-, 75%-, and 100% of its maximum potential) a few times in clusters 1,2,3 and 4, which creates the unique shape of the scatter plot. The same discussion holds true for the commercial network transformer loading scatter plot (figure 5.28).



# Chapter 6

## Conclusions and Recommendations

### 6.1 Introduction

In this closing chapter, the purpose of the project will first be revisited, followed by an evaluation of the project objectives, and a discussion of the project findings and -contributions. The chapter concludes with closing remarks.

### 6.2 Project Purpose

The purpose of this project was to model the technical influence of randomly distributed solar PV uptake on electrical distribution networks. The technical influences considered were voltage rise and equipment overload. In the lack of a national standard dedicated to PV installations in South Africa, and subsequent allowable PV penetration levels on distribution networks, network studies were performed on local distribution networks in Cape Town. The aim was to provide a reference point to Eskom, CCT and other local municipalities with regard to the technical effects of distributed PV on distribution networks, and, more importantly, to provide a reproducible methodology with which network studies can be performed.

### 6.3 Evaluation of Project Objectives

The project objectives, as presented in chapter 1, are evaluated below.

**Provide a firm understanding of PV systems, conventional power systems, and the status quo when PV- and conventional power systems are integrated:**

The objective was fulfilled in chapter 2 and chapter 3, where a literature review addressed all relevant topics.

**Model the network topologies:**

The objective was fulfilled in subsection 4.3.1 in chapter 4, where a topology modelling methodology was presented.

**Model the electrical loads:**

The objective was fulfilled in subsection 4.3.2 in chapter 4, where a load modelling methodology was presented.

**Determine the PV uptake potential, in terms of the amount of available roofs-**

**pace for PV installations:**

The objective was fulfilled in subsection 4.3.3 in chapter 4, where a GIS-based methodology was presented.

**Model the power supply from rooftop PV systems:**

The objective was fulfilled in subsection 4.3.3 chapter 4, where a PV generation modelling methodology was presented.

**Develop software with which to perform network studies:**

The objective was fulfilled in section 4.4 in chapter 4, where DPL-based software was developed in Digsilent Powerfactory.

**Investigate the occurrence of voltage rise and equipment overload when PV is integrated into the networks:**

The objective was fulfilled in section 4.4 in chapter 4, where appropriate DPL-based algorithms were developed for this purpose, as well as in chapter 5, where voltage rise- and equipment overload results were presented and analysed.

**Determine the PV hosting capacities (allowable PV penetration level) of the networks, as well as the restraining technical issues that are the bottlenecks to further PV uptake:**

The objective was fulfilled in chapter 5, which presented results and an appropriate results analysis method with which to conclude the PV hosting capacities.

## 6.4 Project Findings and -Contributions

The literature review in chapter 2 provided sufficient evidence as to the fact that global PV uptake is rapidly increasing. Although large, utility-scale PV plants still dominate the global PV industry, there is a rapid increase in uptake of distributed rooftop PV systems. The global rise in PV uptake can partly be attributed to several environmental-, economic-, social- and technical factors, but remains largely a consequence of government and municipal incentives, -policies and -regulations. There is still a lack of a national standard with regard to grid-connected distributed PV installations. CCT have aligned with the NRS097-2-3 specifications and a self-developed regulatory process in this regard, whereas Eskom seems to be considering applications for grid-connection of distributed PV systems on a case-to-case basis. It seems that there are regulations employed to ensure that individual PV systems are grid-compliant, i.e. they operate within regulatory limits, but knowledge on the cumulative technical effects of a large number of PV systems on the same network, seems to be a grey area for local distribution system operators. The literature review in chapter 3 discussed the technical effects of DG on electrical distribution networks, and presented several technical issues that could arise when distributed PV is integrated into conventional, passive distribution systems. It is evident that rising PV penetration levels can cause significant technical challenges with regards to operation and control of power systems. These technical issues have already started to manifest in some places, as had been seen in some case studies presented.

In terms of collecting data for modelling of networks, it was found that monitoring- and record-keeping practices for LV networks do not seem to be in place in South Africa. This could be observed by the challenges faced when sourcing network data for LV networks. Furthermore, it was observed that in terms of load monitoring, there seems to be no downstream

load data from HV/MV distribution substations, nor higher-resolution than 30-minute data.

Studies on the LV networks concluded that the load supply capability under passive conditions is mostly limited by cable overload, whereas, in the presence of distributed PV generation, some of the LV networks seem to be battling more with overvoltage issues. It was shown that in all instances, line overload or overvoltage will be the constraining factors in terms of PV uptake on the residential LV networks, and that the MV/LV transformers are sufficiently sized to handle PV penetration levels beyond that what is possible due to voltage- and line loading violations. It was also shown that the installation of distributed PV has the ability to reduce line- and transformer loading (and associated losses) on LV distribution networks, but only at low penetration levels. At higher penetration levels, the effect starts to reverse and line- and transformer loading (and losses) will significantly increase. In terms of LV network PV hosting capacity, a wide spectrum of maximum allowable PV installations (187 kW - 373kW) and PV penetration levels (82% - 150%) was observed, as well as differing constraints (for some networks overvoltage, and for others line overload) to PV uptake. The differing results can be attributed to the vast difference between different LV networks in the same area, in terms of transformer rating, amount of customers, as well as network topology and cable composition. It was concluded that no general rule of thumb dictates allowable PV penetration on the LV networks. The results for the LV networks cannot be generalised, and each network needs to be considered on a case-to-case basis. An important conclusion made from the results for the interconnected MV/LV network, is that a higher violation-free cumulative PV capacity can be reached if individual PV generators are size-restricted. This will allow more property owners to participate in PV generation, whilst still keeping network conditions within regulatory limits.

The residential-, commercial- and industrial areas all exhibit significant scope for uptake of PV installations. The amount of PV-eligible roof space in the residential- and industrial areas provide PV generation capabilities that far exceed the load demand in the areas. The result is that it is possible to reach PV penetration levels that could have catastrophic technical influences on the residential- and industrial distribution networks. Although there is significant scope for PV installations in the commercial area, there is simply not enough PV-eligible roof space to cause adverse network effects in terms of voltage rise or equipment overload. The dense, multi-storey loads consume most of the PV power generated on their roofs, leaving little excess power for export to the network. Transformer overload is the main concern in terms of PV uptake in the industrial area, due to large PV-eligible roof spaces making it possible to install PV systems that will cause local transformer overload.

As PV penetration levels start to increase, more case-to-case studies of LV networks will need to be made. The observations made in this project should alarm utilities to sharpen up record-keeping practices for LV networks. Insufficient monitoring of LV networks will lead to utilities being blindsided by the technical effects that distributed PV generation will have on their LV networks. The LV network results show that utilities need to start planning appropriate regulatory frameworks for anticipated high PV penetration levels, in advance. This is in terms of adopting appropriate restrictions on the maximum size of individual PV systems that may be installed, in order to promote fair regulations with regards to PV uptake. Furthermore, revision of regulatory limits, in terms of QoS parameters, is appropriate in order to ensure that PV uptake will not unnecessarily be restricted by stringent regulations.

The available load data restricted the study to consider only steady-state voltage rise and

equipment overload. The observations in this study may encourage utilities to consider reviewing data monitoring processes. As an example, from a utility perspective it may be useful to monitor load data downstream from the HV/MV distribution substation at increased resolution, in order to allow an analyst to simulate network conditions over shorter intervals, in order to promote accuracy and perhaps even the ability to extend the study to include the modelling of transient effects, such as voltage variations due to cloud cover.

The results of this study provide a better understanding to utilities in terms of the technical limits that dictate PV uptake for different types of networks, as well as the corresponding PV penetration levels.

## 6.5 Closing Remarks

The topic of network integration of distributed PV generation presents vast scope for future research. As opposed to technical effects of distributed PV generation, the consideration of the economics of distributed PV generation opens up a vast field of study. As an example, in this project, it was mentioned that transformer resizing could significantly increase the allowable PV uptake in the industrial area - a very relevant follow-up investigation could focus on the economic feasibility of transformer resizing to increase allowable PV uptake in industrial areas. A key technical point of investigation in future studies will be the investigation of methods to increase allowable PV penetration on existing distribution networks. This topic will introduce network upgrade measures, and consequently, consideration of the economic feasibility of specific network upgrades.

This project presented a methodology that can be used as starting point for future studies. With more available data, the capability of the methodology can be extended to consider different technical effects of DG. The methodology is reproducible and can be adapted for certain scenarios. In future work, the load models (which are effectively mean values), can be extended to stochastic load models, in order to perform probabilistic load-flow simulations in conjunction with the randomly distributed solar PV models.

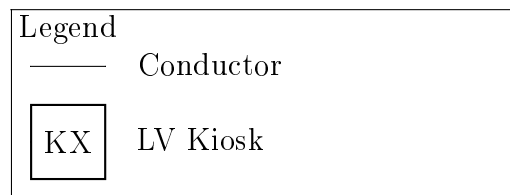
This project presented guidelines as to the PV hosting capacity of a sample residential-, commercial- and industrial network, derived by modelling the technical influence of randomly distributed solar PV uptake on electrical distribution networks. It is but a small sample set of networks, and future work will need to include a wider sample set, with studies on more networks, in order to lay a foundation that will improve the understanding of network integration of distributed PV generation. As the threshold limits of PV uptake, as derived in this project, are approached when PV penetration levels increase, detailed, scenario-specific studies will need to be performed.

# Appendices

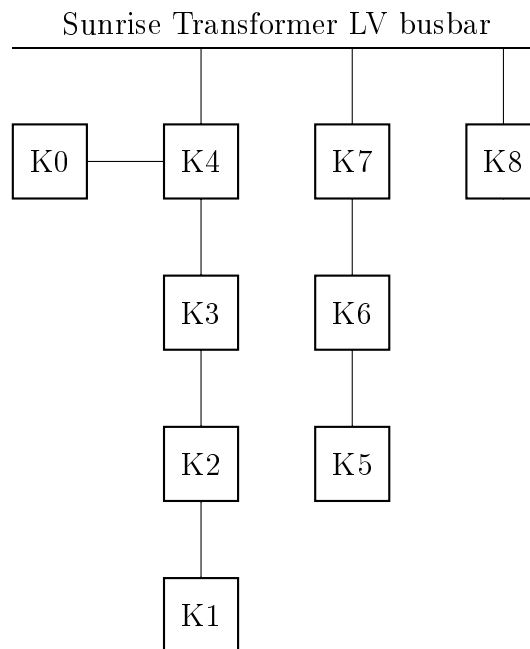
# Appendix A

## Residential Network Information

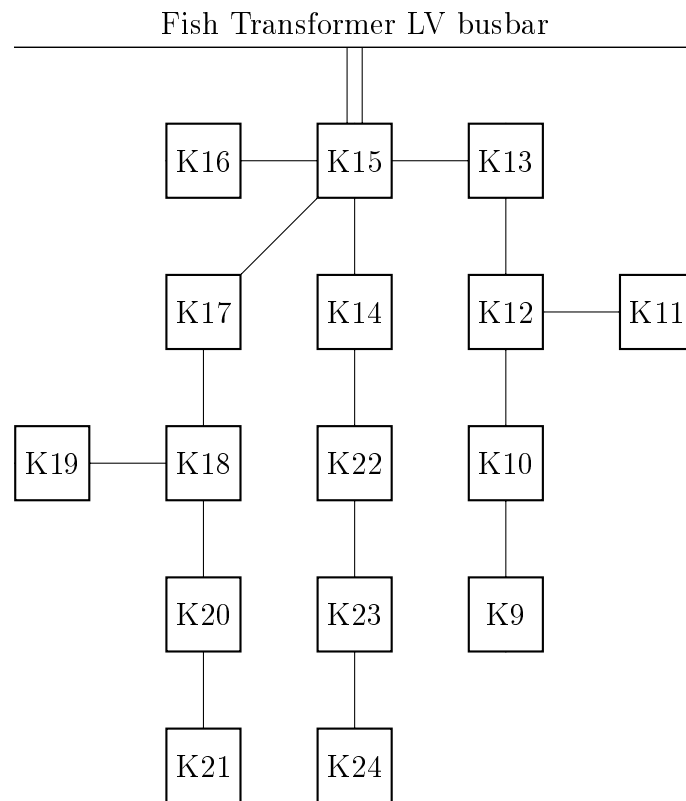
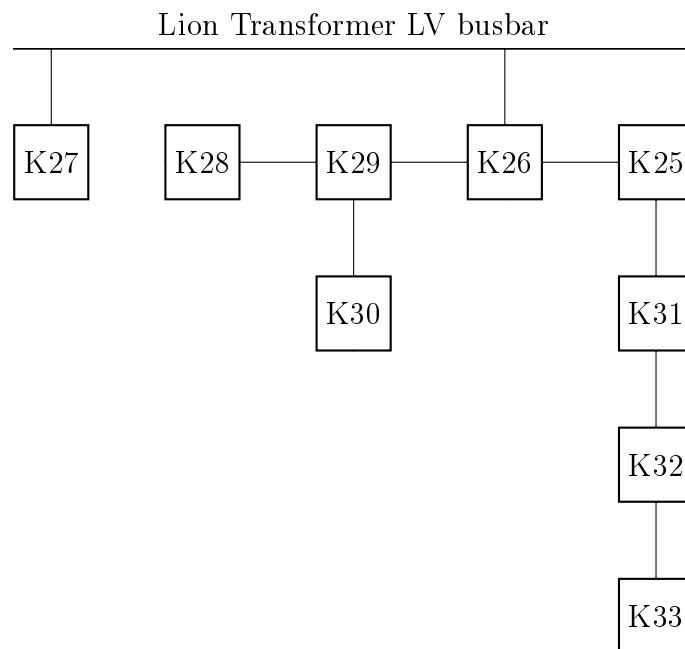
### A.1 Residential Network Topology

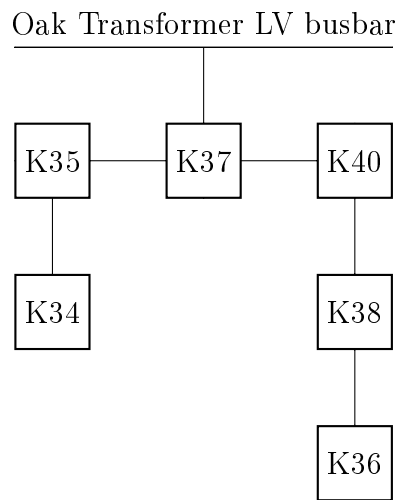
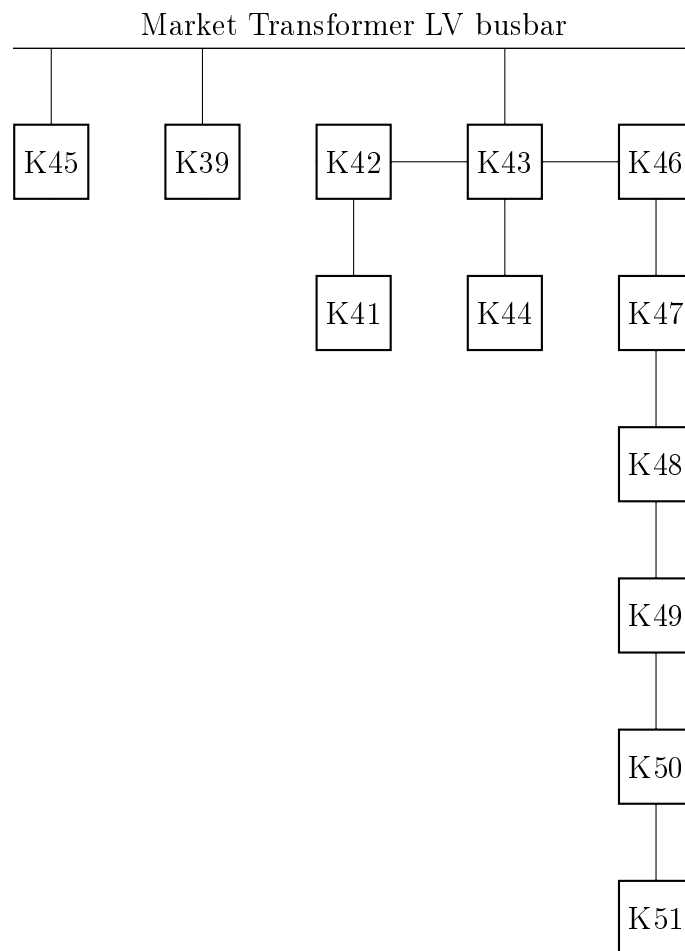


**Figure A.1:** LV Networks SLD Legend



**Figure A.2:** Sunrise LV Network SLD

**Figure A.3:** Fish LV Network SLD**Figure A.4:** Lion LV Network SLD

**Figure A.5:** Oak LV Network SLD**Figure A.6:** Market LV Network SLD



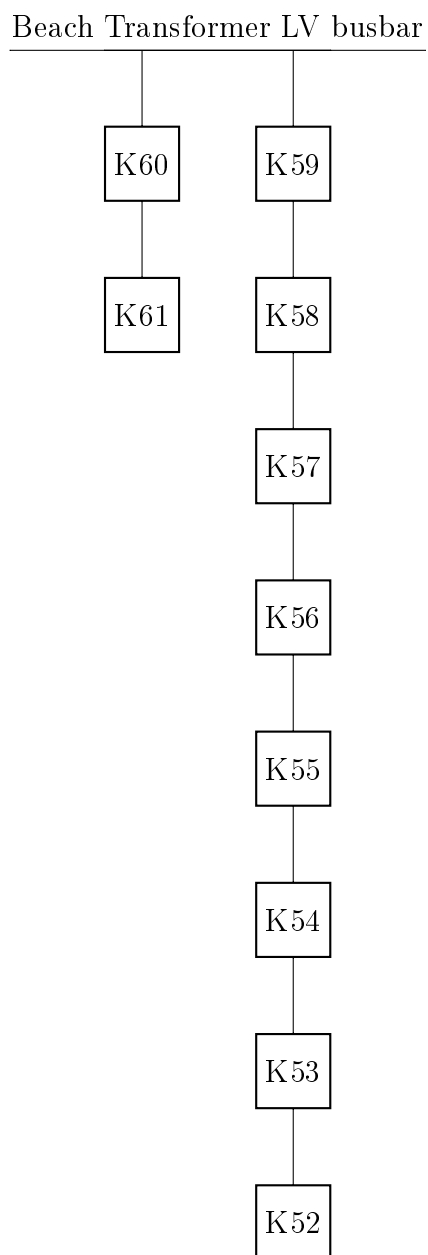


**Figure A.7:** Beach LV Network SLD

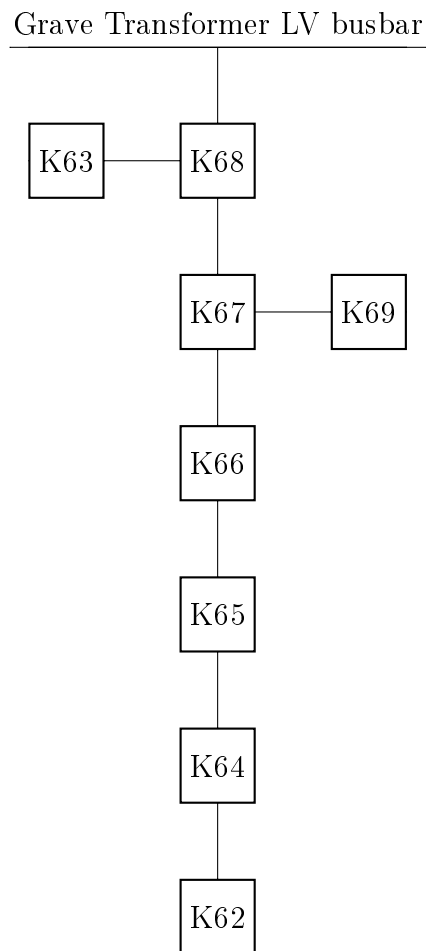


Figure A.8: Grave LV Network SLD

Table A.1: Residential Network LV Kiosks Phase Allocation

Kiosk	Allocated Properties		
	Phase A	Phase B	Phase C
0	2	2	1
1	1	2	2
2	2	1	1
3	1	1	2
4	1	1	0
5	1	1	2
6	1	2	1
7	1	2	1
8	2	1	1
9	1	1	1
10	1	2	1
11	2	1	1
12	1	1	2
13	1	2	1
14	1	1	1
15	0	0	0

Continued on next page

**Table A.1:** Residential Network LV Kiosks Phase Allocation  
- continued from previous page

Kiosk	Allocated Properties		
	Phase A	Phase B	Phase C
16	2	1	1
17	0	1	1
18	1	0	1
19	0	1	1
20	2	2	2
21	2	2	2
22	0	1	1
23	1	1	2
24	1	2	1
25	2	2	1
26	3	3	2
27	2	2	2
28	2	1	1
29	0	2	2
30	2	2	0
31	1	2	1
32	1	1	1
33	2	3	2
34	1	2	1
35	2	2	3
36	1	2	2
37	2	1	1
38	2	2	2
39	0	1	1
40	1	2	1
41	2	2	2
42	2	2	2
43	1	1	1
44	3	2	2
45	2	2	2
46	0	1	1
47	1	0	1
48	1	1	0
49	2	1	1
50	1	1	1
51	1	1	1
52	0	1	0
53	0	0	1
54	1	1	1
55	2	2	1
56	1	1	1
57	2	2	1
58	3	2	2

Continued on next page

**Table A.1:** Residential Network LV Kiosks Phase Allocation  
- continued from previous page

Kiosk	Allocated Properties		
	Phase A	Phase B	Phase C
59	3	3	3
60	3	3	4
61	3	3	3
62	2	2	3
63	3	3	2
64	2	2	3
65	3	3	2
66	1	2	1
67	2	2	1
68	0	1	1
69	1	1	1

**Table A.2:** Residential Network MV Cable Composition derived from [70]

<b>From</b>	<b>To</b>	<b>Cable Segment Composition, In Series: Conductor; Size(mm<sup>2</sup>); Length (m)</b>	<b>Total Cable Length(m)</b>
Church Road	Mountain	Al; 300; 116 + Cu; 161; 29 + Cu; 129; 1010	1155
Mountain	Roy	Al; 120; 771	771
Mountain	East	Cu; 65; 639	639
East	Hill	Al; 50; 372	372
East	Sugar	Cu; 65; 60 + Al; 120; 595	655
Sugar	Oak	Al; 50; 637	637
Oak	Lion	Al; 50; 127 + Al; 65; 405 + Al; 50; 115	647
Lion	Fish	Al; 50; 125 + Al; 65; 58	183
Fish	Sunrise	Al; 65; 44 + Al; 120; 4 + Al; 65; 103 + Al; 50; 5 + Al; 65; 343	499
Sugar	Market	Al; 120; 792	792
Market	Beach	Al; 120; 214 + Al; 50; 256	470
Beach	Grave	Al; 50; 512	512
Market	Disciple	Al; 120; 587 + Cu; 70; 10	597
Disciple	Artillery	Cu; 70; 10 + Cu; 39; 90	100
Artillery	Pole	Cu; 70; 10 + Cu; 39; 522 + Al; 50; 2	534

**Table A.3:** Residential Network LV Cable Composition derived from [70]

<b>From</b>	<b>To</b>	<b>Cable Segment Composition, In Series: Conductor; Size (mm<sup>2</sup>); Length (m)</b>	<b>Total Cable Length(m)</b>
Sunrise LV busbar	K4	Al; 185; 158,8	158,8
K4	K0	Al; 120; 149,53	149,53
K4	K3	Al; 120; 64,15	64,15
K3	K2	Al; 70; 64,73	64,73
K2	K1	Al; 35; 83,8	83,8
Sunrise LV busbar	K7	Al; 185; 4,24	4,24

Continued on next page

**Table A.3:** Residential Network LV Cable Composition derived from [70] - continued from previous page

<b>From</b>	<b>To</b>	<b>Cable Segment Composition, In Series: Conductor; Size (mm<sup>2</sup>); Length (m)</b>	<b>Total Cable Length(m)</b>
K7	K6	Al; 185; 93,89	93,89
K6	K5	Al; 35; 104,34	104,34
Sunrise LV busbar	K8	Al; 185; 59,51	59,51
Fish LV busbar	K15	Al; 300; 15,22	15,22
Fish LV busbar	K15	Al; 185; 6,31	6,31
K15	K16	Al; 120; 105,83	105,83
K15	K17	Al; 185; 144,37	144,37
K17	K18	Cu; 65; 33,27	33,27
K18	K19	Al; 65; 1,96	1,96
K18	K20	Cu; 65; 78,35	78,35
K20	K21	Cu; 65; 97,27	97,27
K15	K14	Al; 185; 29,12	29,12
K14	K22	Al; 120; 54,07	54,07
K22	K23	Al; 120; 65,9	65,9
K23	K24	Al; 120; 67,47	67,47
K15	K13	Al; 185; 88,6	88,6
K13	K12	Al; 120; 87,19	87,19
K12	K11	Al; 70; 60,11	60,11
K12	K10	Al; 120; 101,54	101,54
K10	K9	Al; 120; 97,28	97,28
Lion LV busbar	K27	Al; 120; 77,69	77,69
Lion LV busbar	K26	Al; 185; 111,33	111,33
K26	K29	Al; 185; 87,29	87,29
K29	K28	Al; 185; 32,11	32,11
K29	K30	Al; 185; 50,34	50,34
K26	K25	Al; 120; 34,39	34,39
K25	K31	Al; 70; 145,05	145,05
K31	K32	Al; 70; 52,16	52,16
K32	K33	Al; 120; 53,22	53,22
Oak LV busbar	K37	Al; 300; 100,69	100,69
K37	K35	Al; 120; 116,27	116,27
K35	K34	Al; 70; 81,93	81,93
K37	K40	Cu; 97; 114,09	114,09
K40	K38	Cu; 65; 61,14 + Al; 120; 45,25	106,39
K38	K36	Al; 120; 131,26	131,26
Market LV busbar	K45	Al; 35; 4,9	4,9
Market LV busbar	K39	Al; 185; 336,76	336,76
Market LV busbar	K43	Al; 300; 129,29	129,29
K43	K42	Al; 185; 31,11	31,11
K42	K41	Al; 120; 118,3	118,3
K43	K44	Al; 120; 60,13	60,13
K43	K46	Al; 300; 163	163

Continued on next page

**Table A.3:** Residential Network LV Cable Composition derived from [70] - continued from previous page

<b>From</b>	<b>To</b>	<b>Cable Segment Composition, In Series: Conductor; Size (mm<sup>2</sup>); Length (m)</b>	<b>Total Cable Length(m)</b>
K46	K47	Al; 300; 47,63	47,63
K47	K48	Al; 300; 40,13	40,13
K48	K49	Al; 300; 32,98	32,98
K49	K50	Cu; 26; 74,09	74,09
K50	K51	Al; 70; 66,64	66,64
Beach LV busbar	K60	Al; 300; 93	93
K60	K61	Al; 185; 52,94	52,94
Beach LV busbar	K59	Al; 300; 1,26	1,26
K59	K58	Cu; 97; 198,48	198,48
K58	K57	Al; 300; 33,06	33,06
K57	K56	Al; 300; 28	28
K56	K55	Al; 300; 18,56	18,56
K55	K54	Al; 300; 53,56	53,56
K54	K53	Al; 185; 43,7	43,7
K53	K52	Al; 35; 37,48	37,48
Grave LV busbar	K68	Al; 185; 2,97	2,97
K68	K63	Al; 120; 155,3	155,3
K68	K67	Al; 120; 63,72	63,72
K67	K69	Al; 120; 133	133
K67	K66	Al; 120; 37,49	37,49
K66	K65	Al; 120; 64,73	64,73
K65	K64	Al; 120; 49,01	49,01
K64	K62	Al; 70; 102,35	102,35

## A.2 Residential Network Cables

**Table A.4:** Residential Network Cable Characteristics [70]

Voltage	Type	Conductor	Size (mm <sup>2</sup> )	R ( $\Omega$ /km)	X <sub>L</sub> ( $\Omega$ /km)	C ( $\mu$ F/km)	Ampacity (A)
LV	PVC	Al	35	0,944	0,0895	-	108
LV	PVC	Al	65	0,512	0,087	-	158
LV	PVC	Al	70	0,476	0,087	-	158
LV	PVC	Al	120	0,282	0,086	-	219
LV	PVC	Al	185	0,186	0,084	-	278
LV	PVC	Al	300	0,119	0,0825	-	355
LV	PVC	Cu	26	0,749	0,0915	-	119
LV	PVC	Cu	65	0,305	0,087	-	210
LV	PVC	Cu	97	0,207	0,086	-	251
MV	PILC	Al	50	0,666	0,112	0,3	125
MV	PILC	Al	65	0,515	0,108	0,32	155
MV	PILC	Al	120	0,285	0,099	0,39	210
MV	PILC	Al	300	0,123	0,089	0,59	340
MV	PILC	Cu	39	0,504	0,118	0,25	130
MV	PILC	Cu	65	0,308	0,108	0,32	155
MV	PILC	Cu	70	0,287	0,106	0,33	155
MV	PILC	Cu	129	0,161	0,098	0,41	265
MV	PILC	Cu	161	0,132	0,095	0,57	295

## A.3 Residential Network Transformers

**Table A.5:** Residential Network MV/LV Transformers

MV/LV Transformer	Transformer Rating (kVA) [70]
Sunrise (residential network):	500
Fish (residential network):	500
Lion (residential network):	500
Oak (residential network):	315
Market (residential network):	500
Beach (residential network):	800
Grave (residential network):	315
Roy (broader area):	315
East (broader area):	315
Hill (broader area):	160
Sugar (broader area):	315
Artillery (broader area):	315
Pole (broader area):	100



# Appendix B

## Commercial Network Information

### B.1 Commercial Network Topology

**Table B.1:** Commercial Network MV Cable Composition derived from [70]

From	To	Cable Segment Composition, In Series: Conductor; Size (mm <sup>2</sup> ); Length (m)	Total Cable Length(m)
Metropolitan	Bird busbar	Al; 300; 1206	1206
Metropolitan	Palace busbar	Al; 300; 299	299
Metropolitan	Office busbar	Al; 300; 1084	1084
Bird busbar	T22	Al; 120; 291	291
T22	T23	Al; 120; 200	200
T23	T24	Al; 120; 200	200
T24	T25	Al; 120; 200	200
T25	T26	Al; 120; 200	200
T26	T27	Al; 120; 301	301
Bird busbar	T21	Al; 300; 200	200
Bird busbar	T28	Al; 300; 44	44
T28	T29	Al; 300; 221	221
T29	T30	Al; 300; 75	75
T30	T31	Al; 300; 162	162
T31	T32	Al; 300; 50	50
Palace busbar	T33	Al; 120; 588	588
T33	T37	Al; 120; 81	81
T37	T34	Al; 120; 200	200
T34	T35	Al; 120; 787	787
T35	T36	Al; 120; 37	37
Palace busbar	T3	Al; 120; 456	456
Palace busbar	T2	Al; 120; 5	5
Palace busbar	T1	Al; 50; 223	223
Palace busbar	Bush busbar	Al; 300; 454	454
Bush busbar	T16	Al; 120; 248	248
Bush busbar	T12	Al; 120; 90	90
T12	T13	Al; 120; 196	196

Continued on next page

**Table B.1:** Commercial Network MV Cable Composition derived from [70] - continued from previous page

From	To	Cable Segment Composition, In Series: Conductor; Size (mm <sup>2</sup> ); Length (m)	Total Cable Length(m)
T13	T14	Al; 120; 200	200
T14	T15	Al; 120; 144	144
Bush busbar	T8	Al; 120; 23	23
T8	T9	Al; 120; 207	207
T9	T10	Al; 120; 264	264
T10	T11	Al; 120; 208	208
Bird busbar	Sapphire busbar	Al; 300; 1000	1000
Sapphire busbar	Bush busbar	Al; 300; 377	377
Bush busbar	Office busbar	Al; 300; 1199	1199
Office busbar	T5	Al; 50; 95	95
Office busbar	T4	Al; 120; 241	241
T4	Cell busbar	Al; 120; 252	252
Cell busbar	T7	Al; 120; 5	5
Cell busbar	T6	Al; 120; 195	195

## B.2 Commercial Network Cables

**Table B.2:** Commercial Network Cable Characteristics [70]

Voltage	Type	Conductor	Size (mm <sup>2</sup> )	R (Ω/km)	X <sub>L</sub> (Ω/km)	C (μF/km)	Ampacity (A)
MV	PILC	Al	50	0,613	0,112	0,3	125
MV	PILC	Al	120	0,262	0,099	0,39	210
MV	PILC	Al	300	0,113	0,089	0,59	340

## B.3 Commercial Network Transformers

**Table B.3:** Commercial Network MV/LV Transformers

MV/LV Transformer	Transformer Rating (kVA) [70]
1	1000
2	1000
3	800
4	1000
5	1000
6	800
7	1000
8	800
9	1000

Continued on next page

**Table B.3:** Commercial Network MV/LV Transformers -  
continued from previous page

<b>MV/LV Transformer</b>	<b>Transformer Rating (kVA) [70]</b>
10	800
11	800
12	500
13	800
14	800
15	800
16	1000
21	1600
22	1000
23	1000
24	800
25	800
26	1000
27	800
28	1000
29	800
30	800
31	1000
32	800
33	800
34	500
35	800
36	800
37	800

# Appendix C

## Industrial Network Information

### C.1 Industrial Network Topology

**Table C.1:** Industrial Network MV Cable Composition derived from [28]

From	To	Cable Segment Composition, In Series: Conductor; Size (mm <sup>2</sup> ); Length (m)	Total Cable Length(m)
South	Switching station A	Cu; 185; 2679,1	2679,1
South	Switching station B	Cu; 185; 3966,3	3966,3
Switching station A	Switching station B	Cu; 185; 894,5	894,5
Switching station A	T10	Cu; 95; 165,8	165,8
10	J1	Cu; 95; 59,9	59,9
J1	T9	Cu; 25; 60,6	60,6
J1	T8	Cu; 95; 90,7	90,7
T8	T7	Cu; 95; 266,7	266,7
T7	T6	Cu; 95; 239,3	239,3
T6	J2	Cu; 95; 234,5	234,5
J2	T5	Cu; 25; 202,9	202,9
J2	J3	Cu; 95; 267,4	267,4
J3	T4	Cu; 25; 79,8	79,8
J3	T3	Cu; 95; 42,3	42,3
T3	T2	Cu; 95; 44,3	44,3
T2	T1	Cu; 95; 37,6	37,6
Switching station A	T11	Cu; 95; 196,3	196,3
T11	T12	Cu; 95; 49,7	49,7
T12	T13	Cu; 95; 103,5	103,5
T13	T14	Cu; 95; 155,8	155,8
T14	T15	Cu; 25; 99,2	99,2
T14	T25	Cu; 95; 183,5	183,5
T25	T26	Cu; 95; 53,3	53,3
T26	T27	Cu; 95; 96,7	96,7
T27	B1	Cu; 95; 441,1 + Cu; -; 83,2 *	524,3
B1	T35	Cu; 25; 45,2	45,2

Continued on next page

**Table C.1:** Industrial Network MV Cable Composition derived from [28] - continued from previous page

From	To	Cable Segment Composition, In Series: Conductor; Size (mm <sup>2</sup> ); Length (m)	Total Cable Length(m)
B1	B2	Cu; -; 242,1 *	242,1
B2	T39	Cu; 95; 75,3	75,3
B2	T40	Cu; -; 67,1 * + Cu; 95; 69	136,1
T40	T41	Cu; 95; 37,8	37,8
Switching station B	T44	Cu; 95; 277,2	277,2
T44	T43	Cu; 95; 532,7	532,7
T43	T42	Cu; 95; 88,4	88,4
Switching station B	T28	Cu; 95; 40,2	40,2
T28	T24	Cu; 95; 282,3	282,3
T24	T16	Cu; 95; 162,3	162,3
T16	T18	Cu; 95; 183,8	183,8
T18	T17	Cu; 95; 54	54
T17	T19	Cu; 95; 107	107
T19	T20	Cu; 95; 98,1	98,1
T20	T21	Cu; 95; 140,2	140,2
T21	T22	Cu; 95; 85,3	85,3
T22	T23	Cu; 95; 74,6	74,6
Switching station B	T29	Cu; 95; 225,5	225,5
T29	T32	Cu; 95; 205,8	205,8
T32	T31	Cu; 95; 38,3	38,3
T31	T30	Cu; 25; 87	87
T31	T33	Cu; 95; 115,8	115,8
T33	T34	Cu; 95; 8,1	8,1
T34	T36	Cu; 95; 259,4	259,4
T36	T37	Cu; 95; 46,7	46,7
T37	T38	Cu; 95; 82,5	82,5

\*overhead lines

## C.2 Industrial Network Cables

**Table C.2:** Industrial Network Cable Characteristics [28]

Voltage	Type	Conductor	Size (mm <sup>2</sup> )	R (Ω/km)	X <sub>L</sub> (Ω/km)	C (μF/km)	Ampacity (A)
MV	PILC	Cu	25	0,739	0,391	0,166	115
MV	PILC	Cu	95	0,194	0,266	0,324	245
MV	PILC	Cu	185	0,194	0,266	0,324	345
MV	Overhead	Cu	-	0,281	0,359	0,0128	262

### C.3 Industrial Network Transformers

**Table C.3:** Industrial Network MV/LV Transformers

MV/LV Transformer/ Supply Point	Transformer/ Rating (kVA) [28]	Supply Point
1	500	
2	500	
3	550 (MV supply)	
4	500	
5	500	
6	500	
7	500	
8	500	
9	1000	
10	500	
11	500	
12	315	
13	500	
14	500	
15	500	
16	500	
17	500	
18	500	
19	500	
20	1000	
21	100	
22	200	
23	500	
24	500	
25	500	
26	500	
27	200	
28	500	
29	500	
30	100	
31	200	
32	500	
33	500	
34	500	
35	500	
36	200	
37	1500 (MV supply)	
38	500	
39	315	
40	500	
41	500	
42	500	
43	3000 (MV supply)	
44	1200 (MV supply)	

# List of References

- [1] REN21, “Renewables 2018 Global Status Report,” Paris, Tech. Rep., 2018. [Online]. Available: [http://www.ren21.net/wp-content/uploads/2018/06/17-8652\\_GSR2018\\_FullReport\\_web\\_-1.pdf](http://www.ren21.net/wp-content/uploads/2018/06/17-8652_GSR2018_FullReport_web_-1.pdf)
- [2] L. Scholtz, K. Muluadzi, K. Kritzinger, M. Mabaso, and S. Forder, “Renewable Energy: Facts and Futures,” WWF, Cape Town, Tech. Rep., 2017.
- [3] Eskom, “Coal Power,” 2018. [Online]. Available: [http://www.eskom.co.za/AboutElectricity/ElectricityTechnologies/Pages/Coal\\_Power.aspx](http://www.eskom.co.za/AboutElectricity/ElectricityTechnologies/Pages/Coal_Power.aspx)
- [4] P. Dondi, D. Bayoumi, C. Haederli, D. Julian, and M. Suter, “Network integration of distributed power generation,” *Journal of Power Sources*, vol. 106, pp. 1–9, 2002.
- [5] GreenCape, “Utility-scale renewable energy 2017 Market Intelligence Report,” Cape Town, Tech. Rep., 2017.
- [6] International Renewable Energy Agency and Energy Technology Systems Analysis Programme, “Renewable Energy Integration in Power Grids,” Tech. Rep., 2015. [Online]. Available: [http://www.irena.org/-/media/Files/IRENA/Agency/Publication/2015/IRENA-ETSAP\\_Tech\\_Brief\\_Power\\_Grid\\_Integration\\_2015.pdf](http://www.irena.org/-/media/Files/IRENA/Agency/Publication/2015/IRENA-ETSAP_Tech_Brief_Power_Grid_Integration_2015.pdf)
- [7] Siemens Power Technologies International, “Integration of distributed generation,” 2014. [Online]. Available: [https://w3.usa.siemens.com/smartgrid/us/en/transmission-grid/consulting-and-design/integration-of-dispersed/Documents/PTI\\_FF\\_EN\\_NCRE\\_SystemInteg\\_FT\\_1411.pdf](https://w3.usa.siemens.com/smartgrid/us/en/transmission-grid/consulting-and-design/integration-of-dispersed/Documents/PTI_FF_EN_NCRE_SystemInteg_FT_1411.pdf)
- [8] Energy Research Centre, CSIR, and IFPRI, “The developing energy landscape in South Africa: Technical Report,” University of Cape Town, Cape Town, Tech. Rep., 2017.
- [9] Solargis, “Solar resource maps and GIS data for 200+ countries,” 2018. [Online]. Available: <https://solargis.com/maps-and-gis-data/overview/>
- [10] City of Cape Town, “What is small-scale embedded generation?” [Online]. Available: <http://www.capetown.gov.za/Workandbusiness/Commercial-utility-services/Commercial-electricity-services/What-is-small-scale-embedded-generation>
- [11] A. Rix, K. Kritzinger, I. Meyer, and J. van Niekerk, “Potential for distributed solar photovoltaic systems in the Western Cape Province,” Centre for Renewable and Sustainable Energy Studies, Stellenbosch, Tech. Rep., 2015. [Online]. Available: [http://www.crses.sun.ac.za/files/research/publications/technical-reports/WCGPVReportFinal\[1\].pdf](http://www.crses.sun.ac.za/files/research/publications/technical-reports/WCGPVReportFinal[1].pdf)
- [12] City of Cape Town, “Register your PV system,” 2018. [Online]. Available: <http://resource.capetown.gov.za/documentcentre/Documents/Procedures,guidelinesandregulations/Register-Your-PV-System.pdf>

- [13] —, “Rooftop PV Guidelines for Safe and Legal Installations in Cape Town,” pp. 1–8, 2018. [Online]. Available: <http://resource.capetown.gov.za/documentcentre/Documents/Graphicsandeducationalmaterial/CCT-Energy-PV-Brochure.pdf>
- [14] Electricity Services Department and Environmental Resource Management Department of the City of Cape Town, “Safe and Legal Installations of Rooftop Photovoltaic Systems,” pp. 2–3, 2016. [Online]. Available: <http://resource.capetown.gov.za/documentcentre/Documents/Procedures,guidelinesandregulations/SafeandLegalPVinstallationsMarch2016.pdf>
- [15] City of Cape Town, “City of Cape Town,” 2016. [Online]. Available: <http://resource.capetown.gov.za/documentcentre/Documents/Mapsandstatistics/ElectricityDistributionLicenceandAreaBoundaries.pdf>
- [16] —, “Requirements for small-scale embedded generation: Application process to become a small-scale embedded generator in the City of Cape Town,” pp. 1–43, 2016. [Online]. Available: [http://resource.capetown.gov.za/documentcentre/Documents/Procedures,guidelinesandregulations/CCTRequiremenstforEmbeddedGeneration\\_V4720161103.pdf](http://resource.capetown.gov.za/documentcentre/Documents/Procedures,guidelinesandregulations/CCTRequiremenstforEmbeddedGeneration_V4720161103.pdf)
- [17] —, “Utility Services - Electricity Services (Consumptive),” no. July, pp. 47–49, 2016. [Online]. Available: <https://www.capetown.gov.za/en/electricity/Electariffs201415/ScheduleofConsumptiveTariffs.pdf>
- [18] G. M. Masters, *Renewable and Efficient Electric Power Systems*, 2nd ed. Hoboken: John Wiley & Sons, 2013.
- [19] J. Glover, M. S. Sarma, and T. J. Overbye, *Power System Analysis & Design*, 5th ed., S. Meherishi, H. Gowans, C. Valentine, and S. Gerger-Knechtl, Eds. Stamford: CL Engineering, 2011.
- [20] Eskom, “ESCOM 1923 - 1929 - The Years of Establishment - "Electrifying our beloved country",” 2018. [Online]. Available: <http://www.eskom.co.za/sites/heritage/Pages/1923.aspx>
- [21] C. G. Carter-Brown, “Effect of conductor size on the total cost of electricity distribution feeders in South African Electrification,” Ph.D. dissertation, University of Cape Town, 2006.
- [22] Eskom Generation Communication, “Transmission and Distribution of Electricity,” 2015. [Online]. Available: [http://www.eskom.co.za/AboutElectricity/FactsFigures/Documents/TD\\_0003TransmissionDistributionElectricityRev8.pdf](http://www.eskom.co.za/AboutElectricity/FactsFigures/Documents/TD_0003TransmissionDistributionElectricityRev8.pdf)
- [23] M. Mahmud, M. Hossain, and H. Pota, “Analysis of Voltage Rise Effect on Distribution Network with Distributed Generation,” in *18th IFAC World Congress*, Milano, 2011, pp. 14 796–14 801. [Online]. Available: <https://www.sciencedirect.com/science/article/pii/S1474667016460064>
- [24] C. Masters, “Voltage rise: the big issue when connecting embedded generation to long 11 kV overhead lines,” *POWER ENGINEERING JOURNAL*, vol. 16, no. 1, pp. 5–12, 2002. [Online]. Available: <https://ieeexplore.ieee.org/stamp/stamp.jsp?arnumber=990181>
- [25] C. Carter-Brown, “The impact of rooftop PV on distribution networks,” 2015. [Online]. Available: <http://www.aurecongroup.com/en/thinking/thinking-papers/the-impact-of-rooftop-pv-on-distribution-networks.aspx>



- [26] ABB, “Large distribution transformers (2,500-10,000 kVA ONAN) - Distribution Transformers (Transformers) | ABB.” [Online]. Available: <http://new.abb.com/products/transformers/distribution/large>
- [27] ———, “Small distribution transformers (0-315 kVA) - Distribution Transformers (Transformers) | ABB.” [Online]. Available: <http://new.abb.com/products/transformers/distribution/small>
- [28] Eskom Distribution, “No Title,” 2018.
- [29] Brown & Kysar Inc., “Brown & Kysar Inc. - Voltage Regulator Line Drop Compensation.” [Online]. Available: <http://www.bki.cc/blog/71/>
- [30] A. Kumar, “Distribution System Capacitor Banks And their Impact On Power Quality.” [Online]. Available: <http://www.electricalindia.in/blog/post/id/5458/distribution-system-capacitor-banks-and-their-impact-on-power-quality>
- [31] G&W, “Viper-ST® Solid Dielectric, Triple Option Reclosers | G&W Electric.” [Online]. Available: <http://www.gwelec.com/viper-solid-dielectric-triple-option-reclosers-p-95-len.html>
- [32] J. Chihota and C. Gaunt, “Potential PV Penetration study in the Western Cape Draft Work Package 2 Final Report,” Cape Town, Tech. Rep., 2018.
- [33] A. Toliyat, A. Kwasinski, and F. Uriarte, “Effects of high penetration levels of photovoltaic generation: Observations from field data,” in *2012 International Conference on Renewable Energy Research and Applications (ICRERA)*. Nagasaki, Japan: IEEE, 2012. [Online]. Available: <https://ieeexplore.ieee.org/document/6477269>
- [34] B. Ucar, M. Bagriyanik, and G. Komurgoz, “Influence of PV Penetration on Distribution Transformer Aging,” *Journal of Clean Energy Technologies*, vol. 5, no. 2, pp. 131–134, 2017. [Online]. Available: <http://www.jocet.org/vol5/357-A0116.pdf>
- [35] J. D. Watson, N. R. Watson, D. Santos-Martin, A. R. Wood, S. Lemon, and A. J. Miller, “Impact of solar photovoltaics on the low-voltage distribution network in New Zealand,” *IET Generation, Transmission & Distribution*, vol. 10, no. 1, pp. 1–9, 2016. [Online]. Available: <https://ieeexplore.ieee.org/stamp/stamp.jsp?arnumber=7381747>
- [36] V. H. Méndez Quezada, J. R. Abbad, and T. Román, Gómez San, “Assessment of Energy Distribution Losses for Increasing Penetration of Distributed Generation,” *IEEE Transactions on Power Systems*, vol. 21, no. 2, pp. 533–540, 2006.
- [37] T. Aziz and N. Ketjoy, “PV Penetration Limits in Low Voltage Networks and Voltage Variations,” *IEEE Access*, vol. 5, 2017. [Online]. Available: <https://ieeexplore.ieee.org/stamp/stamp.jsp?tp={&}arnumber=8022856>
- [38] J. M. Nye, “Increasing distributed generation penetration when limited by voltage regulation,” Stellenbosch University, Tech. Rep., 2014. [Online]. Available: <https://www.crses.sun.ac.za/files/research/completed-research/eppei/JMNye.pdf>
- [39] M. ElNozahy and M. Salama, “Technical impacts of grid-connected photovoltaic systems on electrical networks - A review,” *Journal of Renewable and Sustainable Energy*, vol. 5, 2013. [Online]. Available: <https://aip.scitation.org/doi/10.1063/1.4808264>

- [40] G. Yang, F. Marra, M. Juamperez, and S. Hashemi, "Voltage rise mitigation for solar PV integration at LV grids," *Journal of Modern Power Systems and Clean Energy*, vol. 3, no. 3, pp. 411–421, 2015. [Online]. Available: <https://link.springer.com/article/10.1007/s40565-015-0132-0>
- [41] D. Habijan, M. Cavlovic, and D. Jaksic, "The Issue of Asymmetry in Low Voltage Network with Distributed Generation," in *22nd International Conference on Electricity Distribution*, Stockholm, 2013.
- [42] S. Shivashankar, S. Mekhilef, H. Mokhlis, and M. Karimi, "Mitigating methods of power fluctuation of photovoltaic (PV) sources - A review," *Renewable and Sustainable Energy Reviews*, vol. 59, pp. 1170–1184, 2016. [Online]. Available: [https://umexpert.um.edu.my/file/publication/00005361\\_141429.pdf](https://umexpert.um.edu.my/file/publication/00005361_141429.pdf)
- [43] V. Cirjaleanu, "Investigation of Cloud-Effects on Voltage Stability of Distribution Grids with Large Amount of Solar Photovoltaics," Chalmers University of Technology, Gothenburg, Tech. Rep., 2017. [Online]. Available: <http://publications.lib.chalmers.se/records/fulltext/249022/249022.pdf>
- [44] Electricity Suppliers Liaison Committee, *NRS 048-2:2003*. Pretoria: Standards South Africa, 2003. [Online]. Available: <http://www.nersa.org.za/Admin/Document/Editor/file/Electricity/IndustryStandards/NRS048part2.pdf>
- [45] B. Abdi, M. Abroshan, H. Aslinezhad, and A. Alimardani, "Coordination Return of Protective Devices in Distribution Systems in Presence of Distributed Generation," *Energy Procedia*, vol. 12, pp. 263–270, 2011.
- [46] P. Padmavathy and S. Parthasarathy, "Distribution Feeder Protection with and without PV System," *International Journal of Electrical, Electronics and Data Communication*, vol. 1, no. 3, pp. 30–34, 2013.
- [47] E. Csanyi, "The fundamentals of protection relay co-ordination and time/current grading principles," 2018. [Online]. Available: <https://electrical-engineering-portal.com/protection-relay-co-ordination-time-current-grading>
- [48] H. Ravindra, M. Omar Faruque, P. McLaren, K. Schoder, M. Steurer, and R. Meeker, "Impact of PV on distribution protection system," in *North American Power Symposium (NAPS)*, Champaign, 2012. [Online]. Available: [https://www.researchgate.net/publication/261047573\\_Impact\\_of\\_PV\\_on\\_distribution\\_protection\\_system](https://www.researchgate.net/publication/261047573_Impact_of_PV_on_distribution_protection_system)
- [49] NERSA, "Grid Connection Code for Renewable Power Plants (RPPs) Connected to the Electricity Transmission System (TS) or the Distribution System (DS) in South Africa," 2016. [Online]. Available: <http://www.nersa.org.za/Admin/Document/Editor/file/Electricity/TechnicalStandards/NewableEnergy/SAGCRequirementsforRenewablePowerPlantsRev29.pdf>
- [50] W. Peng, Y. Baghzouz, and S. Haddad, "Local load power factor correction by grid-interactive PV inverters," in *PowerTech (POWERTECH), 2013 IEEE Grenoble*, Grenoble, 2013, pp. 1–6. [Online]. Available: [https://www.researchgate.net/publication/261122335\\_Local\\_load\\_power\\_factor\\_correction\\_by\\_grid-interactive\\_PV\\_inverters](https://www.researchgate.net/publication/261122335_Local_load_power_factor_correction_by_grid-interactive_PV_inverters)
- [51] Global Sustainable Energy Solutions, "Power Factor and Grid-Connected Photovoltaics," pp. 1–4, 2015.

- [52] R. Ciric and M. Markovic, "Power Factor Analysis in Distribution Network with Roof Photovoltaic Units," *Journal of Electrical Engineering & Electronic Technology*, vol. 6, no. 4, pp. 1–8, 2017. [Online]. Available: [https://www.researchgate.net/publication/320614632\\_Power\\_Factor\\_Analysis\\_in\\_Distribution\\_Network\\_with\\_Roof\\_Photovoltaic\\_Units](https://www.researchgate.net/publication/320614632_Power_Factor_Analysis_in_Distribution_Network_with_Roof_Photovoltaic_Units)
- [53] A. Latheef, D. Robinson, V. J. Gosbell, and V. W. Smith, "Harmonic impact of photovoltaic inverters on low voltage distribution systems," in *Conference Proceedings of the 2006 Australasian Universities Power Engineering Conference*, 2006, pp. 1–6.
- [54] S. Lewis, "Analysis and Management of the Impacts of a High Penetration of Photovoltaic Systems in an Electricity Distribution Network," Ph.D. dissertation, University of New South Wales, 2010.
- [55] A. Steyn, "Investigation into the harmonics of LED streetlights," Stellenbosch University, Tech. Rep., 2016.
- [56] A. Chidurala, T. Kumar Saha, and N. Mithulananthan, "Harmonic impact of high penetration photovoltaic system on unbalanced distribution networks - learning from an urban photovoltaic network," *IET Renewable Power Generation*, vol. 10, no. 4, pp. 485–494, 2015. [Online]. Available: <https://ieeexplore.ieee.org/stamp/stamp.jsp?tp={&}arnumber=7442736>
- [57] O. Poosri and C. Charoenlarnnoppa, "Harmonics Impact of Rooftop Photovoltaic Penetration Level on Low Voltage Distribution System," *International Journal of Electronics and Electrical Engineering*, vol. 4, no. 3, pp. 221–225, 2016. [Online]. Available: <http://www.ijeee.net/uploadfile/2016/0628/20160628020250756.pdf>
- [58] S. Horvat, "Frequency fluctuations in power systems," University of Bergen, Bergen, Tech. Rep., 2007. [Online]. Available: <https://org.uib.no/energiforumef/Artikler/FrequencyFluctuationsinPowerSystems2007.pdf>
- [59] S. Pourmousavi, A. Cifala, and M. Nehrir, "Impact of high penetration of PV generation on frequency and voltage in a distribution feeder," in *2012 North American Power Symposium (NAPS)*, 2012. [Online]. Available: <http://www.alipourmousavi.com/docs/CPaper1-2012.pdf>
- [60] Transpower New Zealand Limited, "Effects of Solar PV on Frequency Management in New Zealand," Tech. Rep., 2017. [Online]. Available: <https://www.transpower.co.nz/sites/default/files/plain-page/attachments/EffectofSolarPVonFrequencyManagementinNewZealand.pdf>
- [61] R. Yan, T. Kumar Saha, N. Modi, N.-A. Masood, and M. Mosadeghy, "The combined effects of high penetration of wind and PV on power system frequency response," *Applied Energy*, vol. 145, pp. 320–330, 2015. [Online]. Available: <https://www.sciencedirect.com/science/article/pii/S0306261915002214>
- [62] S.-y. Yang and L. Hao, "Research on the Voltage Distribution of Interconnected Distributed Network - Distributed Generation," in *2011 Asia-Pacific Power and Energy Engineering Conference*, Wuhan, China, 2011, pp. 1–4. [Online]. Available: <https://ieeexplore.ieee.org/stamp/stamp.jsp?tp={&}arnumber=5748672>
- [63] R. Bernards, J. Morren, and J. Slootweg, "Maximum PV-penetration in low-voltage cable networks," in *Proceedings of the 7th IEEE Young Researchers Symposium*, Ghent, Belgium, 2014, pp. 1–5.

- [64] A. Nguyen, M. Velay, J. Schoene, V. Zheglov, B. Kurtz, K. Murray, B. Torre, and J. Kleissl, “High PV Penetration Impacts on Five Local Distribution Networks Using High Resolution Solar Resource Assessment with Sky Imager and QuasiSteady State Distribution System Simulations,” *Solar Energy*, pp. 1–17, 2016. [Online]. Available: [https://www.researchgate.net/publication/299382514\\_High\\_PV\\_penetration\\_impacts\\_on\\_five\\_local\\_distribution\\_networks\\_using\\_high\\_resolution\\_solar\\_resource\\_assessment\\_with\\_sky\\_imager\\_and\\_quasi-steady\\_state\\_distribution\\_system\\_simulations](https://www.researchgate.net/publication/299382514_High_PV_penetration_impacts_on_five_local_distribution_networks_using_high_resolution_solar_resource_assessment_with_sky_imager_and_quasi-steady_state_distribution_system_simulations)
- [65] Electricity Suppliers Liaison Committee, *NRS 097-2-3:2014*. SABS Standards Division, 2014. [Online]. Available: <http://pqrs.co.za/wp-content/uploads/2015/03/NRS-097-2-3-final-2014.pdf>
- [66] K. Dartawan, L. Hui, R. Austria, and M. Suehiro, “Harmonics Issues that Limit Solar Photovoltaic Generation on Distribution Circuits,” in *SOLAR 2012, World Renewable Energy Forum*, Colorado, 2012, pp. 1–7. [Online]. Available: [https://ases.conference-services.net/resources/252/2859/pdf/SOLAR2012\\_0482\\_fullpaper.pdf](https://ases.conference-services.net/resources/252/2859/pdf/SOLAR2012_0482_fullpaper.pdf)
- [67] N. Mararakanye, K. Kritzinger, A. Steyn, and A. Rix, “Identifying the rooftop PV potential of residential, industrial and commercial areas in South Africa,” in *SASEC 2018*, Durban, 2018. [Online]. Available: [https://www.sasec.org.za/full\\_papers/70.pdf](https://www.sasec.org.za/full_papers/70.pdf)
- [68] L. Dordley, “These are South Africa’s most expensive streets and suburbs,” 2018. [Online]. Available: <https://www.capetownetc.com/cape-town/south-africas-expensive-streets-suburbs/>
- [69] Esri, “ArcGIS,” 2018. [Online]. Available: <http://www.arcgis.com/home/index.html>
- [70] City of Cape Town: Electricity Directorate, “Potential PV Penetration study in the Western Cape.”
- [71] G. Moodley, G. Jennings, and V. Pillay, “Typical technical behaviour of LV networks with varied levels of renewable penetration,” in *64th AMEU Convention 2014*, Johannesburg, 2014, pp. 62–64. [Online]. Available: <http://www.ee.co.za/wp-content/uploads/2014/11/AMEU-Convention-2014-p62-64.pdf>
- [72] City of Cape Town, “City of Cape Town Open Data Portal - Data Set Description,” 2016. [Online]. Available: <https://web1.capetown.gov.za/web1/opendataportal/DatasetDetail?DatasetName=Buildingfootprints>
- [73] S. Heunis and M. Dekenah, “A load profile prediction model for residential consumers,” *Energize*, pp. 46–49, 2010.
- [74] Solargis, “pvPlanner,” 2018. [Online]. Available: <https://solargis.info/pvplanner/#tl=Google:hybrid{&}bm=satellite>
- [75] J. Szymanowski and P. Swift, “SANS 10400 Building Regulations,” 2017. [Online]. Available: <http://sans10400.co.za/roofs-1/>
- [76] OfficeHolidays, “Public Holidays in South Africa in 2016,” 2018. [Online]. Available: [https://www.officeholidays.com/countries/south\\_africa/2016.php](https://www.officeholidays.com/countries/south_africa/2016.php)
- [77] DIgSILENT GmbH, “Digsilent Powerfactory 2017 User Manual,” Gomaringen, Germany, p. 363, 2017.

- [78] —, “Digsilent Powerfactory Scripting and Automation.” [Online]. Available: <https://www.digsilent.de/en/scripting-and-automation.html>